Master's thesis

NTNU
Norwegian University of Science and Technology
Faculty of Engineering
Department of Geoscience and Petroleum

Mads Berntsen

Drillstring Vibrations

Identification, Classification and Mitigation

Master's thesis in Petroleum Engineering

Supervisor: Dr. Tor Berge Gjersvik

June 2020

NTNU
Norwegian University of
Science and Technology

AkerBP

Mads Berntsen

Drillstring Vibrations

Identification, Classification and Mitigation

Master's thesis in Petroleum Engineering
Supervisor: Dr. Tor Berge Gjersvik
June 2020

Norwegian University of Science and Technology
Faculty of Engineering
Department of Geoscience and Petroleum

NTNU
Norwegian University of
Science and Technology

Preface

This thesis concludes my master`s degree program in petroleum engineering at the Norwegian University of Science and Technology (NTNU). The thesis is a standalone work; however, it uses the theoretical groundwork laid in the specialization report in TPG4560 (Berntsen 2019).

I would like to thank my advisor from Aker BP, Knut Sigve Selnes, for introducing me to this very interesting topic and providing me with an excellent network consisting of highly recognized persons within the topic of drillstring vibrations. His operational background in various positions across both service- and operating companies, has provided me with the practical expertise otherwise unattainable as a student with very limited field experience.

I would also like to direct appreciation to my advisor at NTNU, Dr. Tor Berge Gjersvik, who`s competence within drilling has helped me understand various mechanisms related to the subject of drillstring vibrations.

A huge thanks to my family, who throughout my five years at university have encouraged and supported me.

During my work I have contacted several people from both industry and academia to quality control and inquire further information. Thank you all for being so forthcoming and helpful.

Finally, a huge thanks to Aker BP for granting me the opportunity to write this thesis and giving me access to internal networks and offices.

Abstract

This master`s thesis builds on the work done in the specialization project TPG4560. Some parts are taken directly from the project report, which was titled “Drillstring Vibrations: A Theoretical Foundation”. This thesis was written in collaboration with Aker BP, an operator who recognized the potential in giving engineers at an operating company a solid understanding of drillstring vibrations. The responsibility of handling and mitigating drillstring vibrations is predominantly engineers from service companies. These service providers often have various patented or classified procedures, workflows and tools to combat vibrations. An engineer at an operating company is required to cooperate with several service providers and gaining a solid theoretical foundation of drillstring vibrations will aid the engineer in cooperating with the different service providers. It will also help the engineer to protect the operator`s interests when decisions are to be made where drillstring vibrations pose a serious risk to the operation.

The main objective of this thesis is to provide insight of the various vibration modes, the mechanisms affecting vibrations, potential consequences, ways of identifying the various vibration types and tools and techniques to mitigate detrimental vibrations. The wide scope of the thesis is chosen to provide the engineer with a broad understanding of the vibrational behavior of the drillstring. A combination of longstanding drilling physics and novel technology developments is described in order to tie together the underlying physical principles of drilling with state-of-the-art technology. The recent developments within measurement tools and techniques have “turned the light on” downhole for dynamic behavior. For this reason, particular focus is given to new anti-vibration tools and procedures. The research is mainly based on literature reviews with emphasis on the reported field experiences to ensure that practice complies with theory.

Important findings and takeaways from the thesis are that field trials indicate that many tools are successful in reducing vibration levels. Field validations have shown that whirl and stick-slip, the most common drilling dysfunctions, have been effectively negated through the use of roller reamers, anti stick-slip technology (AST), depth of cut control (DOCC), soft torque rotary systems (STRS) and drilling advisory systems. The thesis also revealed how the increase in measurement technology have illuminated new vibration types, such as high frequency torsional oscillations (HFTO). The limitation in bandwidth of conventional MWD systems highlights the challenges in real time vibration detection as well as highlighting the potential of wired drill pipe (WDP).

Sammendrag

Denne masteroppgaven bygger på arbeidet fra prosjektoppgaven i faget TPG4560. Noen deler er tatt direkte fra prosjektoppgaven, kalt «Drillstring Vibrations: A Theoretical Foundation». Masteroppgaven var skrevet i samarbeid med Aker BP, et operatørselskap som identifiserte et potensiale ved å gi interne ingeniører et solid teoretisk grunnlag om borestrengsvibrasjoner. Hovedansvaret med å håndtere og mitigere borestrengsvibrasjoner foreligger hos ingeniører fra innleide serviceselskap. Disse serviceselskapene har ofte sine egne patenterte eller klassifiserte prosedyrer, arbeidsflyter og verktøy for å redusere vibrasjoner. Ingeniører ved operatørselskap må samarbeide med flere forskjellige serviceselskap og dermed vil besittelse av en god og generell teoretisk base om borestrengsvibrasjoner være behjelpelig i samhandlingen med de forskjellige serviceselskapene. Det vil også hjelpe med å sikre operatørens interesser når avgjørelser må tas i forbindelse med borestrengsvibrasjoner som kan sette boreoperasjonen i fare.

Formålet med denne oppgaven er å gi innsikt om de forskjellige vibrasjonsformene, mekanismene som påvirker vibrasjoner, potensielle konsekvenser, måter å identifisere de forskjellige vibrasjonstypene samt verktøy og teknikker for å mitigere skadelige borestrengsvibrasjoner. Det brede omfanget til oppgaven er valgt for å gi ingeniøren en bred forståelse av hvordan vibrasjoner påvirker borestrengen. En kombinasjon av etablerte borekonsepter og nyvinninger innenfor boreverktøy og prosedyrer er beskrevet for å knytte sammen underliggende fysiske prinsipper med topp moderne teknologi. Nylige utviklinger innenfor målingsverktøy og sensorer har «skrudd på lyset» i brønnen slik at nå har et bedre bildet av den dynamiske oppførselen til borestrengen. Av denne grunn er nye anti-vibrasjonsverktøy og prosedyrer vektlagt. Undersøkelsene er hovedsakelig basert på litteraturstudier med spesielt fokus på felterfaringer for å forsikre at praksis og teori er i overenstemmelse.

Viktige funn i oppgaven er at flere felterfaringer indikerer at de forskjellige verktøyene beskrevet i denne oppgaven gir signifikant bedre vibrasjonsnivåer. Stick-slip og whirl, de vanligste vibrasjonsformene, er bevist redusert gjennom bruken av roller reamers, anti stick-slip teknologi (AST), depth of cut control (DOCC), soft torque rotary systems (STRS) og drilling advisory systemer. Oppgaven avdekte også hvordan nyvinninger og forbedringer innen måleteknologi har ført til oppdagelse av nye vibrasjonsformer, eksempelvis high frequency torsional oscillation (HFTO). Begrensninger av båndbredde for konvensjonelle MWD systemer avslørte utfordringene knyttet til identifisering av vibrasjoner i sanntid i tillegg til å belyse potensialene ved wired drill pipe (WDP).

Table of Contents

List of Figures

List of Tables

List of Abbreviations

AST	Anti stick-slip technology
BHA	Bottom hole assembly
DOC	Depth of cut
DOCC	Depth of cut control
LWD	Logging while drilling
MPT	Mud pulse telemetry
MSE	Mechanical specific energy
MWD	Measurement while drilling
PDC	Polycrystalline diamond compact
ROP	Rate of penetration
RPM	Revolutions per minute
STRS	Soft torque rotary systems
WDP	Wired drill pipe
WOB	Weight on bit

Nomenclature

DOC	Depth of cut	$[in/rev]$
F_s	Whirl severity	
h_p	Pitch of helix	$[ft]$
h	Height of arc during lateral vibrations	$[m]$
I_p	Moment of inertia	$[in^4]$
L	Length of the drillstring	$[ft]$
L_0	Length of a fibre along the drillstring	$[ft]$
L_2	Length of drill pipe, length of twisted drillstring, well length	$[ft]$
ΔL	Change in length of drillstring	$[m]$
R	Radius of drill collar	$[in]$
r_o	Outer diameter of drill pipe	$[in]$
r_i	Inner diameter of drill pipe	$[in]$
ROP	Rate of penetration	$[ft/hr]$
RPM	Revolutions per minute	$[RPM]$
RPM_{avg}	Average rotation speed	$[RPM]$
RPM_{max}	Maximum rotation speed	$[RPM]$
RPM_{min}	Minimum rotation speed	$[RPM]$
s	Length of arc caused by lateral vibrations	[m]
SSI	Stick-slip index	
T	Input torque	$[ft\ lbs]$
TSE	Torsional severity estimate	
v	Tangential slip velocity	$[ft/s]$
WOB	Weight on bit	$[lbs]$
Θ	Total twist of the drillstring	$[rad]$

ϕ	Angle of deflection	$[rad]$
Ω	Whirl velocity	$[rad/s]$
ω	Angular frequency, rate of rotation	$[rad/s]$

1 Introduction

Since the commencement of petroleum drilling, the industry has pursued solutions that increases the speed at which a well is drilled. By reducing the number of days it takes to drill a well, the operator reaps benefits from producing the well as quickly as possible while simultaneously reducing costs related to drilling days. For offshore drilling, the latter is of utmost importance as rig- and equipment rental make up the largest portion of the cost per meter well drilled. The challenge for the operator is to balance fast drilling with low risk while simultaneously producing a high-quality wellbore.

In modern drilling, drillstrings reach several kilometers in length and only a few inches in diameter. This means that the drillstring comprised of solid steel tubulars effectively assume the characteristics of a violin string, prone to vibrate when excited by a force of sufficient magnitude. The industry`s growing demands for increases in rate of penetration (ROP) leads to increased loads on the drillstring and resultingly a higher susceptibility for drillstring vibrations to develop. Vibrating a structure consumes energy, meaning that the energy input through weight on bit and rotation rate intended for increased ROP is being dissipated through the dynamic motion of the drillstring. In addition, drillstring vibrations are identified as one of the most significant causes of premature bit- and component failure. Additional bit runs, replacing components, fishing runs and sidetrack operations lead to huge increased expenses and an overall increased well construction time. Thus, the negation of vibrations is desirable to increase ROP and minimize downhole failures.

The developments in extended reach drilling means well trajectories are now longer and more complex than before. The susceptibility to vibrations is therefore more present now than ever. With the petroleum industry striving to maximize profit, several tools have been developed to negate drilling dysfunctions caused by detrimental vibrations. The complexity of drillstring vibrations makes it impossible for a single tool or system to completely eradicate all vibrations. This, in combination with the limitations of data from the dynamic behavior of the drillstring downhole makes mitigating vibrations a challenge. Despite this, several tools targeting specific vibration types have shown promise from field experiences and stepwise improvements are being made as drillstring vibrations remain an area of intense research.

Aker BP is an operator who is in at the forefront of fast drilling on the Norwegian continental shelf. Minimizing expensive rig days and optimizing drilling performance is an important goal for the company. For these reasons, it is advantageous to minimize drillstring vibrations and the complications they cause. It is also in the best interest of service companies employed by

Aker BP to ensure efficient drilling, as Aker BP have established an alliance structure with service providers. The dynamic of the alliances works so that all parts in the alliance are rewarded with a share of the profits when a project finishes under budget. To achieve the shared goals of both the operator and the service company, continuous work towards negating vibrations must be carried out. Aker BP must be seeking in the pursuit for new technologies and procedures to mitigate vibrations and strive to challenge service companies to experiment with new solutions.

The scope of this thesis is to supply Aker BP with information about state-of-the-art vibration mitigating tools and techniques. An additional goal is to educate the engineer of the various types of vibrations, what affects them, how they are identified and the potential damage they cause. This is done in a chronological order, starting with simple vibratory concepts which are necessary to understand how vibrations travel in the drillstring. The vibrational modes and the most common vibration type within each mode are described in Chapter 3. Chapter 4 describes common consequences from the different vibration modes, which can also be used to determine which vibrations are occurring. Ways to identify the different vibration types are described in Chapter 6 before mitigative techniques and tools are presented in Chapter 7.

2 Vibratory Concepts

In order to understand vibrations in the drillstring, where a multitude of factors affect the dynamic motion of the system, a fundamental understanding of vibratory concepts is necessary. Some of the following sections within this chapter are taken directly from the project report by Berntsen (2019), Chapter 1.

2.1 Wave Propagation

Vibrations travel through a system in the form of waves. A force inducing vibrations in a system will first impact the point of contact, before propagating further along the system. Analogously, a force being felt at one end of a long drillstring will have a time delay before the particles of the other end of the drillstring are affected by the excitation force.

Longitudinal waves are the type of waves where particles are displaced in the same direction as the wave propagates. For this reason, they are often referred to as tensional-/compressional- or axial waves.

Lateral waves are terms used to describe wave motion where the particles are displaced perpendicular to the direction of the wave. The particles slip on top of each other, which is more energy intensive than the motion of their longitudinal counterparts and thus these waves generally move slower. Torsional-, bending- and transverse waves are categorized as lateral waves, however the former does not have a dispersive characteristic, meaning that the wave components that make up the wave all travel at the same speed (Meyers 1994).

2.2 Natural Frequency and Resonance

The natural frequency is the frequency at which an excited object will vibrate if left alone. The natural frequency of an object will depend on geometry as well as material properties. If a force is applied on a spring, the spring will move in the same direction as the applied force until the restoring force in the spring eventually causes the spring to move back to its original position. The frequency at which this happens is termed its natural frequency.

As energy from a force on a system propagates through the system and is reflected, the wave will eventually reach its initial position. If a new force is then applied at the exact time the wave reaches its initial position, the waves from the two different excitation sources will combine to increase the now combined wave`s amplitude. A practical analogy to this can be visualized by a person on a swing. In order to get speed efficiently, the person will induce a movement at the backmost position of pendulum motion because this will generate force at the natural frequency. This phenomenon is termed resonance and can of course be desirable as with the example of the swing. For systems where severe vibrations are undesirable, resonance can be detrimental. This is the case for a drillstring, where resonance of the system will create massive periodical forces on the string which in turn can severely damage the components of the string.

2.3 Damping

Damping is what removes energy from a system. In physics, springs and other systems meant to depict oscillatory motion are typically modelled as ideal systems, where an initial force exerted on the system will keep the energy in the system. This is what is modelled when a spring continuously stays in motion or a pendulum never stops oscillating. Real life experience shows that this is never the case. Damping is what removes energy from a system, causing the spring to eventually come to a standstill in the equilibrium position. In the case of vibrations in a drillstring, this is what prevents resonance energy from inevitably leading to structural failure. Without damping, energy would accumulate in the drillstring until the critical stress/strain limit is reached, causing irreversible damage of the string.

In the borehole, three types of damping are prevalent, namely viscous-, coulomb and hysteretic damping. Viscous damping occurs at the interface between steel and mud. It is generally described to be proportional to the relative velocity between the two ends of the damping device. This means that the dampening effect will increase if the relative movement of the object moving through the viscous fluid is increased. Coulomb friction is the dissipation of energy generated by the movement of materials past one another. The bit/rock interaction while drilling is often regarded as coulomb friction (Tang et al. 2016). Hysteretic damping is often referred to as structural damping. This damping is a result of the internal friction between atoms in a structure. As the atoms move when a force is applied to the structure, energy is lost through interaction with other atoms as the atoms move relative to each other.

2.4 Types of Vibration

Understanding of the different types of downhole vibrations is needed in order to be able to identify dangerous vibration patterns. The specialization project by Berntsen (2019) describes the different types of vibration in a short and concise manner and has been quoted in Section 2.

2.4.1 Free Vibrations

Free vibrations are the type of vibrations resulting from a non-periodic initial excitation from an external source. Once a drillstring is stuck in the well, the firing of a jar in the attempt to free the drillstring will leave the entire system vibrating "freely". Random or non-periodic collisions between the wellbore wall and drillstring are also examples of free vibrations because the external excitation source does not continuously supply energy to the system. The energy in the vibrations will thus in time dissipate through the damping of the system. Factors affecting the damping effect in the system are many, but often viewed as the most essential is the length of the drillstring. Free vibrations without damping are often visualized by an everlasting pendulum, where the initial amplitude of the excitation is sustained indefinitely as a result of damping not continuously taking energy out of the system.

2.4.2 Forced Vibrations

As opposed to the random or non-periodical excitations that characterizes free vibrations, forced vibrations are the term used to describe a system which is continuously excited by an external source of energy in a periodical manner. A drillstring with a mass imbalance is an example of this. The imbalance could for example be caused by a PDM. As the string rotates, it will be excited once per revolution. This in turn means that the excitation frequency is dependent on rotary speed. Rotating at certain RPMs may then cause large vibrations as a result of forced resonance. Accordingly, if the frequency differs from the drillstring`s natural frequency, the amplitude may decrease.

2.4.3 Self-excited Vibrations

Self-excited vibrations carry many similarities to forced vibrations. Whereas forced vibrations are independent of the vibrational response it produces in the system, self-excited vibrations are coupled directly with the response it produces. Self-excited vibrations are caused by a constant energy source as opposed to a periodic excitation mechanism for forced vibrations. Sound feedback from a microphone is an example of self-excited vibrations. Voice sound is amplified through an amplifier and then fed to the speakers. When the sound from the speakers then is coupled with the sound generated by the vocalist, the amplitude is increased for each cycle. Conversely for drilling this may occur as a result between friction between the wellbore wall and the drillstring. The string might stop rotating because there is sufficient friction. Due to the elastic properties of drill pipe, the top drive will still rotate and continuously feed energy into the string while the part of the string in contact with the wellbore wall is stationary and thus displaced from equilibrium. When the top drive has fed enough energy into the system to overcome the frictional disturbing force the string will rotate towards equilibrium. As a result of the elasticity of a drillstring, the string might rotate past its equilibrium position in an oscillatory manner. This over displacement means that the drillstring will require more storage of energy to overcome the friction in the next cycle, which in turn gives rise to further over displacement.

3 Vibrational Modes

Drillstring vibrations are complex due to the diversity of forces that the drillstring is subjected to downhole. Consequently, analysis of downhole vibrations is convoluted. The three primary modes of vibration are axial-, torsional- and lateral vibrations. These three are often superimposed on or even triggered by each other. There are some recognizable patterns within each mode which may help the engineer identify which type of vibration the drillstring is undergoing and thereafter act out appropriate measures. Knowledge of the three modes of vibration and the physical mechanism occurring downhole is therefore essential. This chapter describes the three modes of vibration and the main mechanisms within each. The theory of this chapter is mainly extracted from Berntsen (2019). The source should be studied for a more elaborate picture of the different vibration mechanisms.

3.1 Axial Vibrations

Vibrations along the axis of the drillstring are referred to as axial- or longitudinal vibrations. Together with torsional vibrations, this dynamic behavior of the drillstring has been apparent for many years. This is due to axial- and torsional vibrations` ability to physically manifest at surface (Aadnoy et al. 2009). In the axial case, the manifestation could be seen as the vertical periodical bouncing of surface equipment during drilling (Dareing 2012).
The axial loading on the drillstring is comprised of both a static- and a dynamic component. The static component has upper constrains on the maximum weight on bit that can be applied before the drillstring sustains buckling. The dynamic component originates primarily from bit/rock interactions. These make up the time varying weight on bit (WOB) fluctuations during drilling.

3.1.1 Bit Bounce

The most common form of axial vibrations is experienced when employing roller cone bits. The three lobed pattern induced in the formation when drilling with a tricone bit is particularly commonly encountered. An example of the generated pattern is illustrated by Figure 3.1.

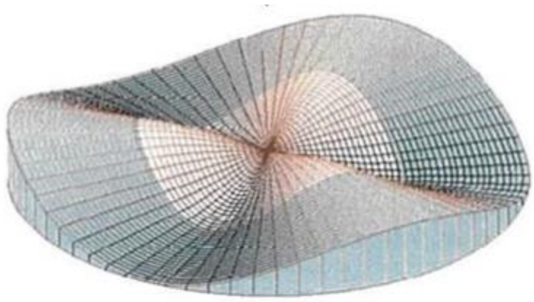

Figure 3.1: Three lobed pattern.

The pattern generated on bottom when drilling with a tricone bit (Aadnoy et al. 2009).

If bit bounce becomes severe, it will cause the drillstring to periodically lift off and disengage the formation. This leads to axial shocks as the bit again impacts the formation. The frequency at which these oscillations occur is typically three times the rotation speed, due to the cones on the bit rolling on the three lobed structure. The amplitude of the axial shocks will increase if the frequency is tuned the axial harmonic frequency of the drillstring, since this induces resonant behavior of the axial mode. An example of this is shown in Figure 3.2 , where the amplitude increases as rotation speed reaches 100 RPM. In the simulations carried out by Berntsen (2019), the first axial harmonic was found to be 108 RPM, which is why amplitude increases as the rotation speed approaches this RPM. The frequency at which the various axial harmonics of the drillstring is found is dependent on various properties of the drillstring, the most important being the length of drill pipes and drill collars and the damping in the drillstring. Drillstring properties for the simulation in Figure 3.2 can be found in APPENDIX A.

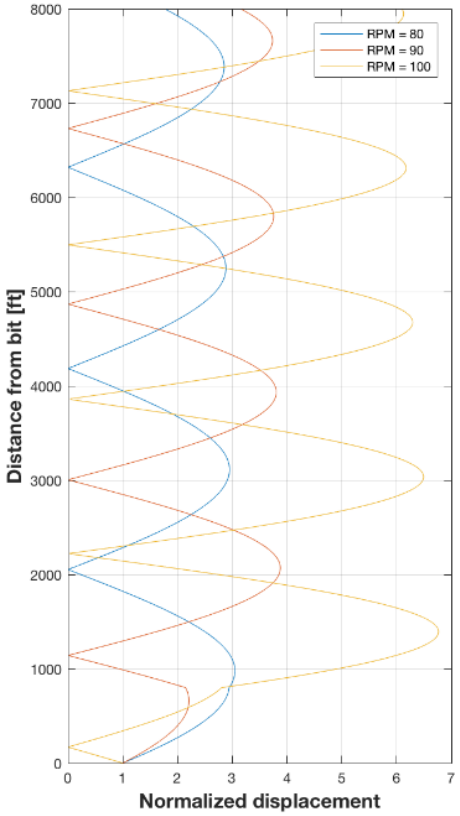

Figure 3.2: Axial displacement amplitudes along the drillstring for varying rotation speeds (Berntsen 2019)

3.2 Torsional Vibrations

Rotary systems are designed to maintain a constant rate of rotation. Dynamic sensors downhole show that this is rarely reflected by the bit and bottom hole assembly (BHA). This is due to the limitations of the drillstring as a transmission system due to the multitude of other demands that are asked of it. As the length of the drillstring increases, the string effectively becomes flexible in torsion (Gallagher et al. 1994). The drillstring is often modelled as a torsional string with a heavy mass at the end of it, representing the BHA. Resultingly, downhole torque usually fluctuates around the surface torque.

3.2.1 Stick-slip

Downhole incidents may cause the drill bit to come to a standstill. Tight hole, severe doglegs, keyseatings or significant drag are some examples that could impair rotation. Once the bit comes to standstill, more torque is needed to start rotation than to keep it moving. Several theories have been proposed as to what is the root cause of stick-slip vibrations. Initially it was hypothesized that the difference in torque input to overcome the static friction in the string was the cause of stick-slip (Kyllingstad and Halsey 1987). This difference between "static" and "dynamic" torque is comparable to that of static and dynamic friction for sliding objects. As drillstring rotation is initiated, energy is stored in the string until the static friction threshold in the system is exceeded. At this point, rotation is started and since the static friction threshold is higher than the dynamic friction threshold, the additional energy is stored as inertial energy in the BHA. The BHA may therefore rotate at speeds higher than the steady state rotation speed (Brett 1992). The torque reduction seen at the bit with higher rotary speeds has later been theorized to be the root cause of stick-slip (Brett 1992). Arguments have later been made that the inverse relationship between torque and rotary speed is a consequence- and not a root-cause of stick-slip (Richard et al. 2004). The latter mentioned theory, commonly referred to as the Richard-Germay-Detournay (RGD) model suggests that the coupling between axial- and torsional vibration of the bit is the primary cause of stick-slip vibrations. Despite differences in root cause analysis of stick-slip vibrations, it is collectively agreed upon by academia that stick-slip can be either bit-induced or friction(drillstring)-induced (Chen et al. 2020).

In the "slip" phase of stick-slip, the bit rotation speed will decrease until the bit eventually comes to a standstill or is even displaced beyond the neutral point. In the latter case, small periods of backward rotation may be seen. This is apparent in Figure 3.3, where field measurements of stick-slip show how the RPM reaches negative values before a new stick-phase is initiated. Eventually the bit comes to a standstill and a new cycle of stick-slip is initiated. Stick-slip is a self-excited vibration type as mentioned in Section 2.4.3, meaning that it is directly dependent on the vibration response it produces in the system. If the bit could be prevented from coming to a standstill, the stick-slip cycle would be interrupted, and steady-state rotation would be resumed. This is because the high torque demands from initiating rotation from standstill would be eliminated.

Polycrystalline diamond compact (PDC) bits are more prone to stick-slip vibrations than roller cone bits due to the former being more aggressive than the latter.

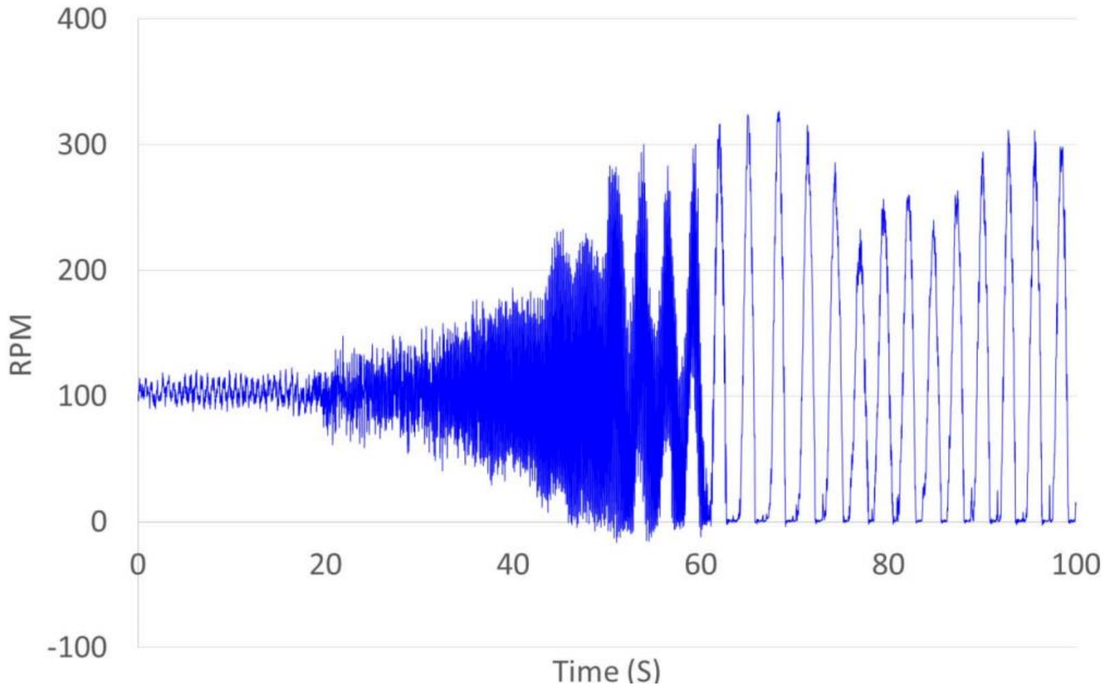

Figure 3.3: Stick-slip manifestation

Downhole measurements of RPM variation during drilling (Shen et al. 2017)

3.2.2 High Frequency Torsional Oscillations (HFTO)

High frequency torsional oscillations, also known as torsional resonance, is a torsional vibration phenomenon with a frequency much higher than that of stick-slip. Warren and Oster (1998) investigated rapid bit wear when drilling a segment of hard rock at Amoco`s test facility in Catoosa. By employing a dynamic drilling sensor (DDS) directly above the bit, dynamic data was sampled at high frequencies. The large sampling rate allow detection of downhole events which normal surface parameter measurements would be unable to detect.

Traditional stick-slip can be analyzed by modelling the entire drillstring as a torsional pendulum. In this case, the angular displacement increases monotonically from the top down towards the bit. This is shown in Figure 3.4.

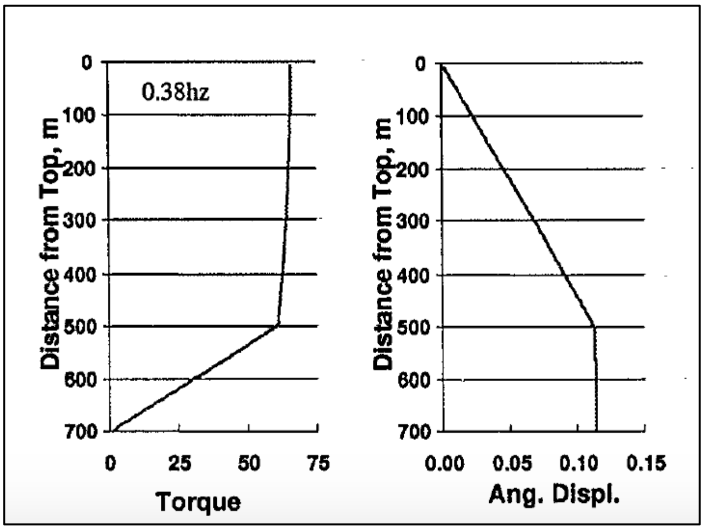

Figure 3.4 Angular displacement and torque profile along the drillstring during a stick-slip cycle of 0.38 hz (Warren and Oster 1998)

In the case of torsional resonance, the drill collars are vibrating at their natural frequencies which are much higher than that of the entire drillstring. The first harmonic for torsional resonance is shown in Figure 3.5. It is apparent that the angular displacement during torsional resonance is much less severe, but is varying along the drillstring. Since the drill pipe is less stiff than drill collar, the BHA is essentially free at the top. These boundary conditions mean that the collars may resonate as a prismatic bar suspended on bearings. Based on DDS vibration data, Warren and Oster (1998) found that the drill collar were also free at the bottom, meaning that the maximum torque is at the middle of the drill collar section. The torque seen at this point is noticeably higher than that seen at surface.

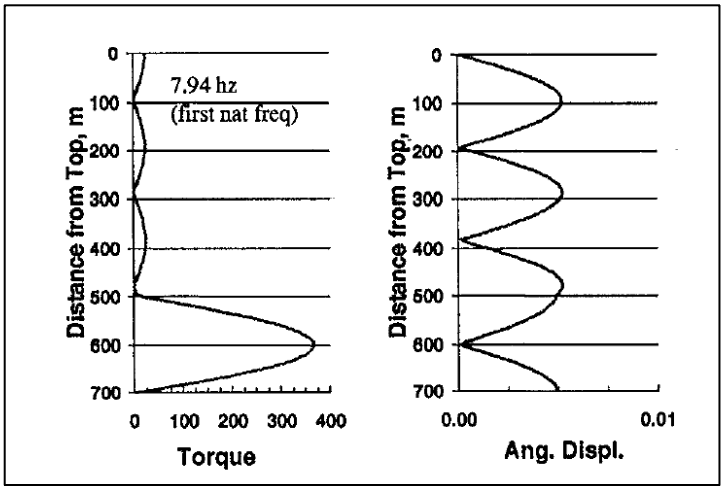

Figure 3.5: Angular displacement and torque profile along the drillstring during torsional resonance (Warren and Oster 1998)

With the more frequent use of dynamic sensors with high frequency sampling rates in the BHA, the occurrence of torsional resonance has been found to be quite common. Lines et al. (2013) found the drill collars to resonate at a frequency of 66 hz and at multiples of this harmonic, despite varying the surface RPM across a large range. The frequency spectrum is demonstrated in Figure 3.6. The authors found the collars to resonate at 66 hz while drilling many different sections of the well, with largely varying amplitude. This means that the severity of the vibrations at this resonant frequency may be highly dependent on the drilling conditions.

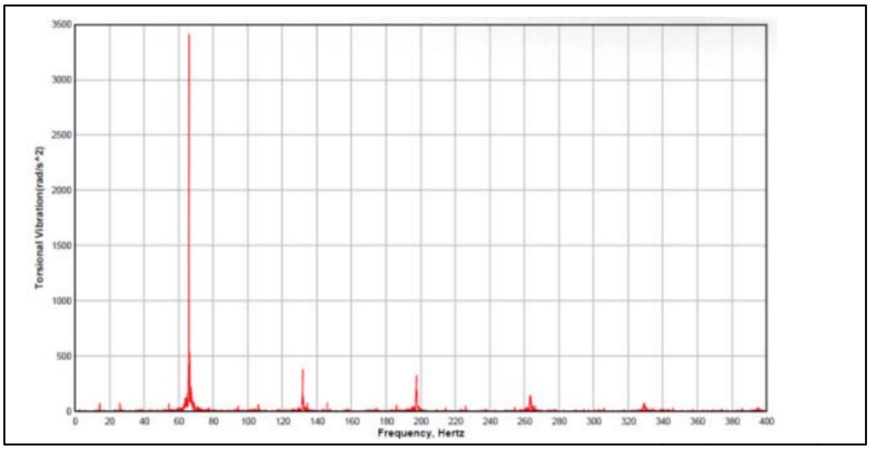

Figure 3.6: Frequency spectrum from a DDS recording (Lines et al. 2013)

At a frequency of 66 hz, the drillstring will undergo 1 million stress cycles in 4.2 hours, which depending on the amplitude of the vibrations mean that fatigue failure may occur very quickly.

3.3 Lateral Vibrations

Lateral vibrations, also referred to as bending-, flexural- or transverse vibrations are vibrations related to the transverse movement of the drillstring. Lack of downhole vibration data and the attenuation of lateral vibrational waves in the drillstring left the impact of lateral vibration unrecognized for extensive amounts of time (Aadnoy et al. 2009). The high frequency coupled with the dispersive characteristic of lateral vibrations are direct causes for the rapid attenuation of lateral vibrations. Paradoxically, this vibrational mode is widely recognized as the leading cause of drillstring and BHA failures (Vandiver et al.).torsional-lateral coupling in the case that the drillstring whips laterally during the slip phase

3.3.1 BHA Whirl

BHA whirl is the term used to describe the bending of drill collar caused by the centrifugal force from rotation. If the center of mass is slightly off the center of the borehole, the centrifugal force will act on the center of mass which in turn creates a curvature of the collar. The eccentricity in this case is the length between center of bit/stabilizer to the center of mass. The magnitude of the centrifugal force is proportional to the mass of the collar, the initial eccentricity and the rotational rate squared (Vandiver et al. 1989). Initial eccentricity may be due to bent drill collar or that the compressive loads resulting from weight on bit drill collar sag caused by gravity. The consequential eccentricity imposes a dynamic imbalance. The deflection between two nodal points of full gauge is demonstrated by

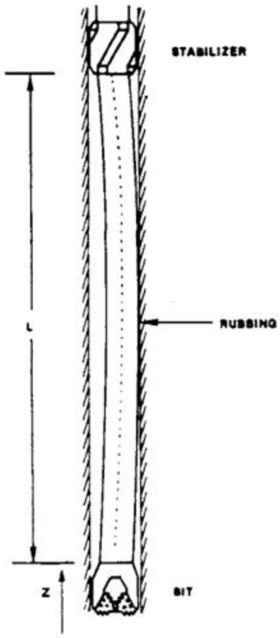

Figure 3.7: Bent drill collar

Deflection of drill collars between two points constrained by the wellbore (Vandiver et al. 1989).

Whirling occurs when the curvature of drill collars is sufficient to create contact between collar and borehole wall. The confinement of the borehole remediates the effect of collar collapse through bending and instead produces the effect of drill collar whirl.

Forward whirl is the term used to describe the drill collar whirling along the borehole wall in the same direction as the drillstring is being rotated. In forward whirl mode, the same point of collar is in contact with the borehole wall during the entire revolution around the borehole. This mode can often be recognized by abrasion on a point on the external wall of the drill collar. The drill collar is then typically flattened on one side (Vandiver et al. 1989). The slip effect between borehole wall and drill collar is what makes this possible. When the whirl rate is equal to the rotational rate of the string it is known as forward synchronous whirl.

Backward whirl occurs when slippage effect is sufficiently small, causing the pipe to roll on the borehole wall. In this mode of whirl, the pipe moves along the borehole wall in a direction opposite to that of drillstring rotation. Pure backward whirl is the term used to describe backward whirl when there is no slippage effect (Vandiver et al. 1989). The low slippage in backward whirl makes it impossible to have a single contact point of drill collar with the borehole wall and thus it can often not be detected by abrasion on the surface of drill collars unless the shocks between contact with the borehole wall are sufficient to cause deterioration of drill collars. High frequency stress cycles occurring at many times the rotational rate may lead to twist offs or connection fatigue failure.

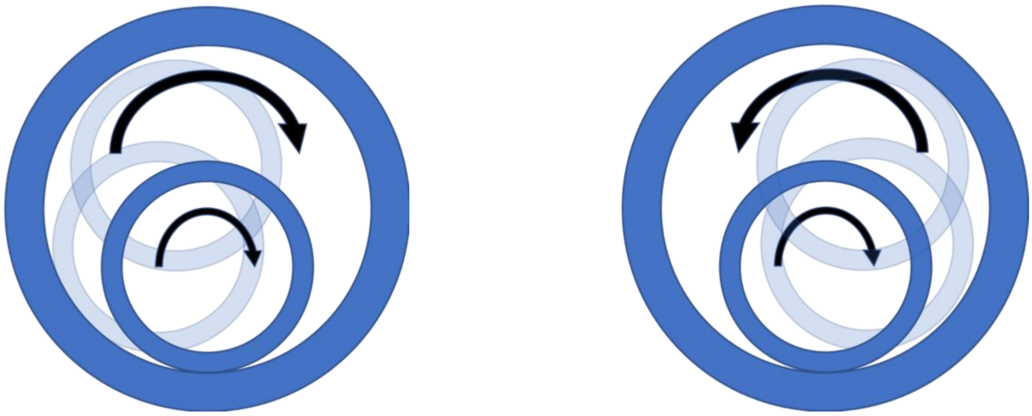

Figure 3.8 Whirl- and pipe rotation directions

Whirl direction indicated by the large arrows and pipe rotation is the conventional clockwise directions as indicated by the small arrows.

Left: Forward Whirl **Right:** Backward Whirl

Table 3.1 demonstrates the bending rate that is seen in the different regimes of whirl, which in turn are determined by the slippage effect between pipe and borehole wall. The table shows that the worst case is backward whirl with no slip, because the bending rate is at a frequency of five times the rotary speed. At this rate, the fatigue life of pipe and especially connections will be severely reduced. The rotary speed used for the calculations in the table is 120 RPM and the formulas for calculating rates and slip velocity are given by Vandiver et al. (1989).

Table 3.1: Whirl- and bending rates with 7” diameter drill collar in an 8 ¾” hole section
A negative rotary speed indicates conventional clockwise rotation. Whirl calculations derived by Vandiver et al. (1989).

Whirl type	Rotary speed $\frac{\omega}{2\pi}$ [Hz]	Whirl rate $\frac{\Omega}{2\pi}$ [Hz]	Bending rate $\frac{\Omega - \omega}{2\pi}$ [Hz]	Slip velocity $\lvert v \rvert$ [ft/s]
Forward synchronous $(F_s = -0.250)$	-2.0	-2.0	0.0	4.58
Forward with slip $(F_s = -0.125)$	-2.0	-1.0	1.0	4.12
Pure rotation $(F_s = 0)$	-2.0	0.0	2.0	3.67
Backward with slip $(F_s = 0.250)$	-2.0	2.0	4.0	2.75
Backward without slip $(F_s = 1.000)$	-2.0	8.0	10.0	0.00

3.3.2 Bit Whirl

Bit whirl is analogical to BHA whirl in that an initial eccentric force will push the bit`s instantaneous center of rotation outwards from the geometric center of the hole. Once the bit makes contact with the wellbore wall an additional friction force comes into play. If there is no slip between bit and formation, the instantaneous center of rotation will be at the point of contact. This is identical to a car tire, where the instantaneous center of rotation will be at the contact point between tire and road.

It is desirable to avoid bit whirl altogether as a detrimental aspect of the whirl type is that it is regenerative. Brett et al. (1989) showed early that both lab- and field measurements indicated the regenerative tendency once bit whirl has commenced. Two factors are primarily the reason why this occurs. The first is the centrifugal force which is highly in effect with whirl kinematics and is exaggerated at high rotary speeds. The centrifugal force in whirl pushes the bit off center, resulting in increased friction with the formation. The second factor is that the design of the bit teeth are designed for the center of rotation being at the geometric center of the well to minimize drilling force imbalance. Once this is violated, the cutters are no longer laid out for full coverage and thus the drilling force imbalance is increased. A whirling bit will drill an over gauged hole and this will continue to occur until the restoring force of the drill collars overcomes the regenerative forces of whirling (Brett et al. 1989). This creates ledges in the well as cyclical periods of over gauge drilling and true gauge drilling. This tendency makes caliper logs a great diagnostic tool for identifying whirling behavior, as these cycles of true- and over gauged drilling may be recognized.

3.4 Coupled Vibrations

Although analysis of the individual modes of vibration serve an essential purpose in identifying the physical mechanisms, the vibrational patterns seen in real cases are often more complex. This is due to the various forces downhole, but also due to the individual vibrational modes` ability to trigger vibrations of a different mode. An example of this is the sudden and erratic movement of the drillstring in lateral direction during the slip phase when experiencing severe stick-slip while drilling. The most commonly encountered coupling mechanisms were elaborately described in the specialization project by Berntsen (2019) and are reused in the upcoming sections.

3.4.1 Coupling Between Axial and Torsional Vibrations

Drillstrings reaching a certain length will always be flexible in torsion. This means that the pipe will not rotate as a rigid object. During stick-slip, the BHA often varies between being under- and over displaced in rotation.

The shear strain is the rotation and the shear stress is the twisting stress in the string. Solid rods subjected to torsional stress will suffer an axial shortening (2013). Axial shortening due to twisting is shown in Figure 3.9. The red line shows the length of one “fiber” along the circular tube. The length of the fibre is constant, but when twisted it`s shape is changed to a helix. This helix can be described by the coordinates:

$$\vec{r}(\theta) = [R\cos\theta \quad R\sin\theta \quad h_p\theta] \tag{3.1}$$

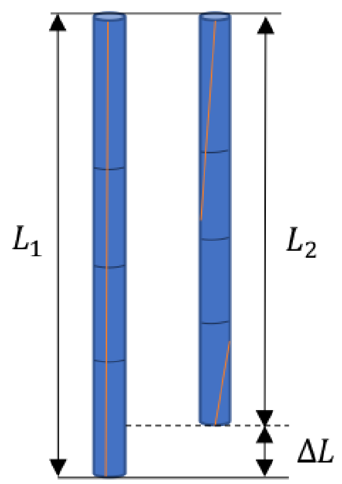

Figure 3.9: Shortening of a circular tube as a result of twisting, the red line indicates a fibre along the tube

Where θ denotes the angle at different points along the helix. The total twist is denoted by Θ. h_p is the pitch of the helix and is calculated by $\mathrm{h_p} = \frac{L}{\Theta}$. This means that the pitch of the helix decreases with increasing twist. From Hooke`s law in shear, assuming constant torque, stiffness and cross-sectional area, the total twist is equal to

$$\Theta = \frac{TL_0}{GI_p} \tag{3.2}$$

The length of the fibre shown in red in Figure 3.9 is constant and for the helix, this can be found by taking the integral of each incremental length from the top to the point of total twist in the bottom:

$$L_0 = \int ds = \int |d\vec{r}| = \int_0^{\Theta} \sqrt{R^2 + h_p^2}$$

$$L_o = \Theta\sqrt{R^2 + h_p^2}$$

Using the relation for the pitch of the helix, $h_p = \frac{L}{\Theta}$, and solving for the length, L, of the circular tube:

$$L_2 = \sqrt{L_0 - R^2\Theta^2} \tag{3.3}$$

A numerical example using a BHA length of 550 ft can be calculated. Assuming that during stick-slip, the BHA is displaced 2 revolutions from the top of drill collars down to the bit, the shortening of the BHA would be equal to:

$$L_2 = \sqrt{550^2 - \left(\frac{7}{2 \times 12}\right)^2 (4\pi)^2} \approx 549.988\ ft$$

Which is approximately equal to 0.15 inches. Assuming a stick-slip frequency of approximately 0.5 Hz, this means that every two seconds, the BHA will slam into the formation with the momentum generated by the weight in the shortening distance. The shortening distance would be even longer if drill pipe had also been considered, due to drill pipe being even more elastic than drill collar.

3.4.2 Coupling Between Axial and Lateral Vibrations

Lateral vibrations may manifest as deflections of the drillstring. How the deflected drillstring relates to the shortening of axial length can be demonstrated by assuming that the entire drillstring assumes a wavy shape. Nodal points and attenuation of lateral waves would counteract this behavior, but the extreme case considering that the lateral deflections will manifest in the entire drillstring can demonstrate the relationship between lateral- and axial vibrational mechanisms. The numerical example in this section is taken from (Larsen 2014).

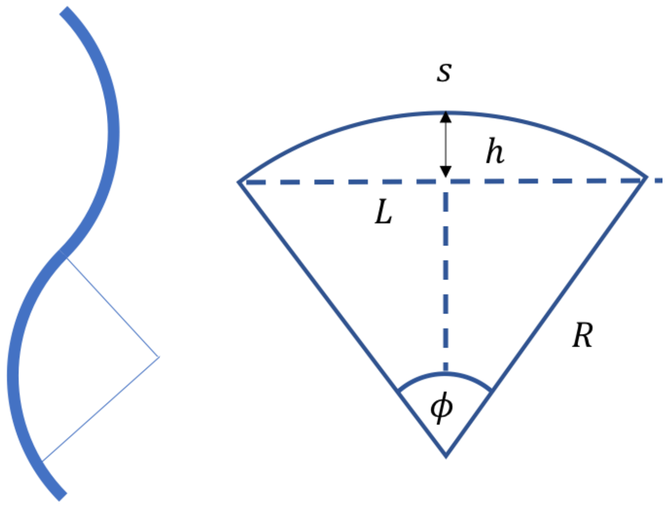

Figure 3.10: A sketch of the deflected shape taken by an unstabilized drillstring subjected to lateral vibrations

When the string gets deflected, the previous straight longitudinal segment s, will become an arc. The new longitudinal length that the arc s spans is denoted L. The arclength s is the product of the radius of curvature R and the angle that the arc spans, ϕ:

$$s = R\phi$$

The string will be shortened by a length ΔL,

$$\Delta L = s - L = R\left(\phi - 2\sin\frac{\phi}{2}\right) \tag{3.4}$$

The lateral displacement h can be determined by

$$h = R\left(1 - \cos\frac{\phi}{2}\right) \quad (3.5)$$

Solving for R and substituting into equation 3.4 yields

$$\Delta L = h\frac{\phi - 2\sin\frac{\phi}{2}}{1 - \cos\frac{\phi}{2}} \quad (3.6)$$

Using the relation between arc length and angle combined with equation 3.5, the angle of deflection may be determined:

$$\phi = \left(1 - \cos\frac{\phi}{2}\right)\frac{s}{h} \quad (3.7)$$

The angle may thus be determined by trial and error until the terms on each side are equal. S and h can be determined by assuming that the deflection of the drillstring is constrained by the size of the wellbore and the size of pipe in the section viewed.

The shortening of the drillstring per cycle can thus be determined. When drilling a 12 ¼“ with 8” drill collars, the lateral displacement $h = 0.1$m. By assuming $s = 10$m, $\phi = 0.08$. Substituting this into the equations derived above, the shortening of the string is found to be $\Delta L = 0.003$m per wave.

3.4.3 Parametric Resonance

Bit/rock interaction is the primary cause of WOB fluctuations. The loss of mechanical stability due to lateral vibrations have been studied to determine under what conditions the axial vibrations (induced by WOB fluctuations) may trigger amplitude increasing lateral vibrations (Dunayevsky et al. 1993). The fundamental theory behind this phenomenon is that the energy associated with axial vibrations may be diverted to lateral vibrations. An example used by Dunayevsky et al. (1993) is depicted in Figure 3.11. Here the frequency of WOB fluctuations are set to twice the natural frequency for lateral vibration.

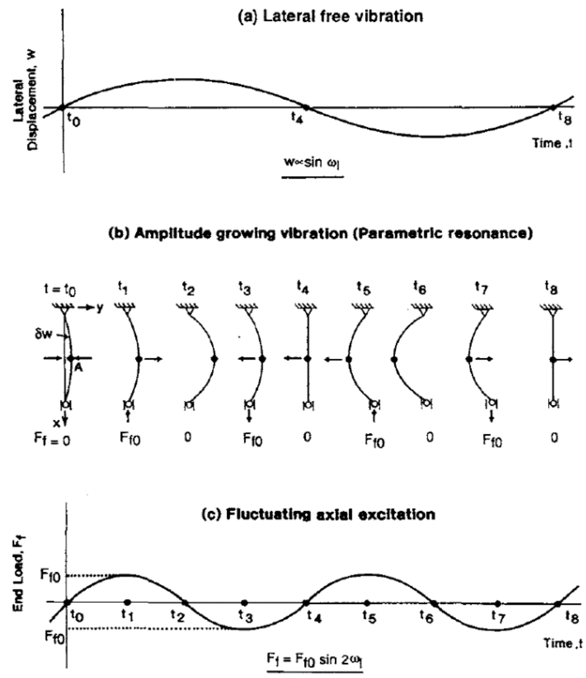

Figure 3.11: a) Lateral free vibration of a drillstring, (b) amplitude-growing vibration (parametric resonnance) and (c) Fluctuating axial excitation

Figure 3.11 (b) demonstrates the lateral deflection of the drillstring. An initial deflection δw which may be insignificantly small is the initial position of the string. Axial force reaches maximum at time t_1 and continues to decrease until maximum lateral deflection is reached at t_2.At this point in time, the axial load changes sign, prompting the deflection to decrease. After the axial force has completed on cycle, the lateral deflection reaches neutral position. An amount of energy δU has been pumped into the lateral vibration mode, manifested as excess kinetic energy (Dunayevsky et al. 1993). This energy increases the amplitude of lateral displacement in the next semi cycle of lateral deflection. The result is infinitely increasing lateral motion amplitude each axial load cycle, which is called parametric resonance. Parametric resonance differs from conventional resonance generally used in drillstring-dynamics models. Instead of the critical frequency spectrum being made up of a discrete set of natural drillstring frequencies as with conventional resonance, the spectrum is a set of bands. These bands depend on WOB fluctuation amplitudes and it is shown that as WOB reaches 0, the bandwidths shrink to zero (Dunayevsky et al. 1993).

3.4.4 Coupled Stick-Slip

Field measurements have revealed bit whirl and BHA whirl to often be closely related. Mechanical specific energy (MSE) measures how much energy is consumed by drilling a unit volume of rock. This definition is adequate for this section, however MSE if further described in Section 6.2. When whirl is apparent, increasing the WOB typically reduces the MSE. This is because increasing the WOB tends to reduce whirling tendencies. This means that less energy is lost to friction and sidecutting. MSE measurements across global operations have revealed that 40% of footage is affected by detectable levels of whirl (Sowers et al. 2009).

Stabilizers and other full gauge components in the BHA function as nodal points, meaning that they are constrained to no lateral movement in the borehole. Side forces are thus concentrated in these points. The strength of the side forces is increased when undergoing large amplitude lateral vibrations. This can often be seen on the blades of the stabilizers as rounded shoulders due to these side forces.

Bit whirl and BHA whirl are related due to bit whirl creating an overgauged hole. This means that the previously mentioned nodal points in the BHA, such as stabilizers, now have room to move laterally. This amplifies the severity of BHA whirl as the BHA now has room to accelerate laterally in. The result is large lateral shocks and side forces on stabilizers and other full gauge equipment. These large side forces lead to increased friction with the borehole, which in turn induces large amplitude torque fluctuations.

4 Mechanisms

An important step towards negating drillstring vibrations is analyzing the root causes leading to vibrations. This chapter views how different aspects of drilling affects the dynamic behavior of the drillstring. The complexity of components in the drillstring combined with the heterogeneity of the subsurface makes it difficult to completely eradicate the sources initiating vibrations. Despite this, understanding the physical effect of different features in the wellbore and drillstring is essential if the engineer endeavors to minimize costs related to harmful vibrations. It is recommended to study this chapter concurrently with Chapter 7, since the latter mentioned chapter describes mitigating measures to many of the root causes and physical relationships described by this chapter.

4.1 Formation

Since many of the sources initiating vibrations are rooted in bit/rock or drillstring/wellbore interaction, the type of formation being drilled is important. In drilling, there is a general tendency for harder rocks to cause more problems. This tendency is also the case for drilling vibrations, as vibrations generally increase with formation strength (Greenwood 2016). A given rock`s hardness is determined by its cementation material, meanwhile the abrasiveness of the rock is determined by particle size and mineral composition. Soft sands and clays with interbedded limestone stringers mean abrupt changes in formation strength. This may be a source of vibrations, especially in cases where these interbedded formations are drilled at a high angle. Drilling through layers with differential hardness at a high angle means that the forces seen across the bit face will fluctuate, giving rise to instable reactive torque.

Hard rock drilling provides several challenges, however drilling soft- or unconsolidated formations may also lead to high levels of vibration. Soft formations are susceptible to washouts which creates overgauged sections of the wellbore.

4.2 Hole size and Hole Angle

Drillstring vibrations are apparent both in vertical and horizontal wells. The different modes of vibrations are however dependent on the hole angle as it affects the inclination- and stability of the drillstring and the orientation of the BHA. The drillstring will be prone to whirl and bit bounce mainly in vertical or near vertical sections. This is due to several factors, with the most important being less contact with the borehole wall. In highly inclined wells, gravity tends to reduce lateral motion of the drillstring (Greenwood 2016). The drillstring is mostly in continuous contact with the wellbore wall along the low side of the well. A hole angle above 15° will reduce the tendency for buckling of the drillstring due to the normal forces that must be overcome once the drillstring is in contact with the wellbore wall. The increased friction resulting from this in wells with high inclination increases the probability of stick-slip vibrations occurring. The increased frictional torque generated along the length of the wellbore reduces the torsional energy reaching the bit. This increases the chance of the system having to build up torque in order to overcome the frictional energy threshold in the system. An additional source of frictional torque is the tortuosity of the wellbore. Smoother wellbores generate less torque, thus small doglegs and high dogleg severity should be avoided.

Drillstring dynamics in relation to hole size is mainly dependent on the outer diameter of the BHA in relation to the wellbore size. This relation determines how much the BHA can deflect laterally before it is constrained by the wellbore. Statistically, large axial- and lateral vibrations can be seen to be related to the larger hole sections, however the relation is essentially rooted from the inclination of these sections moreover than the size of the section itself. An example is bit bounce being more likely to occur in vertical top hole sections due to the nature of roller cone bits mainly being used in these sections combined with the susceptibility of the drillstring to vibrate axially in vertical sections. The borehole size is however related to vibrations when an overgauged- or undergauged hole is drilled. When an overgauged hole is drilled, the BHA will no longer be confined by the wellbore walls. This leads to reduced stabilization and may result in whirling or lateral shocks. An undergauged section will generate increased torque which may lead to stick-slip vibrations.

4.3 Hydraulics

The drilling fluid and cuttings suspended in the fluid affects vibrations in several ways. The viscous damping effect of the fluid directly affects the dynamic movement of the drillstring. The no-slip effect at the contact point between pipe and fluid means that the pipe moves together with this inner-most fluid layer. At the pipe wall, there is then a shear stress when the pipe is moving relative to the fluid. Shear stress along the pipe wall can be integrated to yield an axial force and a torque. The resulting torque and forces are directly proportional to the viscosity of the fluid and the relative movement between the fluid and the pipe. Essentially, sudden movements of the string increase the viscous damping effect. Increasing the viscosity in the drilling fluid will also increase the viscous damping effect.

Mud lubricity directly affects the mechanical friction in the system. Livescu et al. (2014) stated that field measurements indicated a reduction in the coefficient of friction (CoF) of 25% using lubricants. In long reach wells, this could have huge potential in reducing stick-slip tendencies when rotation is initiated and the mechanical static friction in the system must be overcome.

Cayeux et al. (2020) demonstrated that swab and surge will also affect torsional oscillations. The hydraulic pressure in the drilling fluid applies on the surfaces of tubulars. In hydrostatic conditions this is simply the buoyancy force. When there is relative movement in the system due to either pumping or axial movement of the drillstring, there are frictional pressure losses. It can be shown that the partial differential equation that describes the drillstring motion is affected differently depending on whether the system undergoes swabbing or surging (Cayeux et al. 2020). In the case of swabbing, the axial mechanical friction increases and correspondingly the mechanical friction torque is reduced. The result is a positive damping effect on torsional oscillations. When lowering the drillstring, surging pressures are generated and a decrease in the axial mechanical friction brings with a corresponding decrease in the mechanical friction torque. This creates a negative damping effect, amplifying torsional oscillation. Figure 4.1 demonstrates both swab- and surge effects, as well as free rotation.

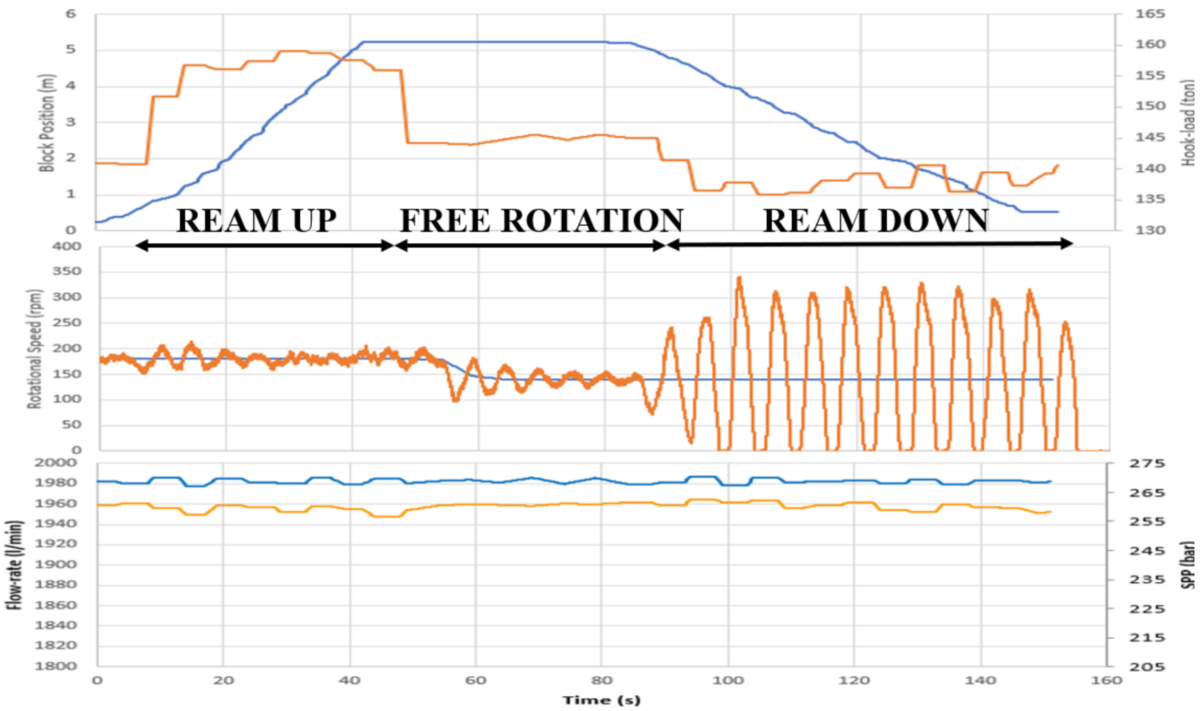

Figure 4.1: Swab- and Surge influencing torsional oscillations

Field measurements from Eldfisk and Ekofisk confirm that during ream up (swabbing), torsional oscillations are damped due to reduced mechanical torque. The opposite occurs during ream down (surging) as mechanical torque is increased and stick-slip is triggered (Cayeux 2019).

The drilling fluid also indirectly affects the frictional torque in the system through hole cleaning. Cuttings may accumulate in deviated wellbores and get caught between tool joints and wellbore wall. An increase of cutting particles passing between borehole and tool-joint results in an increase in grinding torque (Cayeux et al. 2020). As the torque increases, the resulting rotational speed must decrease. A reduction in the rotation speed further reduces the cutting particles that are suspended in the drilling fluid, again leading to a higher grinding torque. This may lead to stick-slip due to the negative damping this creates. This effect is demonstrated through simulation in Figure 4.2, where simulating lower flow rate during cutting transportation leads to stick-slip.

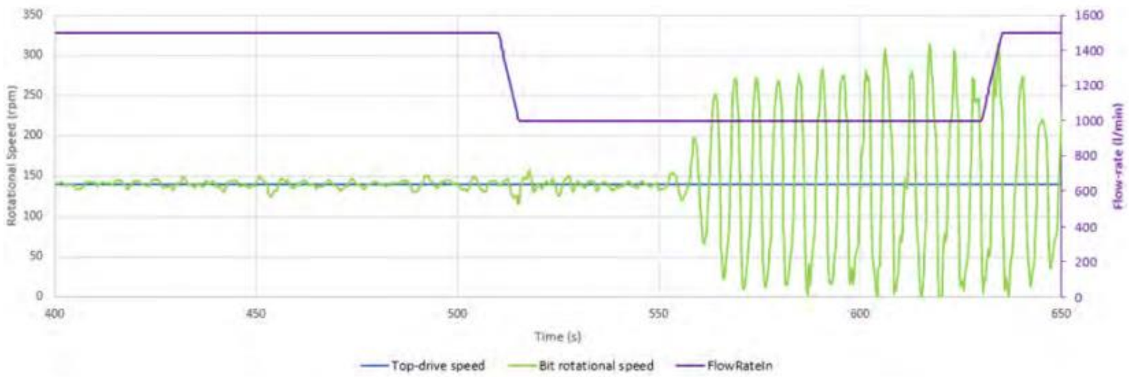

Figure 4.2: Stick-slip resulting from reduced cuttings transport

As flow rate is reduced while transporting cuttings, the amount of cuttings trapped between tool joints and wellbore wall increases, further increasing grinding torque. The end result is initiation of stick-slip (Cayeux et al. 2020)

4.4 Drill Pipe

Much focus has been put into designing the bottom hole assembly least susceptible to suffer severe vibrations while drilling. Drill pipe usually makes up more than 95% of the drillstring, however much less effort has historically been concentrated on optimizing drill pipe to negate vibrations as compared to the BHA. The logic behind this is clearly that the BHA has a larger OD than drill pipe and resultingly is the part of the drillstring in contact with the formation. Drill pipe will have a few contact points in build/drop sections or doglegs.

The design factors for drill pipe with respect to vibrations are the inertia and torsional stiffness of the pipe. The formula for torsional deflection between top drive and BHA of a circular shaft of homogeneous material is given by equation 4.8.

$$\theta = \frac{TL}{GI_p} \tag{4.8}$$

θ is the torsional deflection between the top drive and BHA, T is the resultant torque acting at the cross section, L is the length of the pipe, G is the transverse elastic modulus of the pipe and J is the polar moment of inertia of the cross-sectional area. For a pipe, the polar moment of inertia is equal to:

$$J = \frac{\pi}{2}(r_o^4 - r_i^4) \tag{9}$$

r_o and r_i denote the outer- and inner radius of the shaft, respectively. With the radius impacting the polar moment of inertia as a function raised to the fourth power, increasing the outer diameter of the pipe while keeping the thickness constant will increase its polar moment of inertia. This is demonstrated in Figure 4.3, where an increase in drill pipe diameter from the conventional 5.5 inch to 5.875 inch is calculated. Keeping the torque constant, this would lead to a 19% reduction in torsional deflection when using the same material for both drill pipe sizes (Davis et al. 2012). Resultingly, the torsional elasticity is reduced, meaning that the rotational movement between the top- and bottom of the drill pipe would be more synchronized

5-1/2 inch drill pipe | **5-7/8 inch drill pipe**

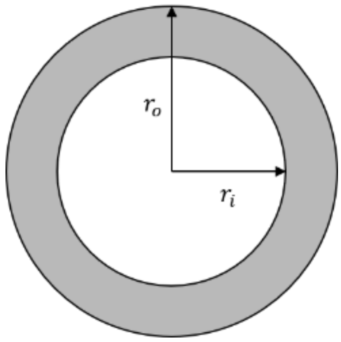

$$J = \frac{\pi}{2}\left[\left(\frac{5.500}{2}\right)^4 - \left(\frac{4.778}{2}\right)^4\right]$$
$$J = 38.699 \text{ in}^4$$

$$J = \frac{\pi}{2}\left[\left(\frac{5.875}{2}\right)^4 - \left(\frac{5.153}{2}\right)^4\right]$$
$$J = 47.737 \text{ in}^4$$

Figure 4.3: Polar moment of inertia of drill pipe

4.5 Mass Imbalance

When an object`s center of gravity does not coincide with its axis of rotation, the object is imbalanced. As mentioned in Section 0, the distance between these two points is the eccentricity and is shown in . Once an eccentricity exists, the centrifugal force comes into play, pushing the rotating object further away from the geometric center. For drill collar, this can be seen as a curve between two nodal points (e.g. stabilizers). This imbalanced drill collar system will have its own natural frequency and if rotation corresponds with the natural frequency of the system, resonance might cause the eccentricity to extend to the wellbore wall. This means that the BHA can make contact with the wellbore wall, leading to high amplitude lateral shocks which may damage the BHA components.

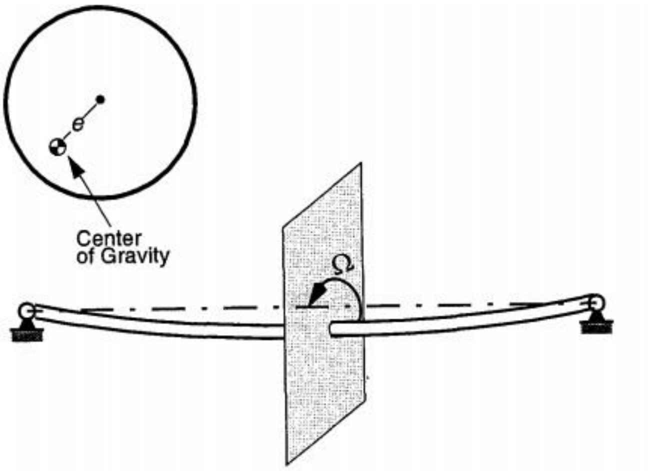

Figure 4.4: Bending of pipe between two nodal points

The distance between the center of gravity and the axis of rotation is the eccentricity (Dykstra et al. 1994).

The imbalance in a drillstring stems from multiple sources. Among them are the imbalance in tools, manufacturing imperfections, wear during service and flawed alignment of connections or tool joints (Dykstra et al. 1994). This makes it impossible to assemble a fully balanced drillstring. The lateral displacement of collar-/sub-assemblies can be visualized by rotating the assemblies at surface with a top drive. Tests conducted doing this by Dykstra et al. (1994) revealed that the eccentricity is especially apparent at the natural frequencies of imbalanced assemblies, as can be seen in Figure 4.5. The deflection increases with rotary speed until the system reaches its first mode of resonance.

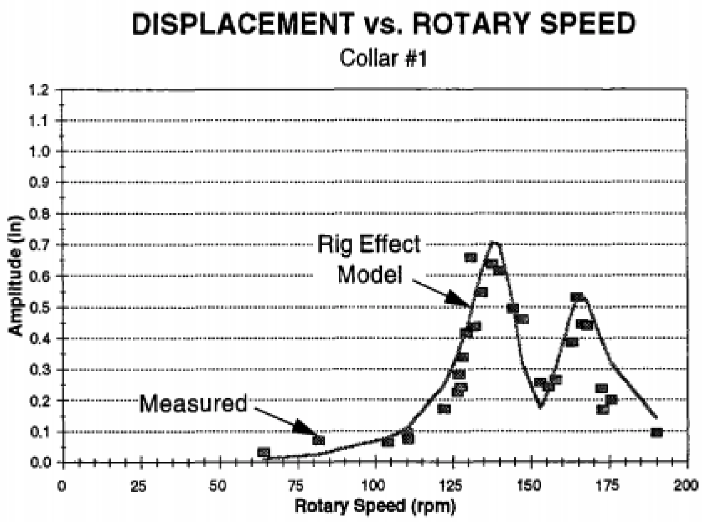

Figure 4.5: Lateral displacement vs rotary speed

The amplitude of lateral deflection of drill collar assemblies rotated at surface (Dykstra et al. 1994).

4.6 Bit Selection

The bit is a very small cost when seen in comparison with total well cost. Often the bit cost makes up less than 1% of total well cost, despite being closely related to more than 75% of the total well cost. This is because the bit is an integral component in determining ROP and number of bit trips. The selection of bit may be directly related to the type of vibrations experienced during drilling.

Roller cone bits induce compression failures of the rock, meaning that most of the formation removal is made with a crushing mechanism. Equivalently to a fixed cutter bit e.g. a PDC bit, the depth of formation penetrated is related to the WOB and the removal of the formation is dependent on the rotary speed. However, PDC bits induce shear stress failures in the formation by a cutting action. The different rock breakage processes generate different torque characteristics as can be seen in Figure 4.6. The large reactive torque experienced by PDC bits at a given weight on bit makes this bit type more susceptible to stick-slip vibrations.

For PDC bits, increased weight on bit at a given rotary speed means more cutter exposure per revolution and resultingly increased reactive torque. Large amplitude torsional vibrations are also experienced in transient periods of drilling like for example while increasing the rotary speed or the applied weight on bit (Langeveld 1992).

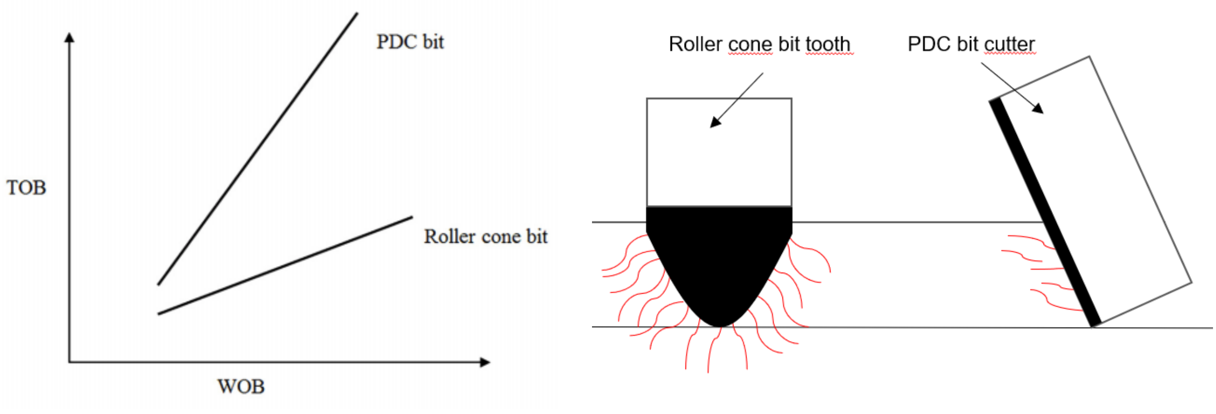

Figure 4.6: PDC vs roller cone bit

a) Sketch of torque characteristics for a PDC and roller cone bit b) Rock breakage processes for a PDC- and roller cone cutter (Niu et al. 2019).

The commonly used tricone roller cone bit is more prone to axial vibrations than its PDC counterpart, due to the three-lobed pattern generation it induces in the formation. Severe axial vibrations are less common for PDC bits, however severe stick-slip may couple with axial shortening of the drillstring as described in Section 3.4.1.

The lack of sidecutters on roller cone bits reduces the tendency for these bits to experience severe bit whirl. It is important to underline that BHA whirl may occur regardless of bit type. Since bit whirl is a phenomenon which causes the bit to roll around on the borehole wall, much focus has been put into balancing the forces of the cutters in order to ensure that the bit`s center of rotation is at the center of the bit. Warren et al. (1990) demonstrated that this condition is extremely hard to maintain under normal drilling conditions. Once the bit is slightly perturbed so that the bit deviates slightly from the geometric center of the wellbore, the instantaneous center of rotation will be displaced from the center of the bit by a relatively large distance, as shown by Figure 4.7. Once the instantaneous center of rotation strays away from the center of the bit, the system becomes prone to whirl. As described in Section 3.3.2, once whirl begins, it is very difficult to stop since the centrifugal force pushing the bit outwards increases as the system is displaced from center.

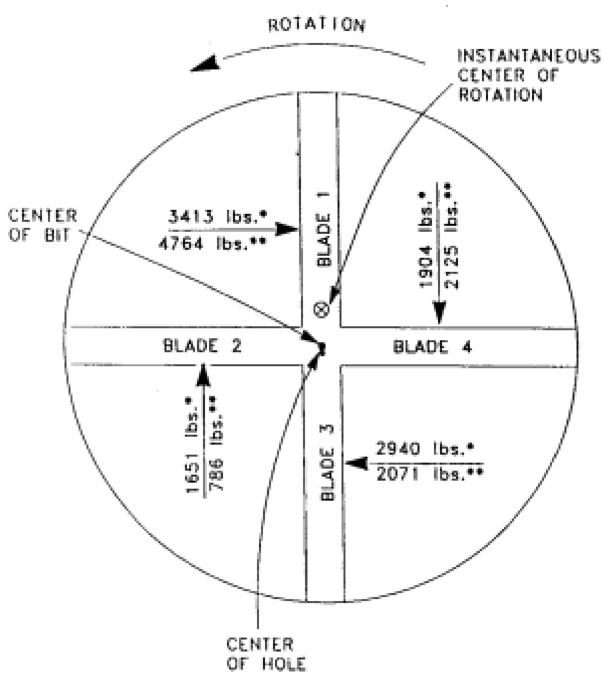

Figure 4.7: Instantaneous center of rotation for a PDC bit which is arbitraliy displaced by 0.050 in (Warren et al. 1990)

4.7 Stabilizers

Early studies in the mechanics of drilling non-vertical wells were based on the assumption that it was possible to drill perfectly vertical holes. It has later been revealed that drilling perfectly vertical holes even in homogeneous formations is impossible (Lubinski and Woods 1955). This has given rise to much research in stabilizers as a tool to control hole inclination and steering as stabilizers are expected to center the BHA in the well. Progress in steering technology has eliminated the need for stabilizers to be used as a tool for steering. Despite this, the expectation for stabilizers to center the BHA in the well has introduced other benefits, among them the prevention of vibrations. This is achieved by reducing the contact area between BHA and wellbore, as well as reducing the sag of pipe between stabilizers. Stabilizer design is a term referring to both the technical aspects of the individual stabilizer as the optimal placement in the BHA. In addition to this, stabilizers are also used to ream out of doglegs and key seatings, however this aspect of stabilizers is not addressed in this thesis. The following subsection addresses the effect of continuous contact between stabilizer blade and wellbore, APPENDIX B.1 can be studied to view the effect of the taper angle of a stabilizer on sliding friction.

4.7.1 Wrap Angle

The wrap angle of the stabilizers is defined as the coverage of all blades. This means that straight stabilizer blades will also have a certain wrap angle depending on the thickness and quantity of blades, as seen in Figure 4.8.

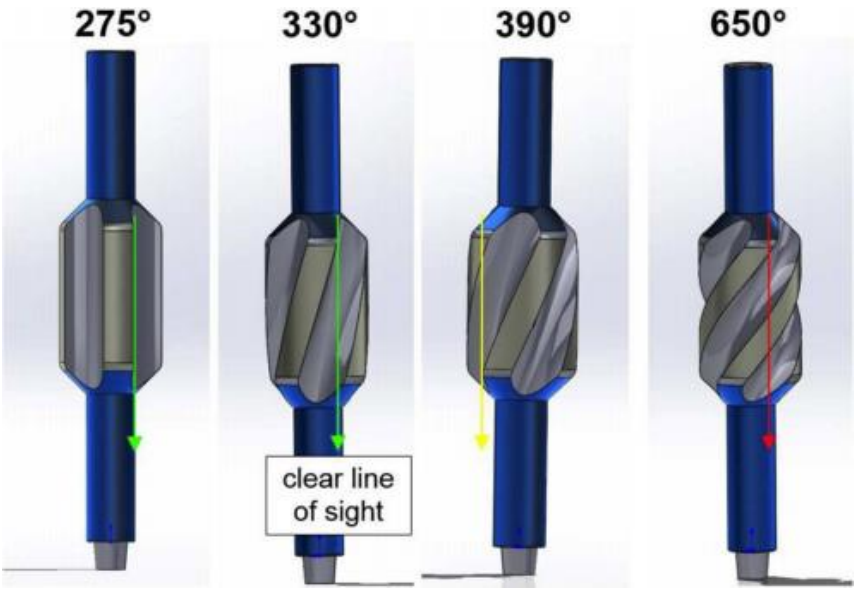

Figure 4.8: 3D cad images of stabilizers with varying wrap angles (Pastusek 2018)

The purpose of increasing the wrap angle of stabilizers is that it provides more continuity of contact with the wellbore wall, which in turn reduces the tendency for the BHA to whirl (Pastusek 2018). Increasing the wrap angle reduces the ease of flow of cuttings through the junk slots, thus one operator`s best practice is to maintain a clear line of sight. This means that the uppermost point of one stabilizer blade does not overlap the lowermost point of the next blade. In low angle holes this may not be desirable as holes with low inclination may tend to whirl. Low angle holes do not form a cuttings bed, meaning that whirl tendencies can be reduced by increasing wrap angle while simultaneously not compromising the hole cleaning ability of the system.

5 Consequences

Bit and BHA damage due to downhole dynamics leads to lost productivity and increased drilling costs. Schlumberger reported in 2012 that failures resulting from shocks and vibration generated hundreds of millions of dollars in loss, constituting more than one quarter of the total losses that year (Bowler et al. 2014). For an offshore operator, drilling operations incur extremely expensive rig rental costs in addition to equipment and crew necessary to carry out the operation. The objective of this chapter is twofold. Firstly, it is essential to shed light on the broad range of repercussions associated with vibrations. Secondly, post-run analysis of the drillstring or wellbore can aid in identifying the origin of the downhole dynamic behavior of the drillstring.

5.1 Wellbore Instability

In the drilling industry, high quality wellbores may be defined to have minimal occurrences of tight hole, hole enlargements or several small doglegs. The wellbore quality may be crucial for the reservoir performance of the well. This is especially pronounced in wells where fracturing is planned, since the wellbore quality will be directly affecting the completion design. Packers require a certain wellbore quality in order to be pressure sealing.

Wellbore instabilities can also be detrimental to the drilling process. Pack offs, time consumed reaming and tripping, sidetracks, mud losses, poor cementing jobs, inability to reach desired depths with casing, stuck pipe and washouts are all problems related to wellbore quality. Mechanically failing the rock leads to the creation of enlarged hole size, reducing the hole cleaning capabilities off the well due to reduced annular velocity. Large amounts of micro doglegs and variations in hole size will also increase the friction in the system, potentially reducing the reach of the well.

Santos et al. (1999) stated that mechanical rock failure will occur once the stress exceeds the rock strength. This assumes singular impacts with the rock. Vibrations occur at various frequencies however, and as shown in Section 3.3, lateral vibrations in the form of whirl easily occurs at rates over ten times per second. Depending on the amplitude of these lateral impacts, the rock will fail due to fatigue at stresses below the strength of the rock. Khaled and Shokir (2017) calculated the number of cycles necessary to cause fatigue failure of formation at different fractions of the rock strength, e.g. 10^4 cycles to cause fatigue failure at 70% of ultimate rock strength. The calculated fatigue forces could be transformed into fatigue accelerations using Newton`s second law in order to directly compare the measurements made by accelerometers in the drillstring. Depending on the amplitude of the accelerations, whirl may cause fatigue failures in the formation in everything from seconds to minutes.

5.2 Rate of Penetration Reduction

For an operator, maximizing ROP means minimizing cost, since time spent drilling is time spent not producing in addition to expenses related to rig rental and drilling equipment. A common misconception in drilling is that high ROP comes at the expense of wellbore quality. In Section 6.2 mechanical specific energy (MSE) is defined. In simple terms, MSE is a measure indicating how much energy input is required to remove a unit volume of rock. By increasing WOB or RPM, one increases the amount of energy put into the system. Conversely, an increase in ROP should be expected. When ROP does not increase after input energy has been increased, it means that energy is dissipated somewhere in the system. Vibrations and drillstring/wellbore interaction are examples through which energy can be lost. Figure 5.1 demonstrates how increased WOB and RPM results in a reduction of ROP. The caliper logs show that the intervals where this occurred coincides with wellbore enlargements. The reflected increase in wellbore size combined with the reduced ROP points to vibrations and eventual interaction with the wellbore wall being the most likely mean through which the lost energy has been transferred (AlBahrani and Al-Yami 2018),

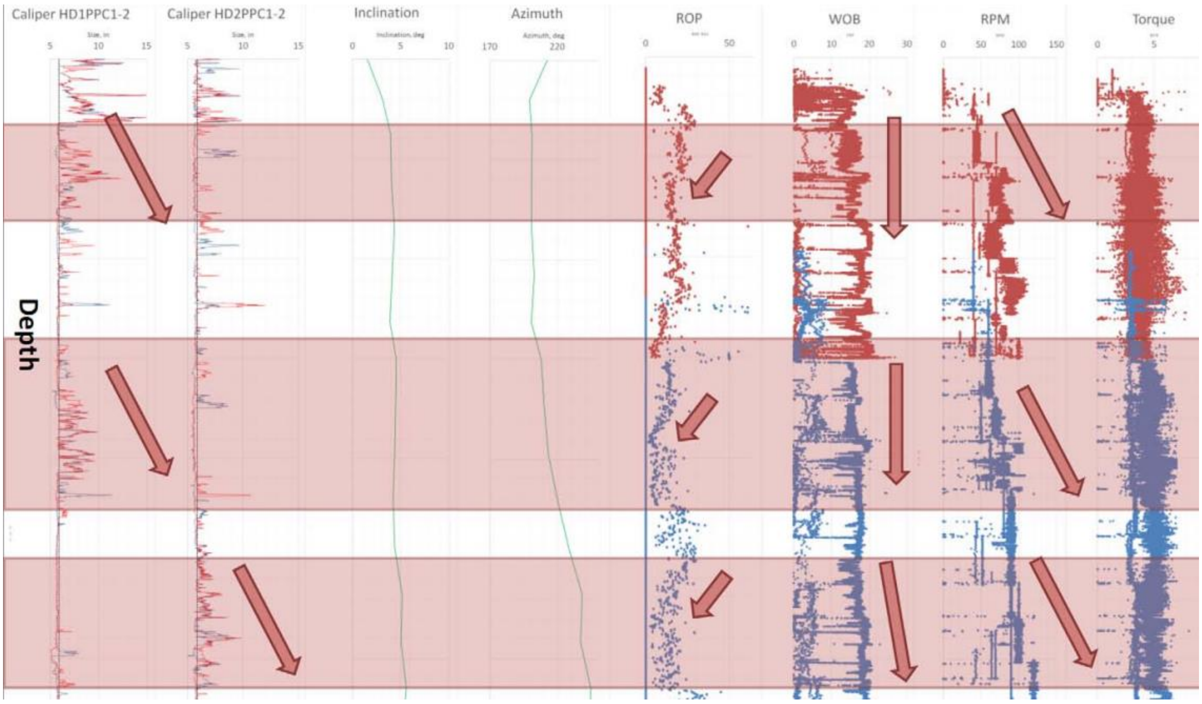

Figure 5.1: ROP reduction despite increasing input energy through WOB and RPM (AlBahrani and Al-Yami 2018)

5.3 Potential Downhole Damage

Damage to tools and components used in the drillstring are often very costly. In addition to the destruction of expensive tools, the continuation of the drilling operation may be relying on the tools being operative. An example is the loss of steerability due to a malfunctioning RSS. To continue drilling in this case could jeopardize the ability to reach the target. The operator would have to trip out of the well, replace the tool and run back in the well, resulting in substantial non-productive time. A thorough investigation of the tools post run should be made in order to better understand the origin of the damage. The different vibrational modes often have characteristic damage on the drillstring; therefore, a post-run inspection may indicate what vibration type is occurring downhole.

5.3.1 Axial Vibrations

As mentioned in Section 3.1.1, the most common form of axial vibration is bit bounce, causing the bit to periodically engage and disengage the formation. The impact loading can damage the seals, bearings and cutting structure of the roller cone bit, as can be seen in Figure 5.2 a). The most commonly encountered form of axial vibrations when using a PDC bit is the resulting axial motion from coupled axial and torsional vibrations. In Section 3.4.1, the numerical example showed that the drillstring must shorten during stick-slip cycles. The drillstring then abruptly increases in length during the slip cycle, causing axial impacts with the formation and bit. The axial shocks lead commonly causes damage to the nose of the PDC bit, as can be seen in Figure 5.2 b). Damage to the drill string may also be seen due to the flexing of pipes and equipment. Surface equipment may also suffer damage in shallow wells, due to a short string being less able to dampen vibrations. The axial impacts resulting from both bit bounce and coupling between stick-slip and axial vibrations may also result in component damage above the bit.

a) Lost cone on a roller cone bit due to bit bounce (Al Hammadi et al. 2018).

b) Axial loading causing ring out on a PDC bit (Hood et al. 2015).

Figure 5.2: Damaged roller cone- and PDC bits from axial vibrations.

5.3.2 Torsional Vibrations

Stick-slip is perhaps the most frequently mentioned type of vibration by both industry and literature. The reason for this is both because it is common to encounter stick-slip when drilling a well, but also because it can have detrimental impacts on drillstring and BHA components if not dealt with. The repeated torque cycling may result in over or under torqued pipe connections. If the stick-slip is severe, backward rotation can in extreme cases back off connections, incurring costly fishing or sidetracking operations. PDC bits are especially susceptible to backward rotation. This is because bit and cutters are designed to face the loads from drilling in forward rotation only and reverse rotation can easily damage cutters, as shown in Figure 5.3.

Damage due to HFTO has gained more attention with the increasing ability to detect this type of vibration. The high frequency of this vibration type leads to fatigue failures in the drillstring. Patil and Ochoa (2020) showed that cracks on tools, loose electronics, squeezed cables, sheared bolts and vibration dust are typical impacts of HFTO.

Figure 5.3: Cutter and shoulder wear due to stick-slip (Hood et al. 2015)

5.3.3 Lateral Vibrations

Lateral vibrations are recognized as the leading cause of BHA- and downhole tool failure (Vandiver et al. 1989). This vibration mode is often manifested as whirl, as described in Section 3.3. Table 3.1 demonstrates the bending rates experienced by the BHA during whirl. Bending stresses at several tens of hertz can be experienced by the drillstring during backward whirl. The repeated flexing of drill collars during this vibration type significantly increases fatigue rates of components in the drillstring. Drill collar connection failures are mainly attributed to cumulative fatigue resulting from bending vibration (Zhao et al. 2018).

Whirling does not necessarily occur in a continuous circular manner but can instead cause the BHA to erratically bite the wellbore wall, leading to lateral shocks which may result in electronic downhole failure. Like backward rotation with stick-slip, backward whirl also subjects the bit and cutters to a force direction that the components are not designed for. An example of bit damage due to backward whirl is demonstrated by Figure 5.4.

Figure 5.4: Bit damage caused by backward whirl (Hood et al. 2015)

Cutters are easily broken and even lost as a result of backward whirl, as highlighted in the red square.

6 Identification

The most important step to solving problems related to drillstring vibrations is firstly to be able to detect vibrations and secondly to accurately identify what mode of vibration is occurring. This chapter is focused on providing the engineer with a fundamental understanding of the typical vibration patterns recorded by downhole tools and surface measurements. A brief description of the variation in measurements, definitions and procedures that exist is also given since it is very likely that the operator will employ several different service companies for dynamic measurements over the course of a field development.

6.1 Drilling Data

Drilling operations bring with them huge amounts of data due to the number of parameters that are monitored to ensure that non-productive time is kept to a minimum. The clear connection between downhole vibrations and non-productive time during drilling has given rise to increased use of mechanics and dynamics measurements. The three main sources of drillstring dynamic data, logging while drilling (LWD), measurement while drilling (MWD) and surface measurements each carry its separate limitation. The two latter sources of data allow real time monitoring and resultingly also intervention.

The majority of MWD equipment uses mud pulse telemetry and is therefore very limited by the rate of data transfer in this type of transmission system. Typical data rates achieved with mud pulse telemetry range from 3 to 40 bits per second (bps)(McCartney et al. 2009). This transmission system also faces challenges such as signal attenuation due to depth, fluid properties, and fluid flow rate due to signal transmission being dependent on flow. Noise due to mud pumps may further obscure the signal. MWD transmission systems using electromagnetic telemetry are not burdened by the difficulties related to the drilling fluid. This telemetry technology is however also limited by poor bandwidth, only reaching up to 20 bps (McCartney et al. 2009). Surface measurements have its own flaws in that it can only detect vibrations that manifest at surface, which becomes increasingly less likely as the well depth progresses. An example of this is shown in Figure 6.1, where fully developed stick-slip is visible through downhole RPM measurements, yet not reflected by the set surface RPM. Finally, LWD offers sufficient resolution and sampling rate, however this data is stored in memory and downloaded after tripping out of the well, meaning that it does not allow real time action to be taken in order to prevent vibrations.

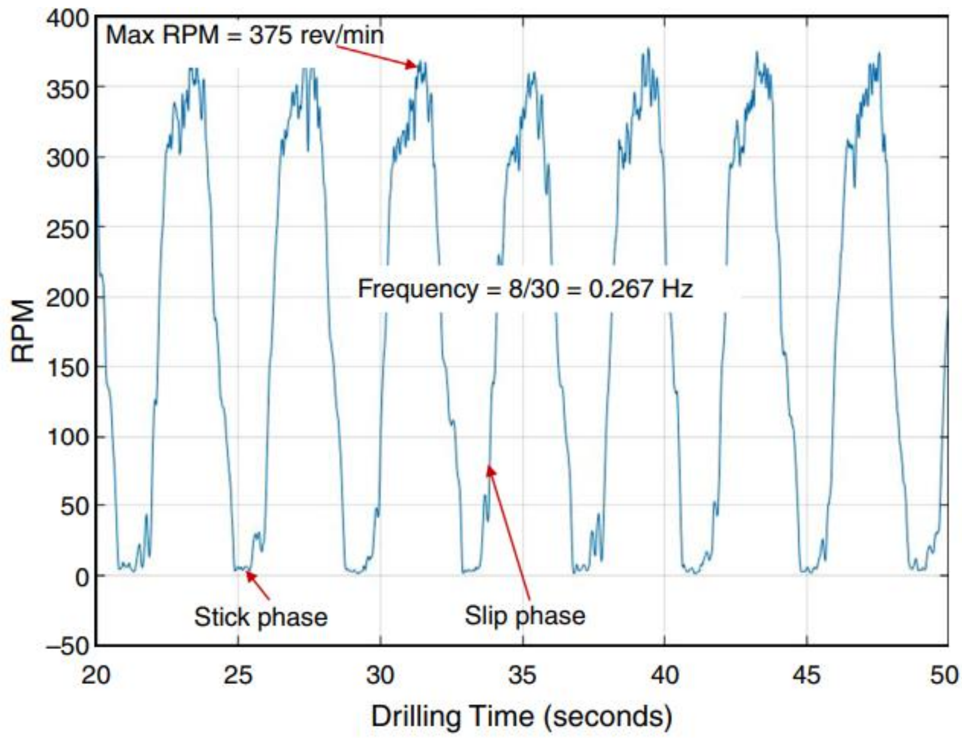

Figure 6.1: Downhole RPM measurements vs surface measurements

Surface RPM is set at 183 RPM, meanwhile the downhole RPM is fluctuating between 0 and 370 RPM (Chen et al. 2020).

6.2 Mechanical Specific Energy (MSE)

Mechanical specific energy (MSE) is a measure of the amount of work a bit uses to drill a volume of rock. The equation for MSE was derived by Teale (1965), however industry wide use of the parameter has been increased in recent years. Equation 6.10 shows how MSE is calculated.

$$MSE = \frac{480 \times T \times RPM}{D^2 \times ROP} + \frac{4 \times WOB}{D^2 \pi} \tag{6.10}$$

Where T is the torque input in ft-lbs, RPM is the rotation speed in revolutions per minute, D is the bit diameter in inches, WOB is the measured weight on bit in lbs and ROP is the rate of penetration in ft/hr.

Increasing WOB should result in a linear increase in ROP, as shown in Figure 6.2. As soon as the ROP deviates from a linear trend, some sort of dysfunction in the system is draining energy which should instead have been used in the rock breakage process. The point where ROP output deviates from the linear trend is called the founder point. The figure points out that numerous factors could affect the position of the founder point, among them vibrations. When the output ROP deviates from a linear trend, an increase in MSE would be seen, as the terms in the nominator of Equation 6.10 would increase without the ROP term in the denominator increasing. An MSE increase could be rooted in several factors, as indicated in Figure 6.2 but the property could serve as an indicator of vibrations downhole.

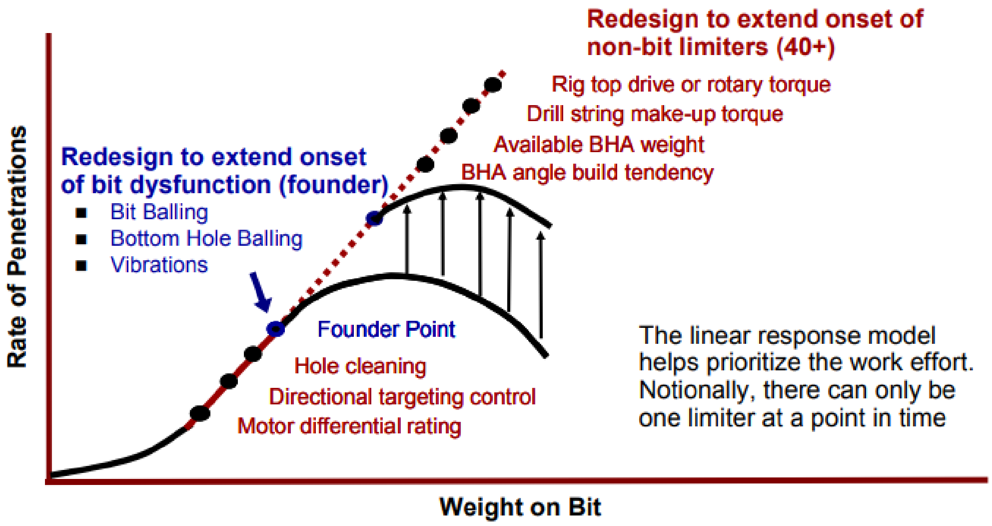

Figure 6.2: Sketch showing the relationship between WOB and ROP (Dupriest et al. 2010)

6.3 Standardization

Drilling a well requires cooperation between the responsible operator and a multitude of service companies. It is well known in the petroleum industry that the desired level of transparency between service providers is often not reached due to several factors, intellectual property being one. An engineer employed by a service provider only needs to deal with the standards and procedures of that sole service company. For an engineer at an operator who wishes to compare dynamic measurement data between service companies, this is not the case. The differences in measurements and data between service providers have made comparisons of drilling dynamics difficult when different service providers have been employed. Several papers recognized this problem, among them Osnes et al. (2009) who focused specifically on standardization of MWD measurements between service companies. Macpherson et al. (2015)

echoed this need but also recognized the limits to which standardization is possible. The authors instead focused on transparency where standardization was not achievable, suggesting that all necessary metadata for the measurements is given. The subsections under Section 6.2 contain elements from the aforementioned papers.

Giving a full description of each service provider`s procedures and definitions when it comes to recording dynamic data is not in the scope of this thesis, neither is it a productive way for an engineer to work. It is however useful to know that there are differences in the way measurements are made.

6.3.1 Sensor orientation:

Acceleration measurements between service companies may vary in several ways. Some service companies use a cylindrical coordinate system, reporting accelerations in radial-, tangential- and axial directions (RTZ configuration). Others may use the cartesian coordinate system with XYZ notation, giving accelerations in two lateral- and one vertical direction, as shown in Figure 6.3. Different service companies have different uses of symbols for the different directions even within the cartesian coordinate configuration. An example is an acceleration in the “X” direction, which may represent lateral motion for one company and the axial direction for another.

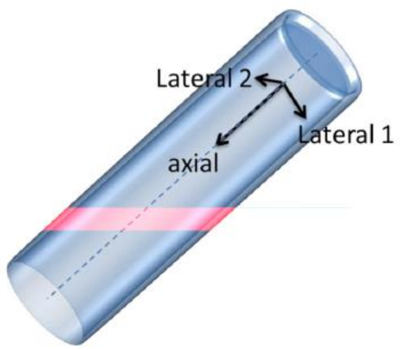

Figure 6.3: Cartesian coordinate system

The principal axis goes along the wellbore axis, with two perpendicular lateral axes defining a plane orthogonally to the principal axis (Macpherson et al. 2015)

6.3.2 Time-Window

Torsional vibration severity or stick-slip index are frequently reported vibrational data calculate by service companies. These numbers are calculated using the difference in maximum- and minimum rotary speed based on a sampled time interval. The equations for stick-slip index and torsional severity estimate are given by 6.11 and 6.12, respectively (Macpherson et al. 2015). In this case it is important to know that the sampled time-window used to calculate these numbers vary between service companies. Some may record data in a 10 second interval, meanwhile other companies may have a standard of recording for 30 seconds. This may in turn result in large differences in output data.

$$SSI = \frac{RPM_{max} - RPM_{min}}{2 \cdot RPM_{avg}} \tag{6.11}$$

$$TSE = \frac{RPM_{max} - RPM_{avg}}{RPM_{avg}} \tag{6.12}$$

SSI is the stick-slip index, RPM_{max}, RPM_{min} and RPM_{avg} are the maximum, minimum and average rotation rates, respectively. TSE is the torsional severity estimate.

6.3.3 Sensor Location and Bandwidth

The location of sensors in the drillstring is essential context when analyzing the measured data. This is because vibrations travel as acoustic waves in the drillstring and thus may attenuate or differ in amplitude depending on where the sensor is located. An example is at positions near a stabilizer. The stabilizer may function as a nodal point for vibrations, minimizing movement in lateral directions. At points further from a stabilizer, the pipe may flex or bend severely without being detected due to sensors being situated at points experiencing less vibrations. The reflection of acoustic waves in the drillstring also means that interfaces between pipes with different dimensions may cause dynamic phenomena. The transition from drill collar to heavy weight drill pipe is an example of a boundary which may give rise to dynamic phenomena at drillstring or BHA-scale (Macpherson et al. 2015). It is also essential to understand the bandwidth that determines the frequency range in which the sensor can measure vibrations.

6.4 Vibration Type Identification

6.4.1 Bit Bounce

As mentioned in Section 3.1.1, bit bounce is primarily an issue when drilling vertical sections with a roller cone bit. In shallow wells, this can be identified by the shaking of surface equipment. With severe bit bounce, logs will show large cyclical axial accelerations, combined with a fluctuating weight on bit. Bit bounce may also manifest on RPM and torque measurements downhole due to the nature of the drillstring cyclically engaging and disengaging the formation. The left side of Figure 6.4 shows regular randomized RPM/WOB variations, meanwhile the logs on the right demonstrate fully developed bit bounce. When drilling with a conventional tricone bit, a frequency of three times the RPM is commonly encountered. The driller`s hook load measurements may show the fluctuations due to bit bounce, however as the drillstring increases in length the WOB fluctuations will become more difficult to detect due to the increased axial damping in the pipes.

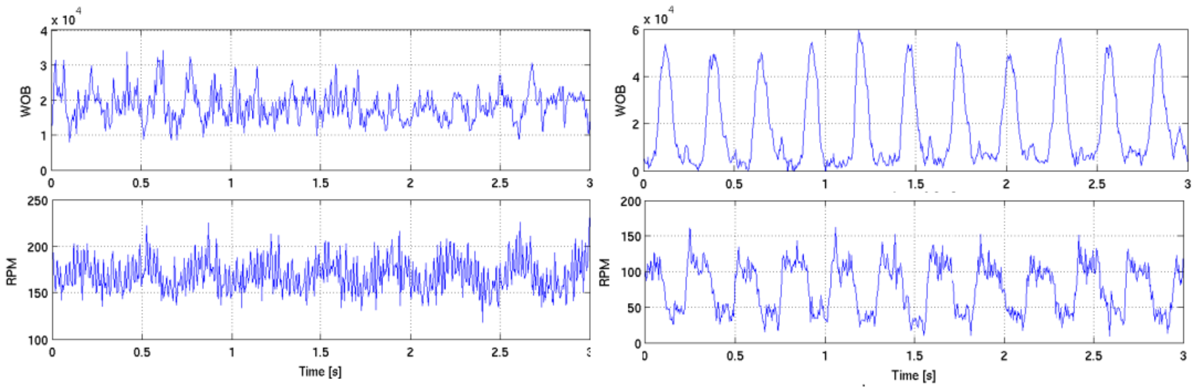

Figure 6.4: RPM/WOB fluctuation during steady-state drilling vs. during bit bounce (Vassallo et al. 2004)

6.4.2 Stick-slip

The increased versatility of PDC bits have resulted in the use of this bit type also in most hard rock drilling. Resultingly, stick-slip incidents are more commonly encountered due to the increased difficulty in drilling in such conditions. The large rotational speeds potentially generated when suffering stick-slip vibrations beg the need for quick identification to minimize the time tools operate outside the design envelope for rotation.

In Section 3.2.1, it was stated that stick-slip could be either friction-induced or bit induced. The latter case is explained by the RGD model to be due to the coupling between axial and torsional vibrations through a rate-independent bit-rock interaction (Chen et al. 2020). In more simple terms, if stick-slip is initiated by the cutting action of the bit, there should be a clear correlation between axial- and torsional vibrations. Figure 6.5 demonstrates this from measurements recorded by on bit sensors

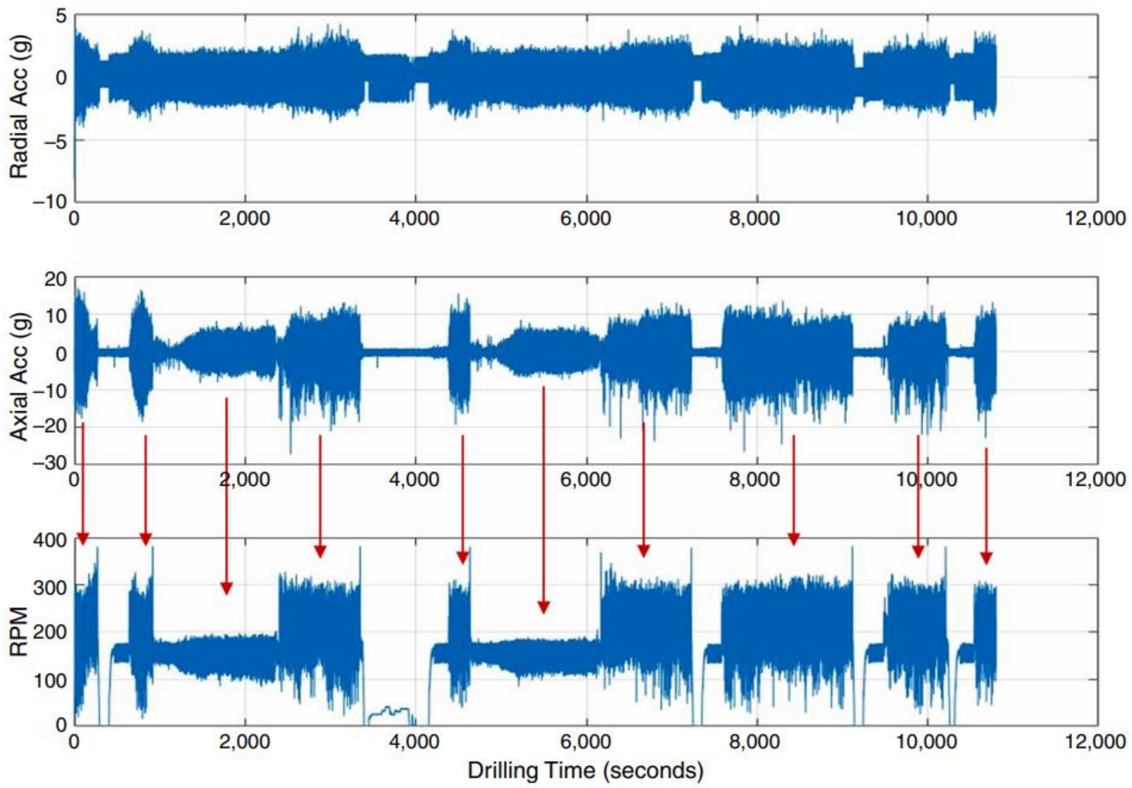

Figure 6.5: Bit induced stick-slip

The RGD model states that bit induced stick-slip is rooted in coupling with axial motion and therefore should be correlated with axial acceleration of the drillstring (Chen et al. 2020).

Kyllingstad and Halsey (1987) showed that frictional torque acting along the drillstring could lead to stick-slip. In this case, the drillstring must be laterally displaced such that it is in contact with the wellbore wall, as demonstrated by Figure 6.6. The axial movement of the string in this case does not contribute to increased frictional torque.

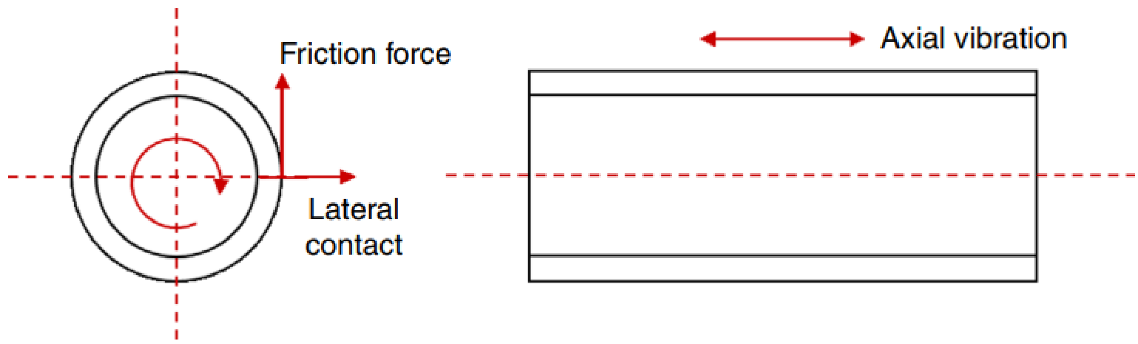

Figure 6.6: Axial vibrations does not affect the friction force (Chen et al. 2020)

Field measurements using bit sensors have identified friction-induced stick-slip in multiple runs and Chen et al. (2020) have demonstrated that it is possible to differentiate between different kinds of friction-induced stick-slip types. However, this reaches beyond the aim of this thesis. The most essential characteristic of friction-induced stick-slip is that the axial- and torsional vibrations are not coupled, as indicated by field measurements in Figure 6.7. The fact that the two vibrational modes are not coupled, does not mean that they can`t coexist. As shown in Figure 6.7 axial vibrations are still occurring, yet they are randomized and occurring during both stick and slip phases.

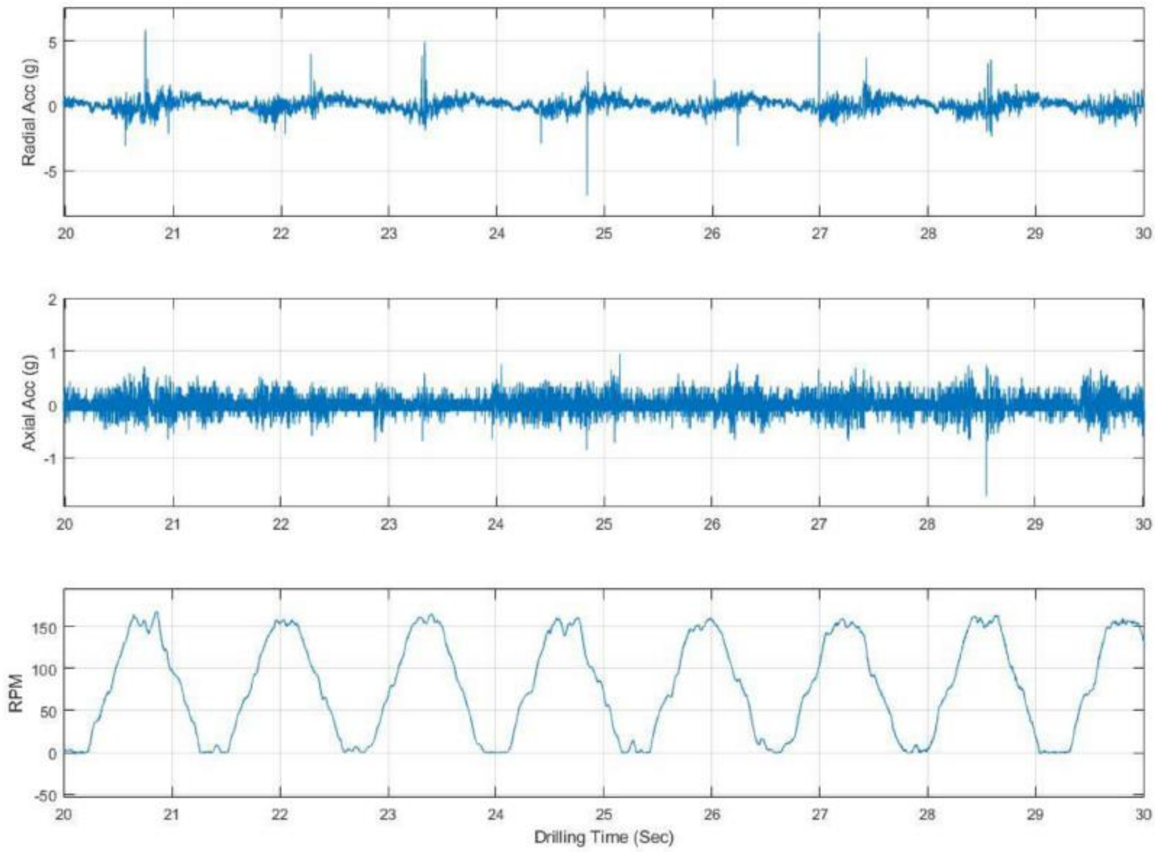

Figure 6.7: Friction-induced stick-slip (Chen et al. 2020)

This type of stick-slip is easily distinguishable from bit-induced stick-slip, as there is no correlation between axial and torsional vibrations.

Differentiating bit-induced and friction-induced stick-slip may seem straight forward in the given examples, however both types may be superimposed on each other. For the bit to rotate without a motor, the applied torque must overcome reactive torque from both cutting action and friction with the wellbore wall. This makes it impossible to attribute stick-slip vibrations to one vibration-inducing mechanism. To summarize the characteristics of bit-induced and friction-induced stick-slip:

- Axial- and torsional vibrations are coupled in bit-induced stick-slip.
- The stick phase of bit-induced stick-slip is characterized by no axial- or lateral vibrations.
- Bit is completely stationary during stick phase of bit-induced stick-slip.
- Axial- and lateral vibrations may occur in stick-phase of friction-induced stick-slip.
- No coupling between axial- and torsional vibrations for friction-induced stick-slip.
- Bit-induced and friction-induced stick-slip may be superimposed.

6.4.3 High Frequency Torsional Oscillations (HFTO)

Torsional harmonic oscillations of the bottom hole assembly at frequencies much higher than that of a torsional pendulum are referred to as high frequency torsional oscillations (HFTO) as explained in Section 3.2.2. Earlier limitations in sampling frequencies downhole have made these vibrations impossible to detect for a long time. HFTO do not propagate to surface, but are instead attenuated in the heavy weight drill pipes, also rendering high frequency surface measurements incapable of detecting the vibrations (Patil and Ochoa 2020). It is highly likely that several concluded root causes of downhole tool failures have been made on false premises due to the limitations in detecting the vibration type. Improvements in the capability of dynamics sensors have later unveiled this type of vibrations. High angular shocks are often linked with HFTO, reaching up to 80g while drilling (Patil and Ochoa 2020). Recent increases in measurement bandwidth of downhole sensors allows recording of frequencies up to 1000 Hz. The recordings can be initiated as the vibrations reach an acceleration threshold or the sensors may be preprogrammed to record at certain time intervals. Post job analysis reveal that HFTO can occur on its own or be superimposed on stick-slip vibrations, as shown on the left- and right side of Figure 6.8, respectively. The spectrogram in Figure 6.8 also shows the high frequencies these torsional harmonics occur at.

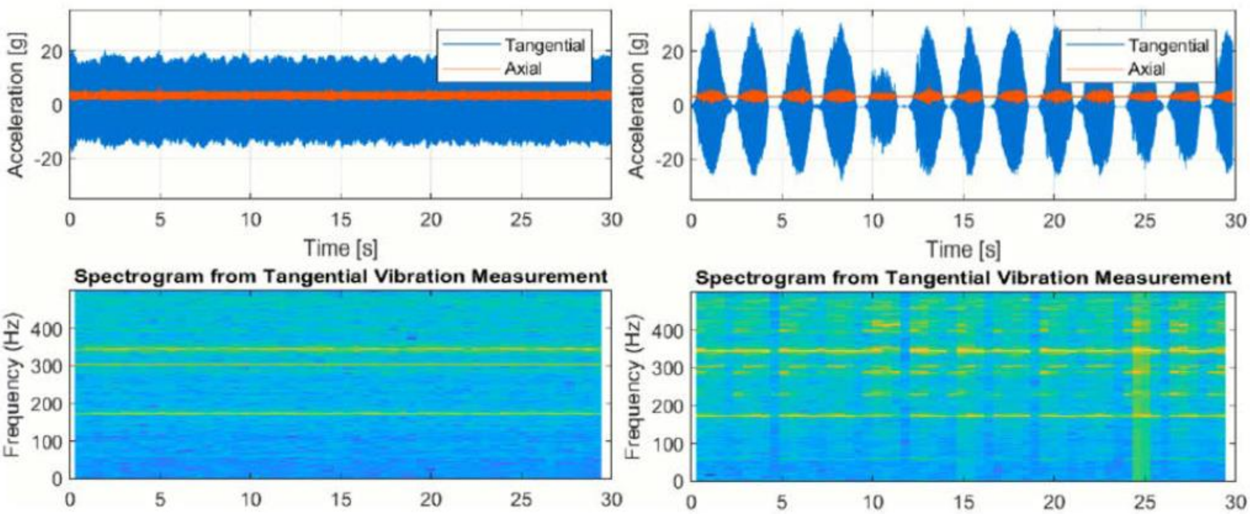

Figure 6.8: HFTO vibrations with (right) and without (left) stick-slip (Patil and Ochoa 2020)

6.4.4 Bit- and BHA Whirl

Whirling motion of bit and BHA must in most cases be identified through post-run analysis. The tendency for lateral vibrations to attenuate rapidly along the string together with the high frequency at which whirling vibrations occur makes it difficult to identify whirl through MWD and mud pulse telemetry. The identification of whirl will in most cases require analysis of memory data. Bowler et al. (2014) used a sub which processed data at high frequency and calculated real-time diagnostics which was sent to surface using mud telemetry, however this equipment is far from an industry standard.

Since bit- and BHA whirl may occur simultaneously or independently, near-bit sensor data must be compared with sensors further from the bit if the whirl type is to be determined. This may in turn affect how the problem is dealt with, as it won`t help to focus on optimizing the BHA to negate vibrations if bit whirl is the root cause of the problem. In either case, whirl is characterized by high frequency bending moments and lateral accelerations, as demonstrated in Figure 6.9, which displays field recorded memory data. Whirl severity is calculated based on the lateral accelerations and bending moments.

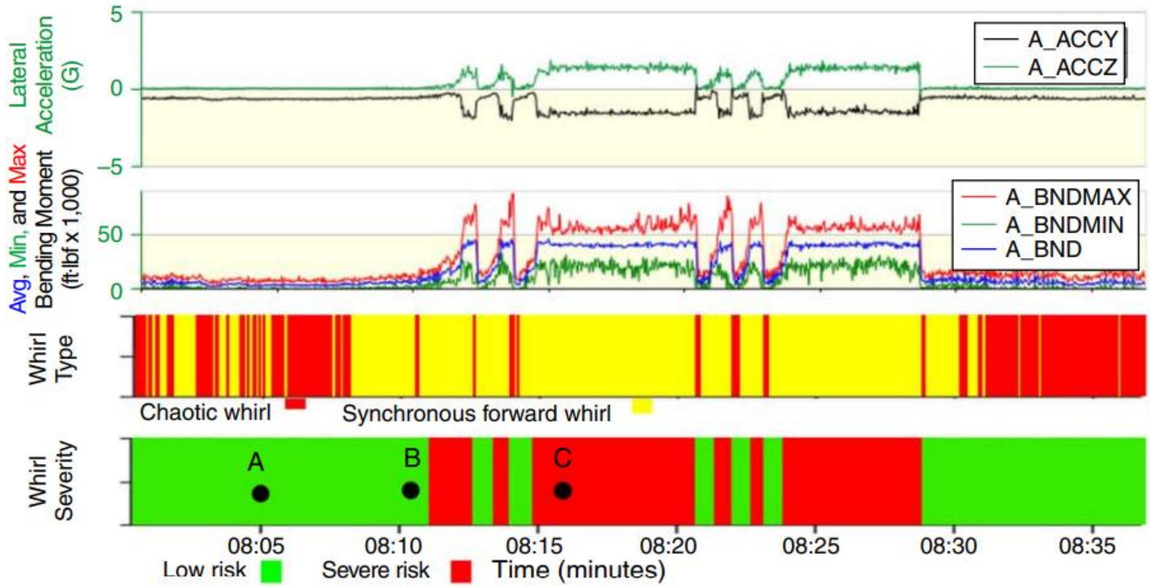

Figure 6.9: Lateral accelerations and bending moments indicating whirl (Bowler et al. 2014)

By converting the bending frequencies to a geostationary reference frame, the distinction between forward- and backward whirl can be made. Also, cross-plots of the lateral motion of the drill collars can be generated for visual purposes (Bowler et al. 2014). The points A, B and C in time show the development from low amplitude chaotic whirl motion to fully developed forward synchronous whirl. Figure 6.10 shows the whirl motion crossplots of the development.

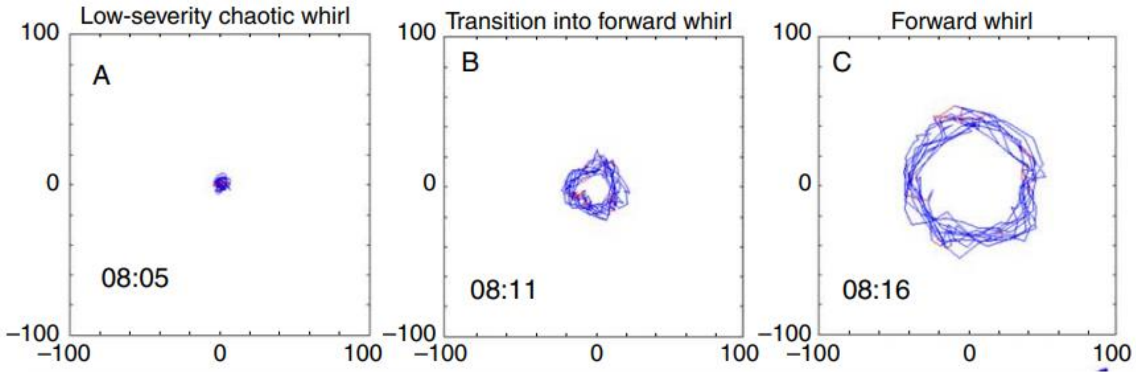

Figure 6.10: Whirl motion crossplots from the high frequency data measured in Figure 6.9 (Bowler et al. 2014)

6.4.5 Summary Table

Using the vibrational modes and primary vibration type of each mode described in Chapter 3 in combination with the root causes from Chapter 4 and the described post drilling evidence from vibrations given in Chapter 4.7, a summary of recognizable traits of the most common vibration modes is shown in Table 6.1.

Table 6.1: Summary of identifiable traits for each of the vibrational modes

Type	Bit Bounce	Stick-Slip	Torsional Resonance	Bit/BHA whirl
Primary mode	Axial	Torsional	Torsional	Lateral
Excitation mechanism	Hard formation Vertical well	Bit reactive torque Drillstring frictional torque	Bit/rock interaction with PDC bits in hard formations.	Sidecutter/formation interaction Overgauge wellbore Mass imbalance
Frequency	1-10 Hz	< 1Hz	10-400 Hz	5-150 Hz
Real-time indications	Shallow well: Axial movement of the drillstring can be detected from surface. This will also be reflected by fluctuations in hook load.	Surface rotary torque may show cyclic variations. Stick-slip severity index (if available in MWD package)	Not possible to detect in real time.	Surface torque and hookload variations (in rare cases) Lateral shock sensor (if available in MWD package). ROP not responsive to WOB/RPM increases.
Post-run evidence	Memory data: Periodic axial axis accelerations. Damage to drill bit structure, bearings and seals. May see damage to drill string due to axial shocks causing severe periodical flexing.	Memory data: Torque- and RPM fluctuations Over- or undertorqued drill collar-/pipe connections Damage to PDC cutters (frequently observed if backward rotation is occurring)	Memory data: High angular acceleration shocks. Memory data: High frequency variations of rotary speed, tangential acceleration and dynamic torsional torque. Cracks on tools, loose electronics, squeezed cables, sheared bolts and vibration dust (Patil and Ochoa 2020).	Memory data: High lateral accelerations. Frequency analysis may indicate dominant peak frequencies of large magnitude. Damage to drill collar connections. Wear on bit blades and damage to PDC cutting structure

7 Mitigation

7.1 Workflow

Many tools have been developed over the course of the last decade aimed at minimizing drilling vibrations, yet the potentially most important mitigative measure may lie in the pre-drilling phase. By implementing a workflow to combat drillstring vibrations as a standard, additional costs may be evaded at a later stage.

In the pre-drilling phase, expected levels of vibration should be found from drillstring dynamic memory data or logs from offset wells. Key personnel should be familiar with the previously experienced vibration levels and what types of vibration to expect. Service companies should model and analyze different BHA configurations in order to increase the likelihood of selecting the least vibration prone BHA when all other design factors have been fulfilled. Significant decreases in vibrations due to BHA vibration modelling has been validated through several field tests, some yielding up to 60% increases in ROP and an increase in length drilled of 150% (Bailey et al. 2016, Bailey et al. 2010).

Surface data and real-time MWD measurements should be closely monitored during drilling. As mentioned in Chapter 6, most vibration types are difficult or even impossible to detect using MWD measurements transmitted through mud pulse telemetry. This means that dynamic memory data should be analyzed thoroughly post-run despite real time measurements not indicating substantial levels of vibration. Counteractive measurements such as RPM, WOB and flow rate manipulation should be taken in the event of high vibration levels in order to determine whether a “sweet spot” exists or to evade combinations parameters giving rise to resonant behavior of the drillstring. Modelling software often give an indication of RPM ranges to operate within, however the complexity of a real case drilling scenario makes it difficult for these models to be precise. Sudden changes in ROP when lithology and operational parameters are kept constant is a quick indication that energy is being dissipated somewhere in the system.

Post-drilling memory logs should be evaluated in order to determine actual levels of vibration downhole. Both problematic and successful runs should be analyzed and reported. If the pre-drilling operational procedures are followed, this increases the probability for successful runs in future operation. Experiences of note during drilling should also be reported. Post-run inspections of equipment and tubulars can reveal vibrations. Different vibration types will often damage the drillstring in characteristic ways. Section 5.3 gives an overview of the most typical imprints and damage patterns for the most common vibration types. A summary of the suggested workflow is given in Table 7.1

Table 7.1: Workflow suggestion

Pre-drilling:
- Offset well analysis
- Risk identification
- BHA modelling
- Identify counteractive actions
- Inform relevant personnel

During drilling:
- Monitor MWD data
- Monitor surface measurements
- Adjust operational parameters to avoid resonant conditions or find sweet spot
- Monitor ROP

Post-drilling:
- Memory data analysis
- Post-run inspection of tools and tubulars
- Report both problematic and successful runs
- Report experiences of note
- Rate BHA configuration

7.2 Parameter Optimization

7.2.1 Bit Bounce

As mentioned in Section 3.1.1, bit bounce is a phenomenon resulting from a lobed pattern in the formation generated by roller cone bits. When this vibrational behavior is initiated, the target should be to destroy the pattern. Reducing the WOB or RPM is a common corrective action when experiencing bit bounce. If the axial vibrations persist, stopping and restarting rotation at a lower WOB/RPM combination may reduce bit bounce behavior. If the axial vibrations are occurring using a PDC bit, it is most likely due to the shortening of the drillstring during stick-slip. Corrective actions should in this case be to increase RPM in order to reduce stick-slip behavior.

7.2.2 Stick-Slip

Stick-slip mitigation is somewhat dependent on whether bit-induced- or friction-induced stick-slip is occurring. Reducing WOB can reduce the frictional torque resulting from bit-induced stick-slip. If friction-induced stick-slip is identified to be the root cause, increasing the mud lubricity can reduce the friction between drillstring and wellbore. Increasing rotary speed will in most cases mitigate the severity of stick-slip vibrations for both bit-induced- and friction-induced stick-slip. Recent research by Cayeux et al. (2020) using downhole RPM measurements at 300 Hz indicate that there seems to be a threshold rotary speed where the downhole RPM oscillations seize to occur. Figure 7.1 a) shows the variability in downhole RPM. At 140 RPM, stick-slip is significantly reduced. Figure 7.1 b) demonstrates how the stick period is reduced from 30% of total rotating time at 100 RPM to close to 0% at 140 RPM. This RPM threshold value will vary depending on the well configuration.

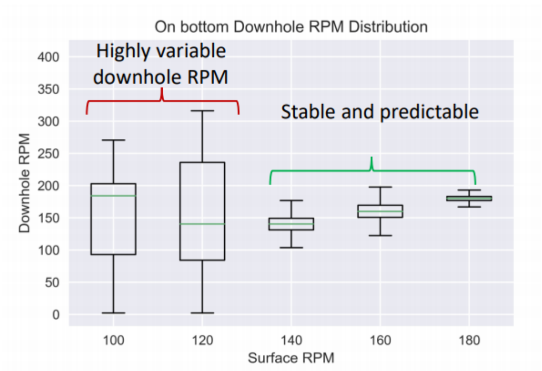

a) RPM downhole vs surface RPM

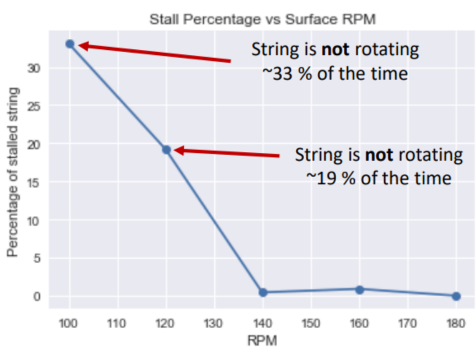

b) Stall percentage at varying surface RPM

Figure 7.1: RPM measurements using downhole high frequency magnetometers (Cayeux et al. 2020)

If stick-slip persists despite parameter manipulation, stopping rotation and picking off bottom may release built up torsional energy in the string.

7.2.3 Whirl

Early empirical studies on the whirling behavior of drill bit and drillstring revealed that whirling effects are amplified at combinations of low WOB and high RPM (Brett et al. 1989). Increasing WOB allows the bit to bite more into the formation, reducing the tendency for the bit to perturbate around the wellbore. Whirling behavior often occurs at the natural frequency of drill collars. Step changes in the RPM while monitoring lateral vibrations may reveal critical rotary speeds to avoid. Whirl is more likely to occur in oversized wellbores. If the creation of an overgauged hole can be attributed to the wellbore hydraulics, reducing flow rate may aid in laterally constraining the drillstring to prevent whirl.

7.2.4 High Frequency Torsional Oscillations (HFTO)

If HFTO have been identified through post-run analysis of dynamic sensor data, BHA modelling should be used to identify a BHA less prone to this type of vibration. Hohl et al. (2020) researched how WOB/RPM combinations affect HFTO amplitudes. HFTO was observed to occur both independently and simultaneously with stick-slip. The essence of the results was that RPM could be increased until stable drilling without both stick-slip and HFTO was realized. The challenge was found to be that the RPM threshold for when HFTO was eliminated could be at very high RPMs (above 150 RPM). At low RPMs, stick-slip and HFTO can occur simultaneously as demonstrated by Figure 7.2. The points A through F indicate step changes in rotary speed at a constant WOB. As RPM is increased, so is the amplitude of the HFTO oscillations. At point E, high amplitude high frequency torsional oscillations are occurring, which may induce a failure in the BHA rapidly. If increasing the RPM with the purpose of reaching the stable area as shown in dark blue is decided as the mitigating action for HFTO, the stable area should be identified according to procedures by Hohl et al. (2015). If the stable drilling envelope is outside operational parameter limit, rotary speed should instead be reduced to reduce the amplitude of the vibrations (Hohl et al. 2020).

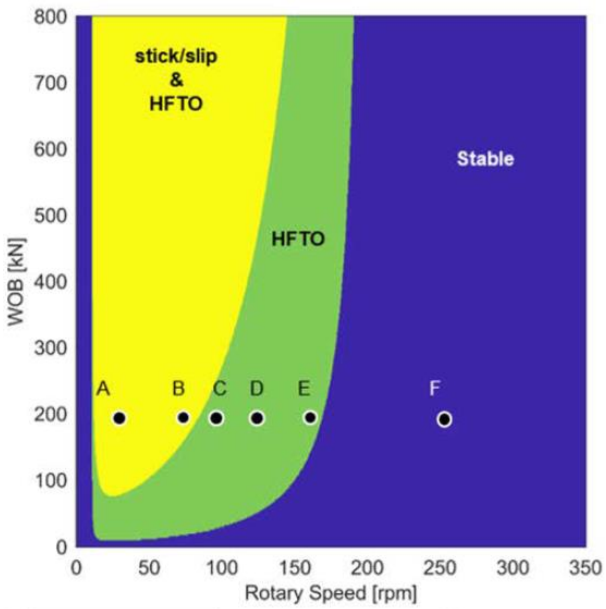

Figure 7.2: Stability map for HFTO (Hohl et al. 2020)

7.2.5 Advisory systems

Real-time monitoring of surface parameters to negate vibrations can be a tedious task for a driller to perform manually. Drilling advisory systems have been developed to relieve the driller of manually analyzing numerous real-time logs of surface parameters. The advisory system helps the driller manage controllable drilling parameters to enable high ROP and low vibrations. Tradeoffs in drilling performance between stick-slip and whirl are examples of limiting conditions that may be difficult for the driller to optimize parameters for. An example of this is shown in Figure 7.3, where suboptimal manipulation of operating parameters can shift the vibration type from stick-slip to whirl. Advisory systems can quickly analyze measured surface parameters to better determine the optimal combination of operating parameters.

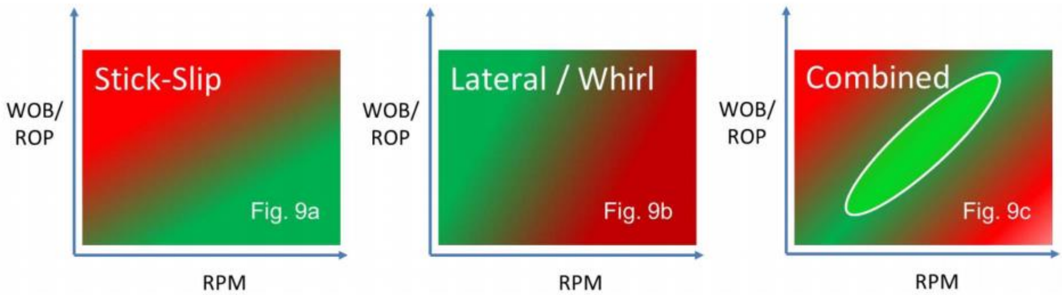

Figure 7.3: Operating parameter optimization problem

Typical tradeoff scenario where adjusting parameters can transition the drilling instability from one vibration type to another with suboptimal parameter manipulation (Payette et al. 2015).

Numerous advisory systems have been developed and tested. The systems may differ in input parameters used in the algorithms which outputs suggested corrective actions. An example is the advisory system used in drilling a lateral section by Payette et al. (2015) which uses MSE, ROP and TSE (torsional severity estimate) to provide a stoplight color-coded display of optimal drilling parameter values. An example of the display and its components is shown in Figure 7.4.

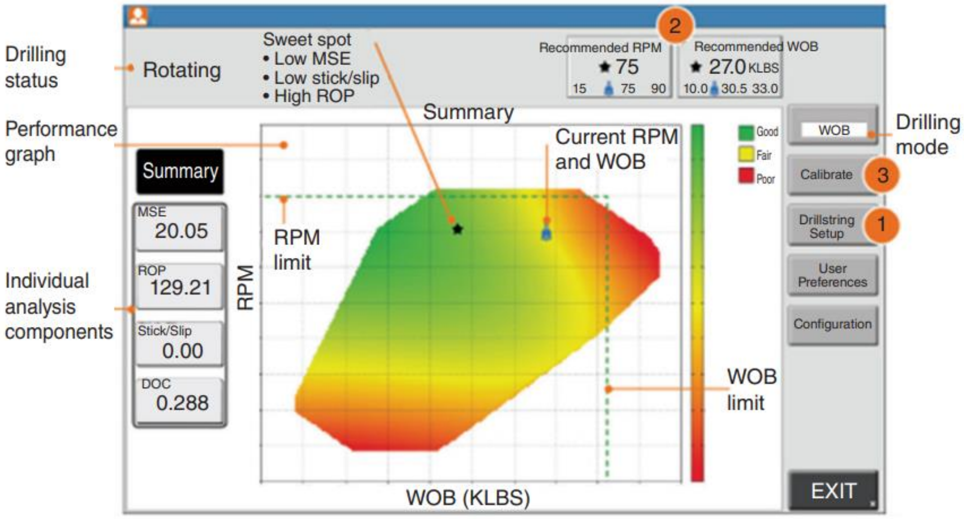

Figure 7.4: Graphical interface of the drilling advisory system DAS by Payette et al. (2015)

It is important to be attentive to the fact that advisory systems use surface parameters due to the insufficient bandwidth of real-time downhole dynamic measurements. This means that vibration phenomena could be occurring downhole without the advisory system being able to detect the vibrations.

7.3 BHA Design Modelling

The purpose of drilling modelling and simulation is to provide crucial information about the drilling system without constructing a real well. Drilling a borehole is a complex process, involving interaction with drilling fluid and surrounding rocks. This makes modelling and simulating every part of the process an impossible endeavor. This is also the case for modelling and simulating downhole drillstring dynamics. Researchers target specific parts of the drillstring dynamics problem, make progress and are then succeeded by new theories, using more complicated models. BHA modelling is the focus in dynamics modelling due to this being the part of the drillstring which is responsible for most of the interaction with the wellbore. Design options for the BHA is very limited for a drilling engineer. RSS-, MWD-, LWD- and other systems often have fixed dimensions, leaving the engineer in charge of only basic configuration issues, e.g. stabilizer placement. Instead of creating an optimized BHA, the focus of the drilling engineer should be to determine whether a given configuration is expected to perform well at a set of operating parameters.

BHA modelling is carried out by service companies. This means that the modelling software and the physics that the software are based on can vary between companies. The models are differentiated into static- and dynamic models. Common for both cases are that most state of the art modelling software use finite element method (FEM). Static models are mostly used in force analysis, trajectory calculation based on side cutting ability, survey sag correction and sensitivity analysis. Dynamic models calculate critical operating parameters for the various vibration modes. There are drawbacks to both static- and dynamic modelling. Some service companies claim that the assumptions made in dynamic models, such as in gauge hole, constant bit weight and constant RPM leads to less alignment between predicted behavior and field experience compared to static models (Larsen 2014). Other service providers supplying mainly dynamic models claim that modelling based on statics leads to underestimation of bending moments.

Although software vary, most BHA optimization software allow the user to input multiple BHA design candidates using a graphical interface, as demonstrated by Figure 7.5. The system is subdivided into short sections of pipe. This is done to create a lumped parameter model with adequate accuracy. Nodes are connected by massless springs. Each nodal point is given a set of parameters, which commonly are lateral displacement, tilt angle, bending moment and beam shear load (Bailey et al. 2008). Depending on the vibration mode to be analyzed, the BHA design is given a force input which induces a dynamic response in the BHA. The magnitude of the response in the BHA is compared to various BHA designs to determine which design is the least prone to detrimental vibrations for the expected loads. Post-drilling of an interval, operating parameters and field measurements may be plotted in a log format and can be compared to expected levels of vibration from model outputs (Bailey et al. 2008)

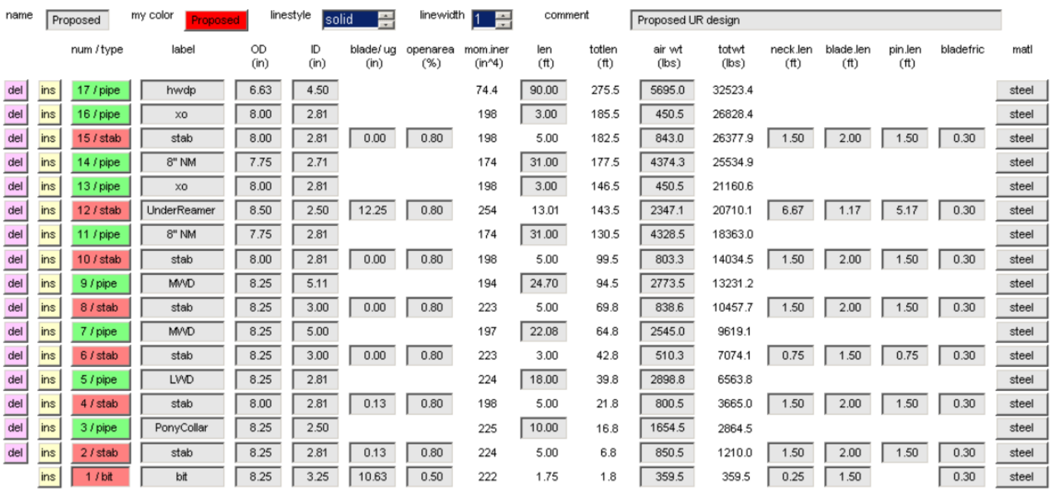

name Proposed | my color Proposed | linestyle solid | linewidth 1 | comment Proposed UR design

		num / type	label	OD (in)	ID (in)	blade/ ug (in)	openarea (%)	mom.iner (in^4)	len (ft)	totlen (ft)	air wt (lbs)	totwt (lbs)	neck.len (ft)	blade.len (ft)	pin.len (ft)	bladefric	matl
del	ins	17 / pipe	hwdp	6.63	4.50			74.4	90.00	275.5	5695.0	32523.4					steel
del	ins	16 / pipe	xo	8.00	2.81			198	3.00	185.5	450.5	26828.4					steel
del	ins	15 / stab	stab	8.00	2.81	0.00	0.80	198	5.00	182.5	843.0	26377.9	1.50	2.00	1.50	0.30	steel
del	ins	14 / pipe	8" NM	7.75	2.71			174	31.00	177.5	4374.3	25534.9					steel
del	ins	13 / pipe	xo	8.00	2.81			198	3.00	146.5	450.5	21160.6					steel
del	ins	12 / stab	UnderReamer	8.50	2.50	12.25	0.80	254	13.01	143.5	2347.1	20710.1	6.67	1.17	5.17	0.30	steel
del	ins	11 / pipe	8" NM	7.75	2.81			174	31.00	130.5	4328.5	18363.0					steel
del	ins	10 / stab	stab	8.00	2.81	0.00	0.80	198	5.00	99.5	803.3	14034.5	1.50	2.00	1.50	0.30	steel
del	ins	9 / pipe	MWD	8.25	5.11			194	24.70	94.5	2773.5	13231.2					steel
del	ins	8 / stab	stab	8.25	3.00	0.00	0.80	223	5.00	69.8	838.6	10457.7	1.50	2.00	1.50	0.30	steel
del	ins	7 / pipe	MWD	8.25	5.00			197	22.08	64.8	2545.0	9619.1					steel
del	ins	6 / stab	stab	8.25	3.00	0.00	0.80	223	3.00	42.8	510.3	7074.1	0.75	1.50	0.75	0.30	steel
del	ins	5 / pipe	LWD	8.25	2.81			224	18.00	39.8	2898.8	6563.8					steel
del	ins	4 / stab	stab	8.00	2.81	0.13	0.80	198	5.00	21.8	800.5	3665.0	1.50	2.00	1.50	0.30	steel
del	ins	3 / pipe	PonyCollar	8.25	2.50			225	10.00	16.8	1654.5	2864.5					steel
del	ins	2 / stab	stab	8.25	2.81	0.13	0.80	224	5.00	6.8	850.5	1210.0	1.50	2.00	1.50	0.30	steel
	ins	1 / bit	bit	8.25	3.25	10.63	0.50	222	1.75	1.8	359.5	359.5	0.25	1.50		0.30	steel

Figure 7.5: Graphical interface in a BHA optimization software (Bailey et al. 2008)

7.3.1 Field Validation

Numerous field trials of BHA designs exist in the literature. Bailey et al. (2008) give the results from drilling with a 10-5/8-inch drill bit with a 12-1/4-inch under-reamer in a vertical well with various LWD components. The employed service company for the job proposed the BHA in orange demonstrated in Figure 7.6.

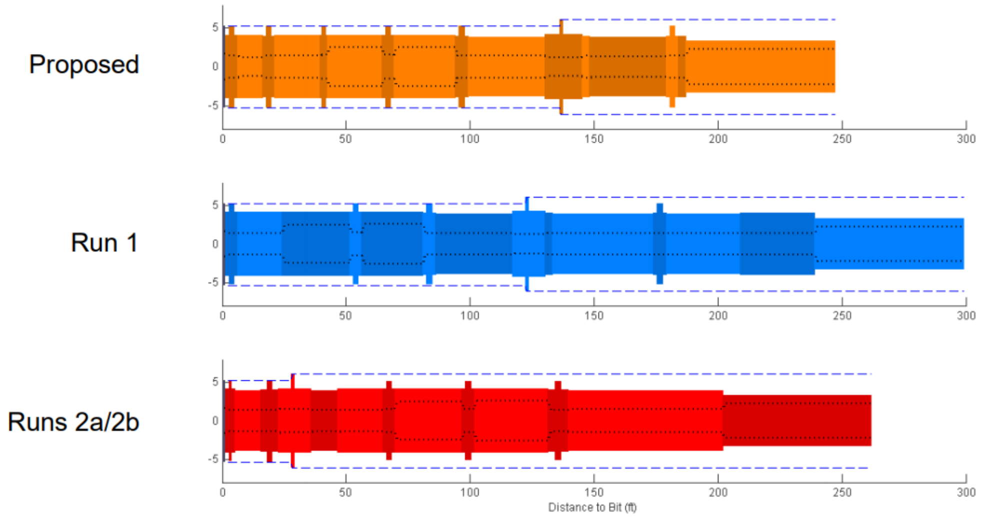

Figure 7.6: BHA configurations

The BHA initially proposed by the service company was not run. The blue design was used in run 1 and the red design were used in runs 2a and 2b(Bailey et al. 2008)

After BHA analysis, the proposed run was not run. Instead, BHA design in blue was selected for run 1 and the red design was used in runs 2a and 2b. The results of each run are given in Table 7.2.

Table 7.2: Bit run details from the case study described in Section 7.3.1 (Bailey et al. 2008).

Color	Bit Run	Footage	ROP	Comments from Morning Reports
Blue	1	1310 ft	15.4 ft/hr	"Had broken chip cutters at point, in gauge. Cutters on under-reamer looked good, grate at a 2."
Red	2a	161 ft	6.4 ft/hr	At end of run, "3 hours without making any new hole, attempted variable RPMs, weight, etc. with no success."
Pink	2b	24 ft	2.8 ft/hr	"Unable to keep bit on bottom due to excessive torque and stalling of bit. Pull string out of hole. Under-reamer wear pad ½ inch out of gauge, first set of cutters worn down."

From Table 7.2, it is clearly visible that the BHA in run 1 performed best from an ROP perspective. BHA modelling predicted that this would be the case, as the BHA used in run 1 performed the best across all dynamic properties. Lateral displacement diagrams for the three BHA designs are shown in Figure 7.7. The proposed BHA exhibited the largest lateral displacement, while the BHA used in run 1 was predicted to experience the least lateral displacement. The BHA in run 1 was also modelled to experience the least beam sheer forces, which is shown in APPENDIX B.2. Figure 7.8 shows measured surface parameters together with downhole MWD dynamic measurements. Collected logs are found to the left of the solid blue BHA demonstration in the figure and to the right are predicted index values calculated by the model. It is clear to see that the model correlates relatively well with the actual recorded lateral vibration data, which can be seen in the log track “vib lat”. This can be seen by comparing the “twirl” log which indicates predicted centrifugal forces affecting the BHA. The predicted twirl can be correlated to several lateral vibration spikes from the MWD logs, as highlighted by the rectangles. The transition from blue to red BHA is also companied by a step increase in vibrations, as was predicted by the software. Bailey et al. (2008) conducted several other case runs which also showed a relatively accurate correlation with predicted index values. Modelling and drilling simulation often can`t predict dynamic behavior accurately, but it can be used as a way to compare BHAs and their susceptibility to vibration.

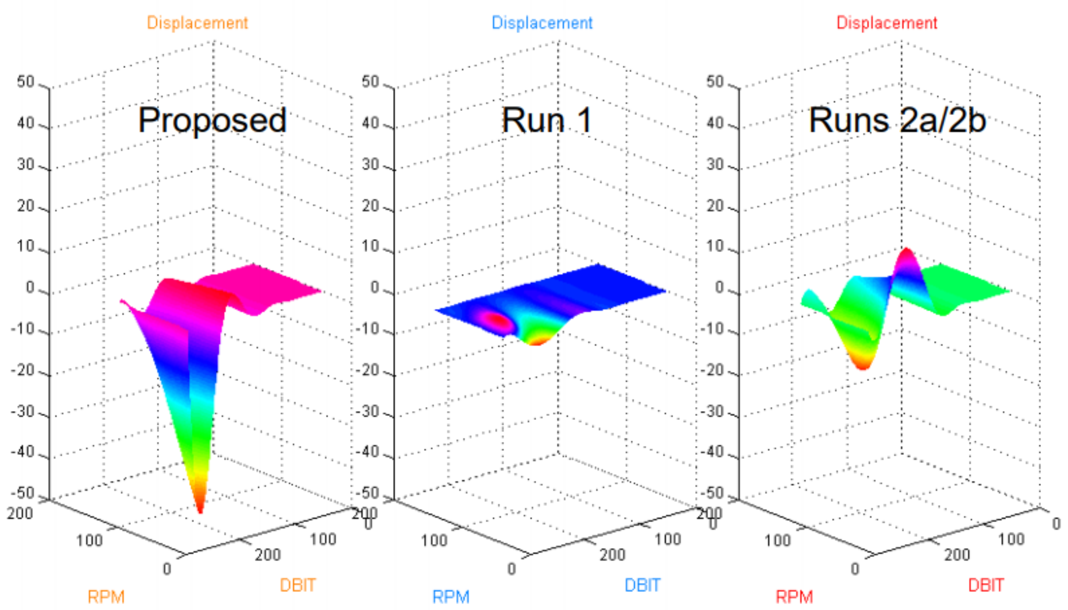

Figure 7.7: Displacement diagrams for the three BHAs (Bailey et al. 2008)

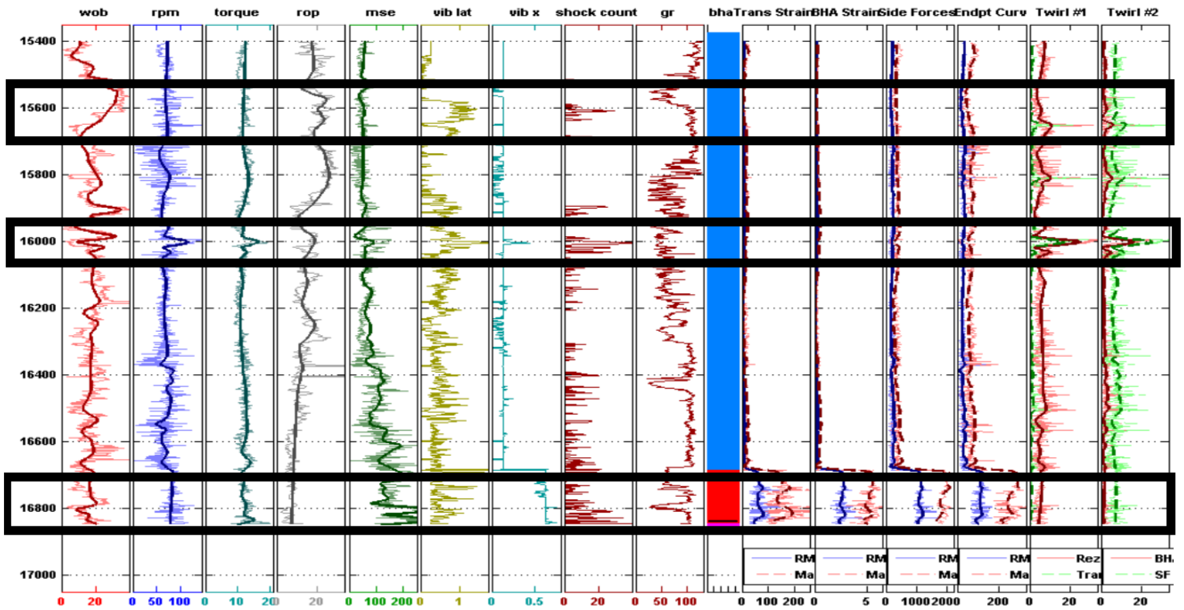

Figure 7.8: Measured surface parameters and MWD measurements compared to model predicted index values (Bailey et al. 2008)

The log tracks to the right of the BHA depth indicator displays predicted index values and the left side displays field measurements.

7.4 Roller Reamers

Section 3.4.4 described what in the industry is often referred to as “coupled stick-slip”. In coupled stick-slip, bit whirl increases the magnitude of BHA whirl due to the overgauged hole induced by bit whirl, allowing BHA whirl to become more severe. This severe BHA whirl produces large lateral shocks and side forces which in turn increases the friction forces with the wellbore wall. Large torque fluctuations are then induced and give rise to the term “coupled stick-slip”. When whirl is occurring exclusively, it is common to increase WOB to reduce whirl tendencies. With coupled stick-slip, this measure may often not be taken as increasing WOB shows a tendency to increase the torsional vibrations or even exceed the operating torque limits of drilling equipment. This means that the driller cannot operate with the desirable parameters to reduce whirl. By replacing conventional stabilizers with roller reamers, low friction bearings will reduce the torque generation between the contact points with the wellbore wall as demonstrated by Figure 7.9. The reduction of torque fluctuations allows additional WOB to be applied without exceeding the torque limitations of drilling equipment.

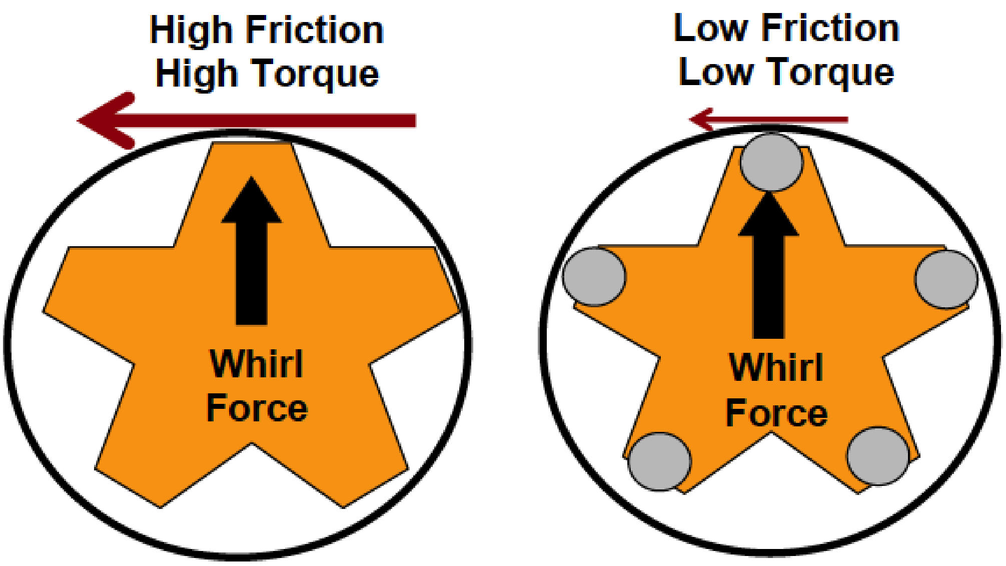

Figure 7.9: Reduction of torque increase when experiencing BHA whirl

The resulting torque in the contact point between BHA and wellbore wall is reduced due to reduced friction when using roller reamers as opposed to conventional stabilizers (Sowers et al. 2009).

The additional WOB may then reduce the initial bit whirl tendencies which create whirl-induced patterns on the wellbore wall. The result is a smoother, more in-gauge hole (Sowers et al. 2009). The BHA does not have room to accelerate in, reducing the side forces experienced by the BHA and resultingly also torque fluctuations. In summary, roller reamers reduce whirl tendencies by allowing optimal operating parameters to avoid whirl, which consequently reduces torque fluctuations created by the side forces experienced during whirl.

Roller reamers are often run with tungsten-carbide inserts which may help in eliminating whirl-induced patterns in the wellbore wall (Sowers et al. 2009). An example is instantaneous doglegs created by whirl. The tungsten-carbide inserts will then remove rock to reduce the severity of the instantaneous dogleg.

7.4.1 Field validation

A study was made by a major operator, drilling four extended reach wells in one field (Sowers et al. 2009). The BHAs used in the 12¼ in sections of the four wells are shown in Figure 7.10. Post run BHA analysis revealed that BHA A and B had less propensity for lateral vibrations than BHA C and D. The BHA in Well C had more propensity to vibrate than Well D. This means that the BHAs employing roller reamers should record higher lateral vibrations than those only using conventional stabilizers (BHA A&B).

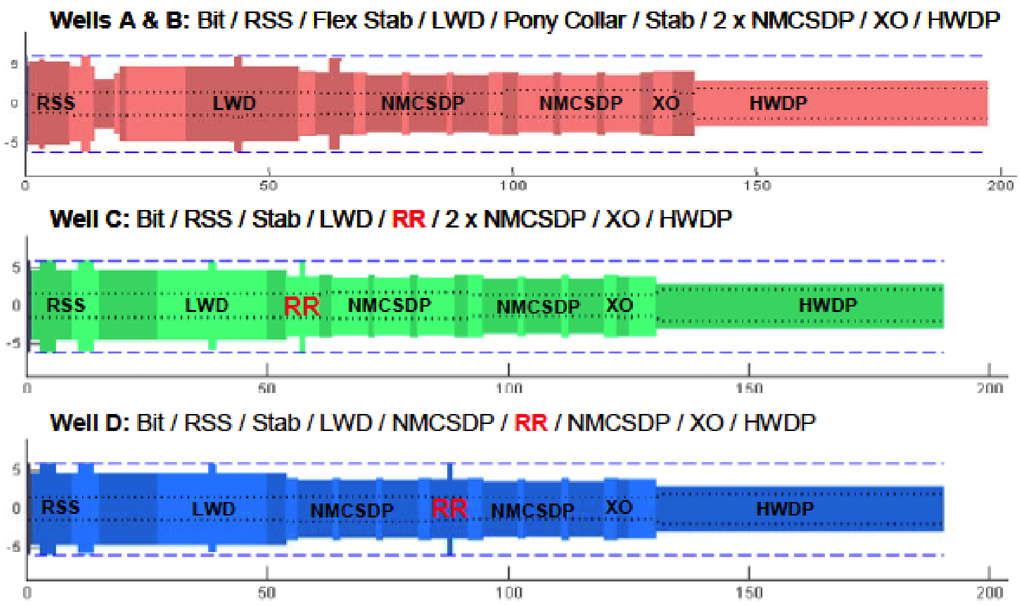

Figure 7.10: BHA comparison of 4 wells drilled in the same field by a major operator (Sowers et al. 2009)

Vibrations measurements for the four wells are shown in Figure 7.11. It is apparent that wells A and B experienced less lateral vibrations than wells C and D, however the vibrations for these wells are connected to more severe stick-slip vibrations. The wells employing roller reamers show little tendency to experience severe torsional vibrations. The fact that Well C experienced more lateral vibrations than Well D is explained by the post BHA analysis. Since the roller reamer BHAs allowed more torque to be delivered to the bit, a higher WOB was applied for wells C and D. These wells required less energy to drill and drilled smoother wellbores than well A and B. Less energy was then lost to friction and whirl, which is reflected by MSE measurements shown in Figure 7.12.

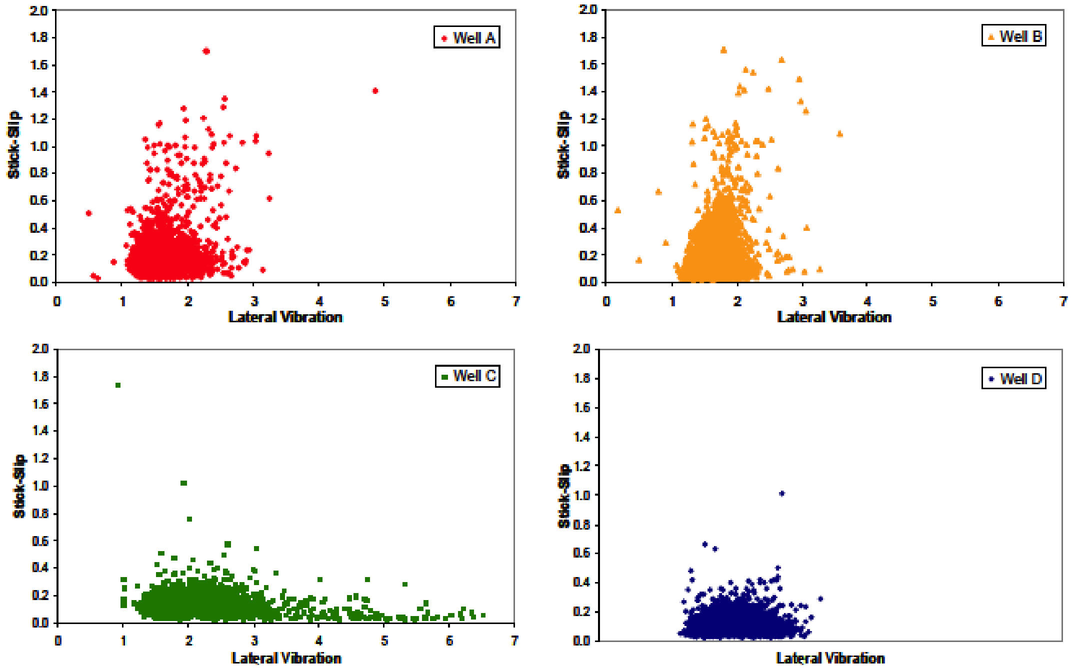

Figure 7.11: Stick-slip and lateral vibration severity in the 12 ¼ in section of four different wells

Post BHA analysis showed that the increased lateral vibration levels of Well C and D was due to the BHAs propensity to laterally vibrate. Well C and D show a clear reduction in stick-slip, theorized to be due to less whirl.

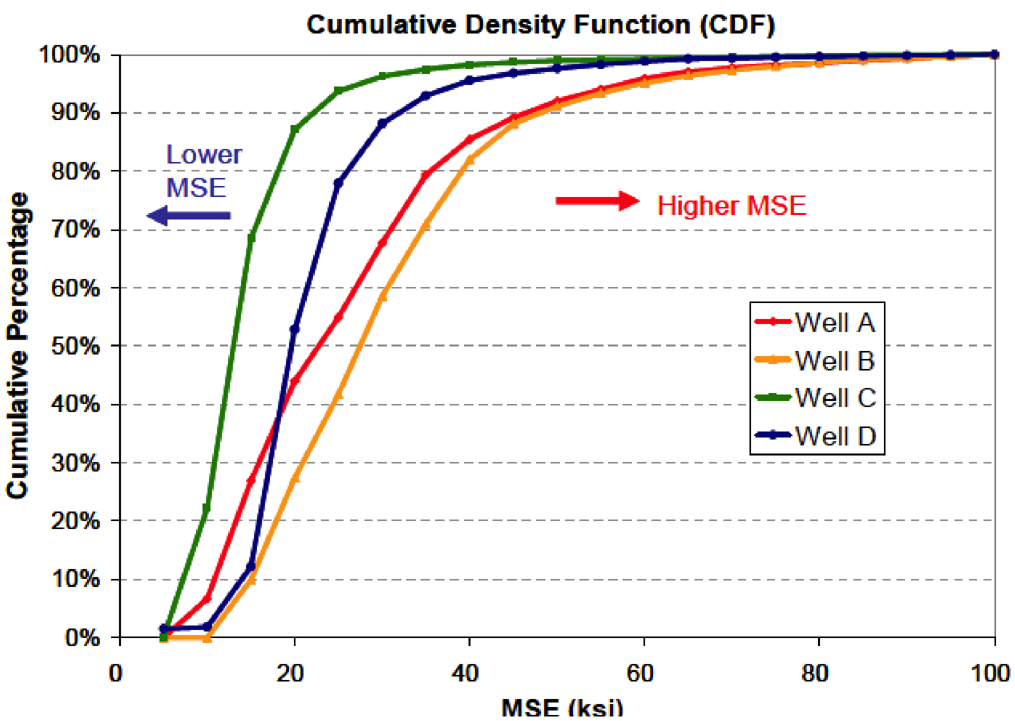

Figure 7.12: MSE measurements from four wells drilled

Well C and D used roller reamers in the BHA which allowed additional WOB to be applied. This in turn reduced energy lost to whirl and friction, lowering MSE.

7.5 Anti Stick-Slip Technology (AST)

The need for predictable results has driven the development of drilling technology and vibration mitigating tools. The Anti Stick-Slip Technology addresses stick-slip behavior resulting from bit/rock interaction, more specifically cutter induced stick-slip. Since its arrival to the petroleum drilling industry the tool has made its way around the world and is often used a standard by many operators.

A preloaded spring in the tool contracts once the reactive torque on bit is increased past a threshold value set by the preloaded spring. The contraction leads to a reduction in weight on bit and consequentially a reduction in depth of cut, as indicated by Figure 7.13. Whereas conventional bottom hole assemblies would stall out in order to build up enough torque for the bit to break free, the reduction in depth of cut and consequentially reduction of torque required to shear the rock allows for continuous drilling. The reactive torque that initially caused the spring to contract is released gradually, allowing the tool to be ready for the next cycle of torque variations.

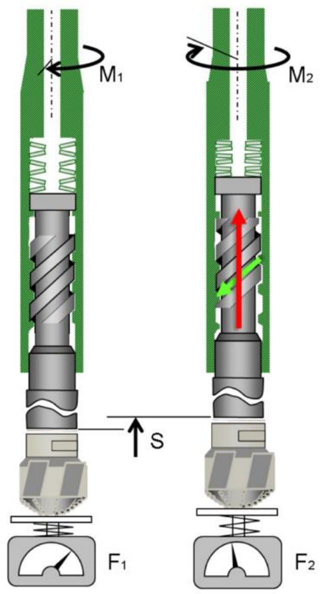

Figure 7.13: A simplified model of the antistall tool

An increase in reactive torque from M_1 to M_2 causes the preloaded spring to contract, reducing WOB and depth of cut (DOC).

7.5.1 Field Validation

Results from running the AST tool in formations known to induce stick-slip and damage to PDC cutters at test rigs show that the tool gives several benefits (Selnes et al. 2009). The results from running the AST tool was compared to a reference run without the tool, but with all other parameters kept equal, including the increase in weight on bit over the drilling interval. Drilling parameters from the two runs on the test facility is shown in Figure 7.14. The test showed a significant reduction of min/max torque interval, as well as increased ROP despite a reduction in WOB.

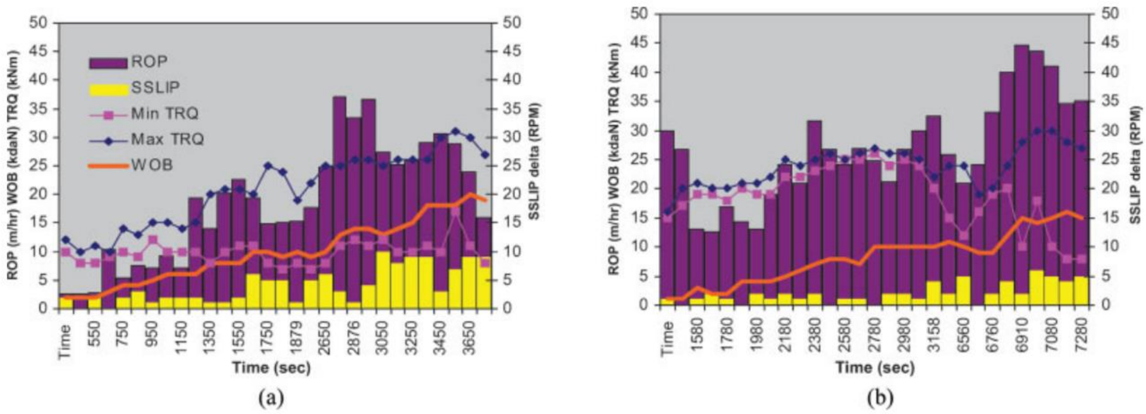

Figure 7.14: Drilling parameters from test rig (a) With AST (b) Without AST

Field tests were also carried out based on the promising test rig results. Field tests were found to be concurrent with the previous test facility findings, indicating the following results (Selnes et al. 2009):

- More stable levels of drilling torque
- Stick-slip severity reduced
- No occurrences of MWD failures
- No occurrences of overtorqued pipe connections
- Faster drilling

7.6 Depth of Cut Control (DOCC)

The constantly increasing range of formation hardness in which PDC bits are being used have resulted in increased attention to the torsional dysfunctions related to this bit type. Operator`s constantly increasing ROP demands leads to increased weight on bit applied when drilling with PDC bits. Increased weight on bit means increased depth of cut and resultingly, increased reactive torque. The latter is what often triggers stick-slip vibrations. By adding rubber elements to PDC drill bits, the indentation depth of the cutters can be limited, despite variations in WOB. This is demonstrated in Figure 7.15, where it is clearly visible that standard cutter exposure (left) will allow a high DOC before the bit body engages the formation. With DOCC, rubber elements or part of the bit body can be used to control the amount of bite into the formation. Real images from industry run bits with DOCC can be seen in APPENDIX B.3.

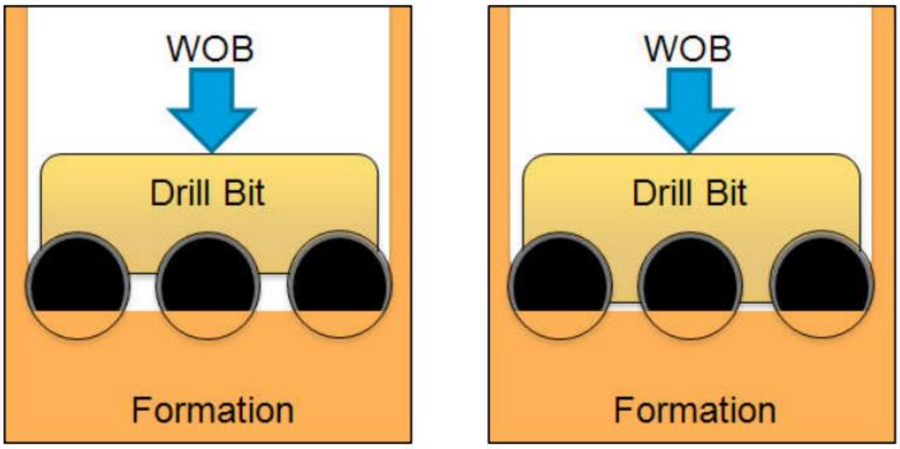

Figure 7.15: Sketch depicting WOB applied to bit without- (left) and with (right) DOCC control (Schwefe et al. 2014)

Once adequate WOB is applied for these rubber elements to contact the bottom of the well, additional WOB is supported by these bearing rubber elements instead of leading to increased depth of cut. Equally, reactive torque will also decrease when increasing applied WOB beyond DOC element engagement. Figure 7.16 demonstrates how the reactive torque deviates from the conventional linear relationship with WOB after the bearing elements engage the formation.

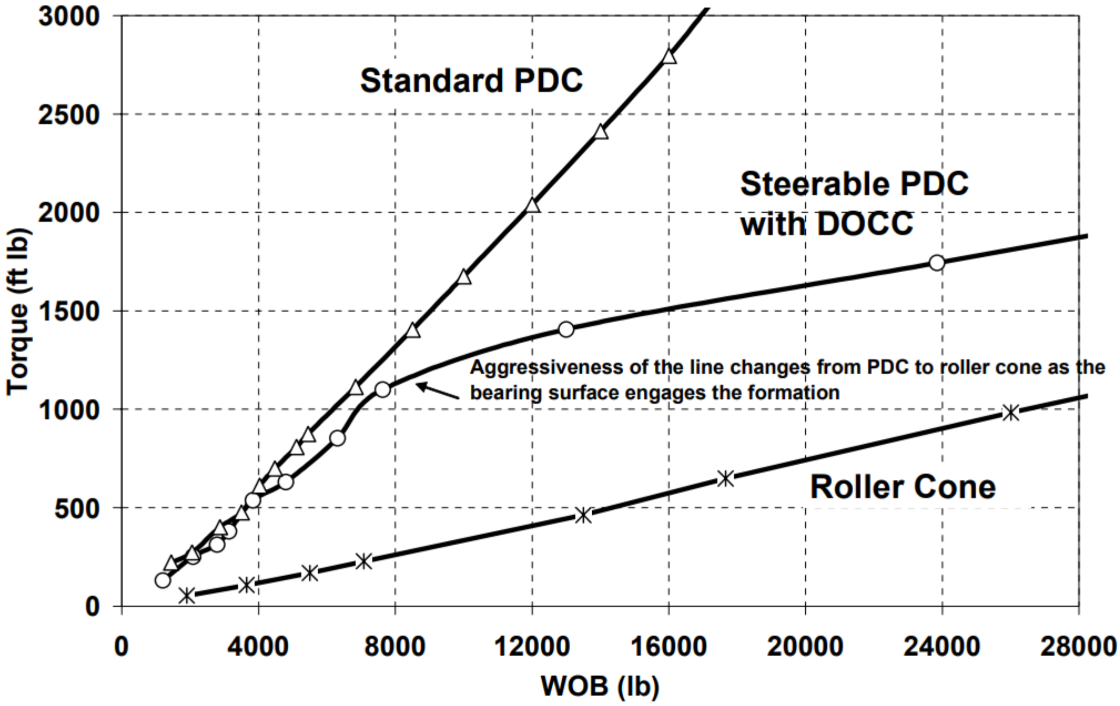

Figure 7.16: WOB/torque relationship for different bit types (Jaggi et al. 2007)

7.6.1 Field Validation

Schwefe et al. (2014) ran tests using five different PDCs bits on a full-scale research rig. The objective was to characterize the optimal type and extent of DOC control capable of negating stick-slip vibrations. Downhole vibration sensors positioned in the shank of the bit capable of measuring high-frequency data were used to determine the severity of stick-slip vibrations. Bits were labelled A, B, C, D and E with A to D having an increased depth of cut control i.e. decreasing cutter exposure. Bit E had identical amount of DOC control as bit B, however this bit used feature-based DOC control (rubber element) as opposed to DOCC using the bit body. DOC is calculated using Equation 7.13.

$$DOC\ [in/rev] = \frac{ROP}{RPM} = \frac{[m/hr]}{1.5\ \times [RPM]} \tag{7.13}$$

Accordingly, increasing the ROP implicates increased cutter exposure when the RPM is kept constant. Figure 7.17 shows the DOCC profile as cutter exposure increases. It is noticeable that increasing depth of cut with bit A activates very little depth of cut control. Contrarily, bit B exhibits depth of cut control as soon as drilling commences.

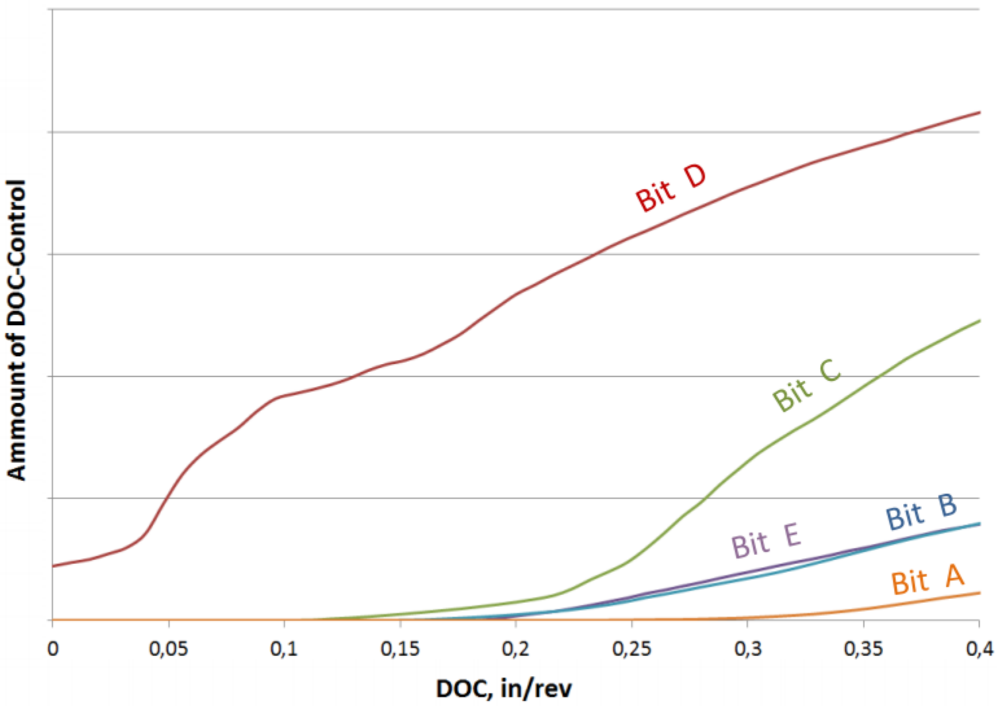

Figure 7.17: Depth of cut control vs depth of cut for five different bit PDC bits (Schwefe et al. 2014)

Bit A had little to zero depth of cut control and exhibited stick-slip tendencies at 10-15 k-lb WOB. Bit B also exhibited stick-slip tendencies; however, this bit pushed the WOB capabilities before stick-slip was initiated to 30 k-lb WOB. Bit C exhibited stick-slip at very low rotary speeds (below 30 RPM), however it was difficult to initiate stick-slip with this bit at rotary speeds above this value. WOB had to be increased to above 50 k-lb to initiate stick-slip with bit C. The results demonstrate a clear trend of DOCC pushing the WOB limit before stick-slip is initiated. Stability maps depicting the results are given in APPENDIX B.3.

Results indicating that increasing DOCC pushes the limit before drilling dysfunctions set in gives rise to the question: to what degree should DOCC be used before it has a negative impact on drilling performance? Tests run with bit B, C and D were run in limestone formations. The results are demonstrated in APPENDIX B.3. Bit B exhibited stick-slip vibrations at low WOB for all RPM values. Bit C did not exhibit stick-slip above 90 RPM. Bit D showed a marginal improvement in stick-slip behavior compared to bit C, as WOB could be increased beyond 30 k-lb before stick-slip was initiated.

Drilling efficiencies are demonstrated in Figure 7.18. Despite the improvements in propensity to develop stick-slip vibrations, bit D drilled less efficiently than bit B and C. The two latter mentioned bits exhibited lower values of MSE at any given ROP, indicating more efficient drilling. Bit B, with the least depth of cut control, drilled the most efficiently in this comparison. Tests were then conducted to compare bit B to the bit with no DOCC (bit A). Results from this test are given in APPENDIX B.3. Bit B drilled more efficiently than the bit with zero DOCC and also more efficiently than bit C with more DOCC. These tests led the authors to conclude that DOC can be tuned to find the optimal relationship between vibration mitigation and energy loss reduction. In conclusion, DOCC improves the WOB threshold at any given RPM, but excessive DOCC may lead to inefficient drilling.

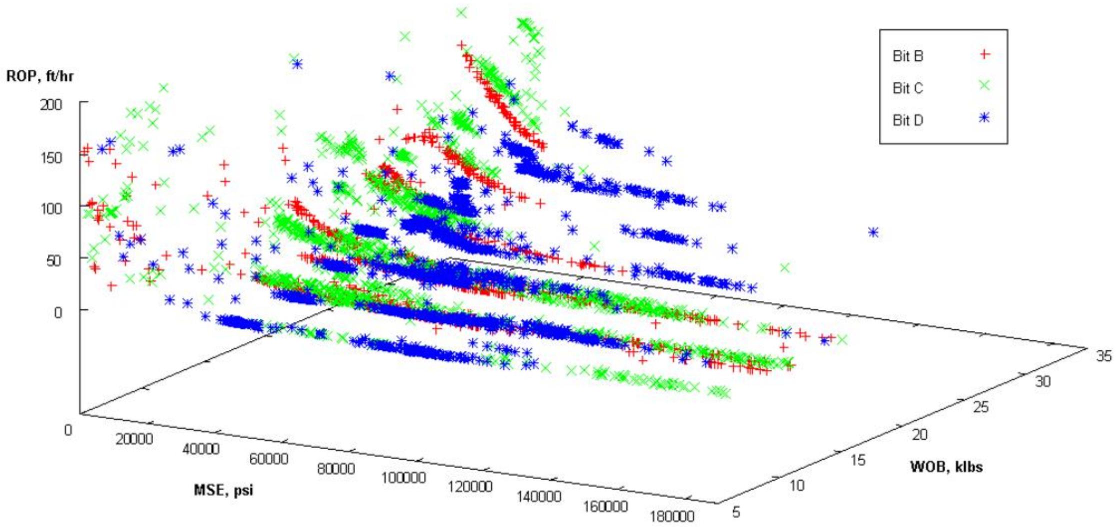

Figure 7.18: Drilling efficiency as determined by mechanical specific energy (MSE) for the different bit types (Schwefe et al. 2014)

7.7 Soft Torque Rotary Systems (STRS)

Drill pipe essentially works as a transmission line for torsional waves. A variation in the downhole torque will propagate upwards to the top drive. Most top drives are designed to maintain a constant RPM, unaffected by these torsional waves that reach the surface. Since the top drive attempts to keep the same rotational rate independent of torque loads, it works as a fixed end, reflecting the torsional waves back down. Effectively, a torsional wave reaching surface slows down the rotation speed due to increased torque demands. This triggers the control system to increase the rotary drive current, which leads to the reflection of the torsional wave, as mentioned earlier. Soft torque softens the response of the top drive by decreasing the increase in speed when the torsional wave reaches the top drive. In summary, soft torque rotary systems works as a compromise between maintaining constant RPM and constant torque. Drill pipe and BHA will then experience lower torque variations while the RPM of the system will vary around a set value. Even though the system is then designed to vary RPM at surface slightly, the RPM downhole will be much more constant than in the case of stick-slip vibrations.

The physics behind soft torque shows that theoretically, it has a large potential to dampen out torsional vibrations. Despite this and the fact that many rigs have STRS installed, field experiences are not as positive as the physics and modelling have predicted. This has resulted in the system often being disabled. Dwars (2015) reviewed some of the drawbacks of STRS and summarized some of the drivers for improvement:

- STRS requires the driller to manually enter different stiffness and damping values for every stand of drill pipe added. The lack of devotion to this labor-intensive process may often be the reason why the potential of STRS is not realized. The driller may be occupied with several other tasks making another added manual labor process excessive.
- Real drillstrings have multiple eigenfrequencies due to the system being made up of several components. Lumped mass, lumped stiffness models give the drillstring one stiffness and one BHA inertia which in some cases will be inaccurate.
- Soft torque models the drillstring as a second order inertia-stiffness system with no time delay (Dwars 2015). With 3 km of drill pipe, a total of 2 seconds is used by torsional waves from the BHA to the top drive and back downhole. Stick-slip manifests in 2-10 seconds and therefore this discrepancy reduces the dampening effect of STRS.
- Global feedback from STRS technology shows that there is an envelope where the system performs well. This envelope is between 1500- and 4500-meter length of the drillstring. Outside this envelope, the system still functions, yet the best results are achieved within the stated range of drillstring length.

7.7.1 Field Validation

STRS was used drilling offshore in Qatar in an effort to reduce failures related to stick-slip vibrations (Attar et al. 2014). The wells being drilled were a part of the Pearl GTL development wells in a simultaneous operations campaign. Several failures had been attributed to stick-slip vibrations in previous drilling operations. STRS was used in the final 7 wells and were compared to the previous wells drilled by a sister rig, identical in design but not equipped with STRS. The two rigs operated in the same field, however differences in formation thicknesses, depths and formation strengths will give rise to some random variation.

Studying the effect of the physical principles used by STRS, namely varying RPM in order to dampen out torque fluctuations, a segment where torque fluctuations was observed is examined. The section is shown in Figure 7.19, where torque fluctuations trigger the STRS to vary RPM around the set value. Torque fluctuations are immediately reduced as the STRS sets in and the damping increases as time progresses. The tables showing ROP, stick-slip percentage and bit wear are given in APPENDIX B.4.

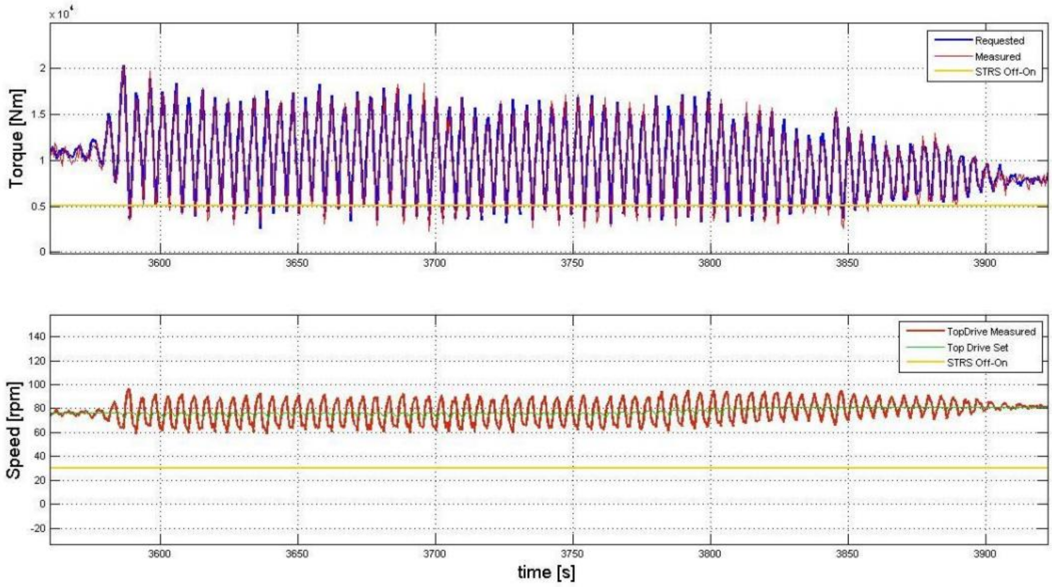

Figure 7.19: Torque fluctuations trigger STRS to vary RPM around set value (Attar et al. 2014)

Comparing the experiences from using or not using STRS on a well level, the authors state that a 30% increase in ROP, a 41% reduction in stick-slip phenomena and 35% less bit teeth damage was experienced while drilling the troublesome 8 ½" sections (Attar et al. 2014).

7.7.2 Future Rotary System Developments

New developments within top drive technology target the limitations of STRS given in Section 7.7. Z-torque is a novel technology which views the system as waveguides or transmission lines (Dwars 2015). Waves propagating along the drillstring will be partially reflected at abrupt variations in a physical parameter called wave impedance. This is the case for geometric interfaces such as between tools in the BHA, the transition from BHA to drill pipe and the interface between drill pipe and top drive. When two components have identical wave impedances, the wave continues with no reflection. Z-torque uses this physical principle to manipulate the impedance of the top drive so that it is identical to the impedance of drill pipe. In this manner, the torsional wave travelling to surface would reach the top drive and travel on. This stops the self-exciting vibration behavior since the torque does not propagate back downhole. In doing this, the manual tuning of present soft torque rotary systems would be eliminated.

7.8 Wired Drill Pipe (WDP)

Wired drill pipe applications have been mentioned frequently by literature since the introduction of the technology. Much focus has been concentrated on the time savings of WDP since it reduces time spent on downlinking and running wireline logging trips. An additional benefit to the technology is the drastically improved downhole dynamic picture, uncovering a huge potential in real time diagnostics.

The drawbacks of mud pulse telemetry (MPT) listed in Section 6.1, namely data rate transfer and problems related to noise and signal attenuation is what has given rise to wired pipe telemetry. Wired drill pipe offers a bandwidth more than 1000 times greater than that of conventional MPT. Data rates achieved with wired pipe reach up to 57,600 bps, compared to 20-40 bps achieved with mud pulse transmission (McCartney et al. 2009). The low bandwidth of MPT MWD systems meant that parameters must be sent to surface in a prioritized order. Dynamic data has historically not been prioritized since parameters more crucial to the operation has instead taken precedence. The low data rate with MPT has in some cases been an ROP limiter to secure sufficient data density when attempting to optimize wellbore placement within a reservoir (McCartney et al. 2009). With wired drill pipe the bandwidth is large enough to yield real time monitoring with a high sample rate of all parameters, regardless of ROP.

7.8.1 Wired Drill Pipe components

Conventional drill pipe is modified to accommodate a high-speed data cable stretching along the length of the joint. The cable transitions to inductive coils contained in the pin nose and corresponding box shoulder of every connection, as seen in Figure 7.20. After being threaded together, the coil within both pin- and box end are in proximity. An alternating current flowing through the coil in either end produces a changing electromagnetic field in the other end, inducing current flow in the adjacent coil (Reeves et al. 2005)

.

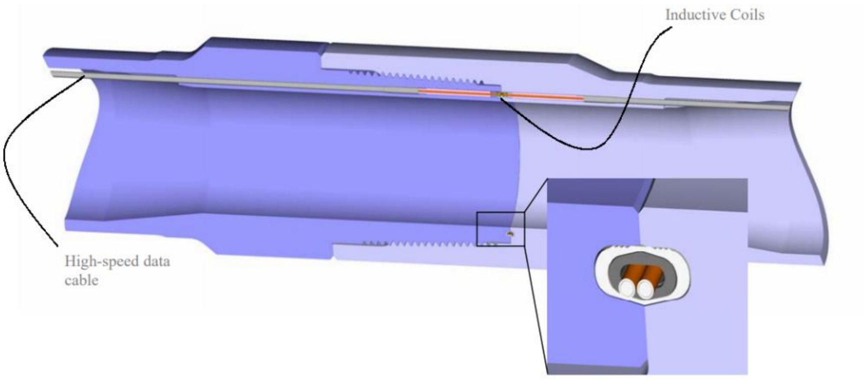

Figure 7.20: Made-up wired drill pipe coupling (Reeves et al. 2005)

After being threaded together, the coil within the pin end and the coil within the box end are in proximity. An alternating current flowing through the coil in either end produces a changing electromagnetic field, inducing current flow in the adjacent coil.

The signal is carried through the drill pipe, reaching an interface sub which allows bi-directional transmission to the BHA tools. Data boosters are contained within tool joints which amplify the signal approximately every 1500 ft in order to increase the signal to noise ratio (McCartney et al. 2009). Finally, on the surface end of the drill string, a top drive swivel extracts the signal from the rotating drillstring to a surface data acquisition system. The entirety of the system is shown in Figure 7.21.

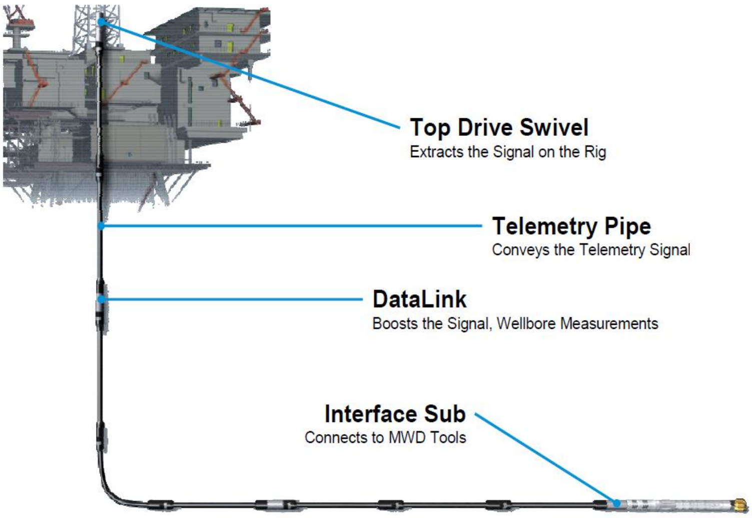

Figure 7.21: Wired drill pipe system (McCartney et al. 2009)

7.8.2 Field Validation

McCartney et al. (2009) used both MPT and WDP to record and transfer downhole vibration data with the aim of visualizing the difference in resolution for the two transmission systems.

The results are shown in Figure 7.22, where it is clearly visible that a large amount of torsional vibrations is overlooked by conventional MPT. In this case several minutes of relatively severe stick-slip go by unnoticed, which could be detrimental for the bit and downhole components.

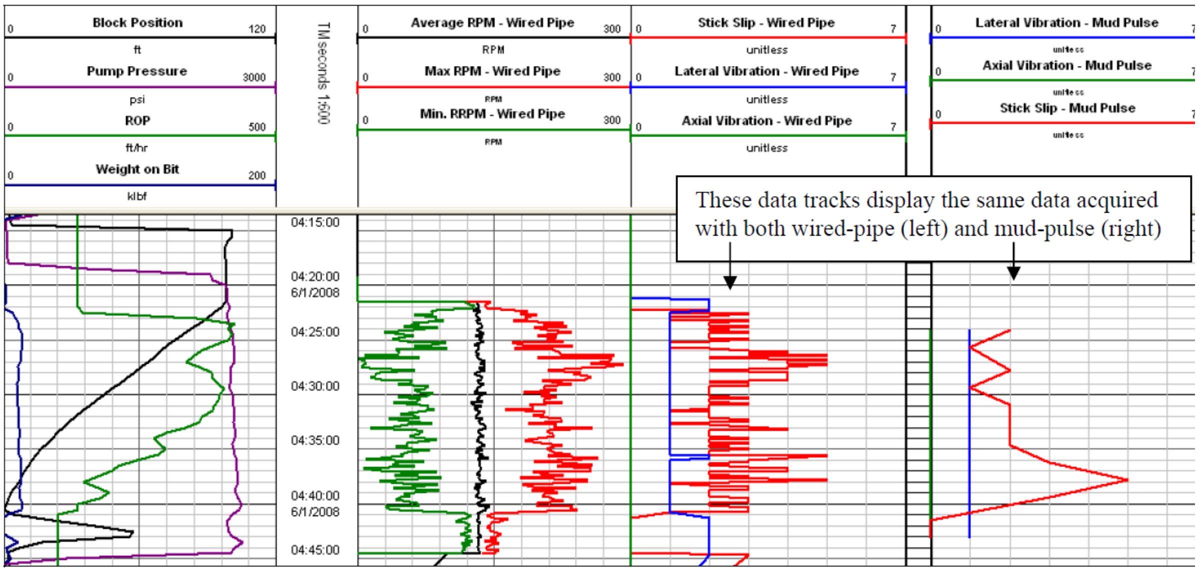

Figure 7.22: Vibrations downhole according to WDP (left track) and MPT (right track) (McCartney et al. 2009)

Section 6.4.4 described that whirl and lateral vibrations can be identified when a non-linear response of ROP to WOB occurs. This is also marked by an increase in MSE, since energy that should be used in increasing ROP is instead dissipated elsewhere in the system. Giltner et al. (2019) demonstrated that wired drill pipe allows accurate detection of this in real time. The event is demonstrated in Figure 7.23, where lateral vibrations were apparent. The decision was to lower the RPM, which resulted in more weight being transferred to the bit due to reduced whirling tendencies. A clear ROP increase was seen after the change was made, as indicated by the blue line in the right track of Figure 7.23. Correspondingly, MSE decreased as the energy being consumed by vibrations were instead directed to increasing the ROP.

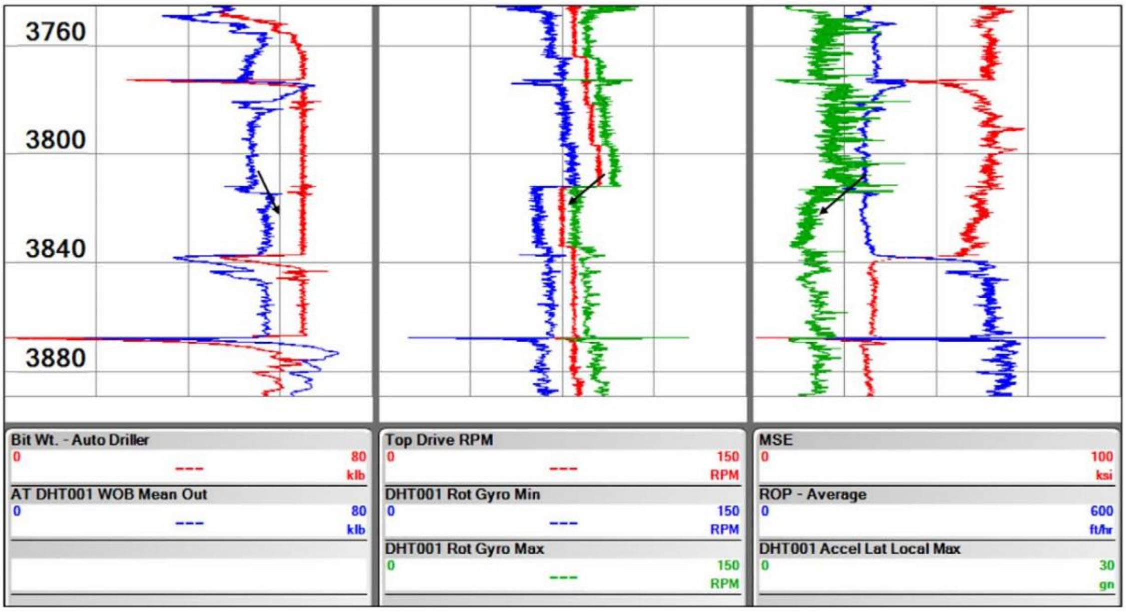

Figure 7.23: Lateral vibrations detected using WDP (Giltner et al. 2019)

The decision to reduce RPM resulted in increased weight being delivered to the bit and increased ROP.

7.9 Mass Imbalance

As mentioned in Section 4.3, assembling a perfectly balanced drillstring is impossible due to the existing imbalance in many tools and the manufacturing difficulties in creating perfectly balanced drill collar and drill pipe. However, preventative measures can be made to decrease the severity of lateral vibrations due to mass imbalance. Dykstra et al. (1994) demonstrated that rotating drill collar assemblies at surface can be done to visually inspect the severity of imbalance in a given drill collar joint or assembly. In this manner, nearly balanced collars should be used near the bit. If severe imbalance seems to be apparent in all assemblies, shortening the distance between stabilizers will decrease the lateral deflection between these nodal points. This will in turn prevent resonance of lateral modes to affect the bit.

Since large lateral shocks coincide with the natural frequency of drill collars, adjusting the rotary speed according to downhole acceleration measurements is an easy preventative measure to avoid potentially damaging vibrations.

The interaction between wellbore and BHA/drill collar due to mass imbalance can be observed as large increases in torque due to the transition from forward to backward whirl (Dykstra et al. 1994). In this manner, the onset of backward whirl can be monitored from torque logs

.

8 Conclusions

Drillstring vibrations occur in axial, torsional or lateral directions and can occur in coupled modes as combinations of the three. Coupling between axial and torsional or axial and lateral modes are common due to periodic shortening of the drillstring when it assumes a wound up- or curved shape. Severe vibrations can lead to huge costs as damaged components downhole may result in otherwise unnecessary trips in and out of the hole and in the worst case, the need to sidetrack.

The consequences of vibrations go beyond damages to the drillstring exclusively. Wellbore instabilities can be induced by fatigue failure of the formation, which can readily occur when lateral vibrations displace the drillstring to interact with the wellbore wall. A common misconception in drilling is that a high-quality wellbore comes at the expense of ROP, however when taking the potential complications resulting from wellbore instabilities into account this is rarely the case.

Ways of identifying the various vibration types have been addressed. The potential of MSE as a measure to identify drilling dysfunctions and therein vibrations was demonstrated. The variation in measurement tools, sensors and definitions between different service companies have been addressed to make the engineer aware of the challenges when comparing results between service providers. The limitations in bandwidth of conventional mud pulse MWD systems was described to emphasis the difficulty in identifying vibrations downhole in real-time.

Several tools and techniques designed to mitigate and negate the different types of drillstring vibrations described and their validity through field studies were analyzed:

- BHA design modelling has been used to determine the susceptibility of various BHA designs to different vibration types. Field experiences indicate that BHA modelling software is able to predict the dynamic behavior of BHAs to a certain degree. Instead of accurately identifying all vibrations bound to incur in a given run, it is more helpful to determine which BHA design that will be least likely to experience severe vibrations.
- Roller reamers were identified as a good substitute for conventional fixed stabilizers, as the rolling motion decreases friction with the wellbore wall. This allows the driller to increase WOB to reduce whirl without the onset of stick-slip due to the overall reduced reactive torque in the system. Field validation showed that

more WOB could be applied and the wellbore quality was higher due to reduced levels of lateral vibrations.

- Experiences from field use of Anti Stick-Slip Technology indicated a substantial reduction in the variation of minimum and maximum torque. The stick-slip severity was reduced, and occurrences of MWD failures and overtorqued pipe connections were reduced to zero.
- Depth of cut control (DOCC) was described and field experiences indicate that DOCC pushes the limitations in WOB and RPM before stick-slip occurs. Tests with varying degree of depth of cut demonstrated the depth of cut control can be exaggerated to a point where drilling becomes less efficient.
- Field studies using wired drill pipe (WDP) instead of conventional drill pipe demonstrated how the increased bandwidth in WDP allowed the driller to identify lateral vibrations where conventional mud pulse did not indicate any drilling dysfunction. The driller increased WOB which resulted in reduced vibration levels and increased ROP.
- Recommendations of parameter manipulation was given to address the various vibrational types. Drilling advisory systems were described and the potential of these systems in quickly identifying inefficient drilling or vibrations were highlighted.
- The limitations in real-time mitigation of vibrations underline the importance in pre-run preparation and design. A suggested workflow was proposed to improve preparation for future runs and improve learnings from previous runs.

9 Recommendations for Future Work

The wide scope of this thesis has opened many doors for further research. The thesis was intended to increase drillstring vibration knowledge of engineers employed by operating companies. It is not efficient for this type of engineer to specialize at particular tools or techniques to mitigate vibrations. Instead this engineer must be agile and able to adapt to working with several service providers. In this regard, it could be useful to explore the variations in measurement techniques and data provided by the various service companies. In doing this, a proposal to standardization could be made which would increase transparency between service companies. The different practices in response to the various vibration modes could be compared between service providers.

The introduction of wired drill pipe has enabled real time high frequency data of downhole dynamic behavior. Combining this with a drilling advisory system could potentially allow real-time rapid correcting actions without the use of human interaction. This would in turn require that the correct mitigating actions have been implemented in an algorithm which is used by the advisory system. A complete system able to mitigate any dysfunction would be a major endeavor, however the stepwise implementation of for individual vibration types, as for example stick-slip could be experimented with. The increased cost of wired drill pipe could also be compared to the cost of conventional drill pipe when increase bit- and component lifetimes are taken into consideration

10 References

Elastic Waves. In *Dynamic Behavior of Materials*, 23-65.

2019. Axial Shortening, (accessed 01.12.2019 2019).

Aadnoy, B.S., Aadnøy, B.S., and Engineers, Society of Petroleum. 2009. *Advanced Drilling and Well Technology*: Society of Petroleum Engineers.

Al Hammadi, Yousef, Al Harbi, Ahmed, Hermawirawan, Lutfi et al. 2018. Hybrid Bit Technology: Transforming Tricone-Bit Drilling to New Levels. Presented at the Abu Dhabi International Petroleum Exhibition & Conference, Abu Dhabi, UAE. 2018/11/12/. https://doi.org/10.2118/193178-MS.

AlBahrani, Hussain and Al-Yami, Abdullah. 2018. Drillstring Vibrations and Wellbore Quality: Where Drillstring Design Meets Geomechanics. Presented at the Abu Dhabi International Petroleum Exhibition & Conference, Abu Dhabi, UAE. 2018/11/12/. https://doi.org/10.2118/193253-MS.

Attar, F., Grauwmans, R., and Ikhajiagbe, O. 2014. Soft Torque Impact on Drilling Performance in Qatar. Presented at the International Petroleum Technology Conference, Doha, Qatar. 2014/1/19/. https://doi.org/10.2523/IPTC-17651-MS.

Bailey, J. R., Pastusek, P. E., Junaibi, H. Al et al. 2016. An Integrated Workflow to Mitigate Drilling Vibrations and Increase Daily Footage. Presented at the Abu Dhabi International Petroleum Exhibition & Conference, Abu Dhabi, UAE. 2016/11/7/. https://doi.org/10.2118/183550-MS.

Bailey, Jeffrey R., Biediger, Erika, Gupta, Vishwas et al. 2008. Drilling Vibrations Modeling and Field Validation. Presented at the IADC/SPE Drilling Conference, Orlando, Florida, USA. 2008/1/1/. https://doi.org/10.2118/112650-MS.

Bailey, Jeffrey R., Wang, Lei, Tenny, Matthew et al. 2010. Design Tools and Workflows To Mitigate Drilling Vibrations. Presented at the SPE Annual Technical Conference and Exhibition, Florence, Italy. 2010/1/1/. https://doi.org/10.2118/135439-MS.

Berntsen, Mads. 2019. *Drillstring Vibrations: A Theorethical foundation*Specialization Project, Norwegian University of Science and Technology, Trondheim.

Bowler, Adam Ian, Logesparan, Lojini, Sugiura, Junichi et al. 2014. Continuous High-Frequency Measurements of the Drilling Process Provide New Insights into Drilling System Response and Transitions between Vibration Modes. Presented at the SPE Annual Technical Conference and Exhibition, Amsterdam, The Netherlands. 2014/10/27/. https://doi.org/10.2118/170713-MS.

Brett, J. F. 1992. The Genesis of Bit-Induced Torsional Drillstring Vibrations. *SPE Drilling Engineering* **7** (03): 168-174. https://doi.org/10.2118/21943-PA.

Brett, J. F., Warren, T. M., and Behr, S. M. 1989. Bit Whirl: A New Theory of PDC Bit Failure. Presented at the SPE Annual Technical Conference and Exhibition, San Antonio, Texas. 1989/1/1/. https://doi.org/10.2118/19571-MS.

Cayeux, Eric. 2019. *Stick-slips and side-effects from downlinking procedures during drilling operations in the Eldfisk and Ekofisk fields*. DrillWell SFI seminar (Reprint).

Cayeux, Eric, Ambrus, Adrian, Øy, Lars et al. 2020. Analysis of Torsional Stick-Slip Situations Observed with Downhole High-Frequency Magnetometer Data. Presented at the IADC/SPE International Drilling Conference and Exhibition, Galveston, Texas, USA. 2020/2/25/. https://doi.org/10.2118/199678-MS.

Chen, Shilin, Wisinger, John, Dunbar, Brad et al. 2020. Identification and Mitigation of Friction- and Cutting-Action-Induced Stick/Slip Vibrations with PDC Bits. *SPE Drilling & Completion* **Preprint** (Preprint): 12. https://doi.org/10.2118/199639-PA.

Dareing, D. W. 2012. *Mechanics of Drillstrings and Marine Risers*: ASME Press.

Davis, Joshua, Smyth, Gregory F., Bolivar, Neil et al. 2012. Eliminating Stick-Slip by Managing Bit Depth of Cut and Minimizing Variable Torque in the Drillstring. Presented at the IADC/SPE Drilling Conference and Exhibition, San Diego, California, USA. 2012/1/1/. https://doi.org/10.2118/151133-MS.

Dunayevsky, V. A., Abbassian, Fereldoun, and Judzis, Arnis. 1993. Dynamic Stability of Drillstrings Under Fluctuating Weight on Bit. *SPE Drilling & Completion* **8** (02): 84-92. https://doi.org/10.2118/14329-PA.
Dupriest, Fred E., Elks, William Curtis, Ottesen, Steinar et al. 2010. Borehole Quality Design and Practices To Maximize Drill Rate Performance. Presented at the SPE Annual Technical Conference and Exhibition, Florence, Italy. 2010/1/1/. https://doi.org/10.2118/134580-MS.
Dwars, Sicco. 2015. Recent Advances in Soft Torque Rotary Systems. Presented at the SPE/IADC Drilling Conference and Exhibition, London, England, UK. 2015/3/17/. https://doi.org/10.2118/173037-MS.
Dykstra, M. W., Chen, D. C. K., and Warren, T. M. 1994. Experimental Evaluations of Drill Bit and Drill String Dynamics. Presented at the SPE Annual Technical Conference and Exhibition, New Orleans, Louisiana. 1994/1/1/. https://doi.org/10.2118/28323-MS.
Gallagher, John, Waller, Mike, and Ruszka, John. 1994. Performance Drilling: A Practical Solution to Drillstring Vibration. Presented at the SPE/IADC Drilling Conference, Dallas, Texas. 1994/1/1/. https://doi.org/10.2118/27538-MS.
Giltner, Molly, Earle, Linsay, Willis, John et al. 2019. Performance Impact of Downhole Data from Wired Drill Pipe and Downhole Sensors. Presented at the SPE/IADC International Drilling Conference and Exhibition, The Hague, The Netherlands. 2019/3/4/. https://doi.org/10.2118/194093-MS.
Greenwood, Jeremy A. 2016. Improvements in the Root Cause Analysis of Drillstring Vibration. Presented at the IADC/SPE Drilling Conference and Exhibition, Fort Worth, Texas, USA. 2016/3/1/. https://doi.org/10.2118/178819-MS.
Hohl, Andreas, Hohl, Carsten, and Herbig, Christian. 2015. A Combined Analytical and Numerical Approach to Analyze Mud Motor Excited Vibrations in Drilling Systems. V009T24A004. https://doi.org/10.1115/GT2015-42144.
Hohl, Andreas, Kulke, Vincent, Kueck, Armin et al. 2020. The Nature of the Interaction Between Stick/Slip and High-Frequency Torsional Oscillations. Presented at the IADC/SPE International Drilling Conference and Exhibition, Galveston, Texas, USA. 2020/2/25/. https://doi.org/10.2118/199642-MS.
Hood, James, Taylor, Richard, Morris, Paul et al. 2015. Expert Real-Time Drilling Performance Prevents Twist-offs and Reduces Bit Damage in the Permian Basin. Presented at the SPE/IADC Drilling Conference and Exhibition, London, England, UK. 2015/3/17/. https://doi.org/10.2118/173170-MS.
Jaggi, Anil, Upadhaya, Sunil, and Chowdhury, Ashabikash Roy. 2007. Successful PDC/RSS Vibration Management Using Innovative Depth-of-Cut Control Technology: Panna Field, Offshore India. Presented at the SPE/IADC Drilling Conference, Amsterdam, The Netherlands. 2007/1/1/. https://doi.org/10.2118/104388-MS.
Khaled, Mohamed Shafik and Shokir, Eissa M. 2017. Effect of Drillstring Vibration Cyclic Loads on Wellbore Stability. Presented at the SPE Middle East Oil & Gas Show and Conference, Manama, Kingdom of Bahrain. 2017/3/6/. https://doi.org/10.2118/183983-MS.
Kyllingstad, A. and Halsey, G. W. 1987. A Study of Slip-Stick Motion of the Bit. Presented at the SPE Annual Technical Conference and Exhibition, Dallas, Texas. 1987/1/1/. https://doi.org/10.2118/16659-MS.
Langeveld, C. J. 1992. PDC Bit Dynamics. Presented at the IADC/SPE Drilling Conference, New Orleans, Louisiana. 1992/1/1/. https://doi.org/10.2118/23867-MS.
Larsen, Lena Kyrvestad. 2014. *Tools and Techniques to Minimize Shock and Vibration to the Bottom Hole Assembly*, University of Stavanger, Stavanger.
Lines, L. A., Stroud, D. R. H., and Coveney, V. A. 2013. Torsional Resonance - An Understanding Based on Field and Laboratory Tests with Latest Generation Point-the-Bit Rotary Steerable System. Presented at the SPE/IADC Drilling Conference, Amsterdam, The Netherlands. 2013/3/5/. https://doi.org/10.2118/163428-MS.
Livescu, Silviu, Craig, Steven Henry, and Watkins, Thomas. 2014. Challenging the Industry''s Understanding of the Mechanical Friction Reduction for Coiled Tubing Operations.

Presented at the SPE Annual Technical Conference and Exhibition, Amsterdam, The Netherlands. 2014/10/27/. https://doi.org/10.2118/170635-MS.
Lubinski, Arthur and Woods, H. B. 1955. Use of Stabilizers in Controlling Hole Deviation. Presented at the Drilling and Production Practice, New York, New York. 1955/1/1/. https://doi.org/.
Macpherson, John D., Paul, Pastusek, Behounek, Michael et al. 2015. A Framework for Transparency in Drilling Mechanics and Dynamics Measurements. Presented at the SPE Annual Technical Conference and Exhibition, Houston, Texas, USA. 2015/9/28/. https://doi.org/10.2118/174874-MS.
McCartney, Chris, Allen, Scott, Hernandez, Maximo et al. 2009. Step-Change Improvements With Wired-Pipe Telemetry. Presented at the SPE/IADC Drilling Conference and Exhibition, Amsterdam, The Netherlands. 2009/1/1/. https://doi.org/10.2118/119570-MS.
Meyers, M.A. 1994. *Dynamic Behavior of Materials*: Wiley.
Niu, Shi-wei, Zheng, Hua-lin, Yang, Ying-xin et al. 2019. Experimental research on torque characteristic and weight distribution of the polycrystalline diamond compact–roller hybrid bit. *Advances in Mechanical Engineering* **11**: 168781401984974.
Osnes, Svein Magne, Amundsen, Per Amund, Weltzin, Tore et al. 2009. Vibration Measurements: A Time for Standardisation. Presented at the SPE/IADC Drilling Conference and Exhibition, Amsterdam, The Netherlands. 2009/1/1/. https://doi.org/10.2118/119877-MS.
Pastusek, Paul E. 2018. Stabilizer Selection Based on Physics and Lessons Learned. Presented at the IADC/SPE Drilling Conference and Exhibition, Fort Worth, Texas, USA. 2018/3/6/. https://doi.org/10.2118/189649-MS.
Patil, Parimal Arjun and Ochoa, Oscar Nicolas. 2020. Identification of Optimal Drilling Parameters for Reduction of High-Frequency Torsional Oscillations by Combined Approach with Modeling and Real-Time Analysis of High-Frequency Measurements. Presented at the IADC/SPE International Drilling Conference and Exhibition, Galveston, Texas, USA. 2020/2/25/. https://doi.org/10.2118/199680-MS.
Payette, Gregory S., Pais, Darren, Spivey, Benjamin et al. 2015. Mitigating Drilling Dysfunction Using a Drilling Advisory System: Results from Recent Field Applications. Presented at the International Petroleum Technology Conference, Doha, Qatar. 2015/12/6/. https://doi.org/10.2523/IPTC-18333-MS.
Reeves, Michael E., Payne, Michael L., Ismayilov, Anar G. et al. 2005. Intelligent Drill String Field Trials Demonstrate Technology Functionality. Presented at the SPE/IADC Drilling Conference, Amsterdam, Netherlands. 2005/1/1/. https://doi.org/10.2118/92477-MS.
Richard, Thomas, Germay, Christophe, and Detournay, Emmanuel. 2004. Self-excited stick–slip oscillations of drill bits. *Comptes Rendus Mécanique* **332** (8): 619-626. http://www.sciencedirect.com/science/article/pii/S1631072104001135.
Santos, Helio, Placido, J. C. R., and Wolter, Claudio. 1999. Consequences and Relevance of Drillstring Vibration on Wellbore Stability. Presented at the SPE/IADC Drilling Conference, Amsterdam, Netherlands. 1999/1/1/. https://doi.org/10.2118/52820-MS.
Schwefe, Thorsten, Ledgerwood Iii, L. W., Jain, Jayesh R. et al. 2014. Development and Testing of Stick/Slip-Resistant PDC Bits. Presented at the IADC/SPE Drilling Conference and Exhibition, Fort Worth, Texas, USA. 2014/3/4/. https://doi.org/10.2118/168026-MS.
Selnes, Knut Sigve, Clemmensen, Carl C., and Reimers, Nils. 2009. Drilling Difficult Formations Efficiently With the Use of an Antistall Tool. *SPE Drilling & Completion* **24** (04): 531-536. https://doi.org/10.2118/111874-PA.
Shen, Yuelin, Zhang, Zhengxin, Zhao, Jie et al. 2017. The Origin and Mechanism of Severe Stick-Slip. Presented at the SPE Annual Technical Conference and Exhibition, San Antonio, Texas, USA. 2017/10/9/. https://doi.org/10.2118/187457-MS.
Sowers, Steven Frank, Dupriest, Fred E., Bailey, Jeffrey R. et al. 2009. Use of Roller Reamers Improves Drilling Performance in Wells Limited by Bit and Bottomhole Assembly

Vibrations. Presented at the SPE/IADC Drilling Conference and Exhibition, Amsterdam, The Netherlands. 2009/1/1/. https://doi.org/10.2118/119375-MS.
Tang, Liping, Zhu, X., Shi, C. et al. 2016. Investigation of the damping effect on stick-slip vibration of oil and gas drilling system. *Advances in Vibration Engineering* **4**: 79-86.
Teale, R. 1965. The concept of specific energy in rock drilling. *International Journal of Rock Mechanics and Mining Sciences & Geomechanics Abstracts* **2** (1): 57-73. http://www.sciencedirect.com/science/article/pii/0148906265900227.
Vandiver, J. K., Nicholson, J. W., and Shyu, R. J. 1989. Case Studies of the Bending Vibration and Whirling Motion of Drill Collars. Presented at the SPE/IADC Drilling Conference, New Orleans, Louisiana. 1989/1/1/. https://doi.org/10.2118/18652-MS.
Vassallo, Massimiliano, Bernasconi, Giancarlo, and Rampa, Vittorio. 2004. Bit Bounce Detection Using Neural Networks. Presented at the 2004 SEG Annual Meeting, Denver, Colorado. 2004/1/1/. https://doi.org/.
Warren, T. M. and Oster, J. H. 1998. Torsional Resonance of Drill Collars with PDC Bits in Hard Rock. Presented at the SPE Annual Technical Conference and Exhibition, New Orleans, Louisiana. 1998/1/1/. https://doi.org/10.2118/49204-MS.
Warren, Thomas M., Brett, J. Ford, and Sinor, L. Allen. 1990. Development of a Whirl-Resistant Bit. *SPE Drilling Engineering* **5** (04): 267-275. https://doi.org/10.2118/19572-PA.
Zhao, Dapeng, Hovda, Sigve, and Sangesland, Sigbjørn. 2018. Whirl Simulation of Drill Collar and Estimation of Cumulative Fatigue Damage on Drill-Collar Connection. *SPE Journal* **23** (02): 286-300. https://doi.org/10.2118/187964-PA.

APPENDIX A Matlab code

APPENDIX A.1 Program Calculating Axial Amplitudes Along the Drillstring

Definitions

```
% L_1        [ft] Length of drill collars
% D_2        [in] DP OD
% d_2        [in] DP ID
% A_2        [in^2] Cross-sectional DP area
% D_1        [in] DC OD
% d_1        [in] DC ID
% A_1        [in^2] Cross-sectional DC area
% L_well     [ft] Well MD
% L_2        [ft] Placeholder
%
% %% Operating parameters
% WOB        [lbf] Weight on bit
% RPM        [RPM] Rotational rate
% f          [Hz] Excitations per sec
% w          [rad/s] angular velocity
%
% %% Steel properties
% E          [psi] Modulus of elasticity for steel
% c          [ft/s] Acoustic velocity in steel
% gamma_1    [(lb/ft)/(sec/ft)]Damping ratio of DC
% gamma_2    [(lb/ft)/(sec/ft)]Damping ratio of DP
%
% %% Topside properties and Miscellaneous
%
% k         [lbs/ft] Spring constant of drawworks
% M         [lbs*s^2/ft] Mass of swivel and travelling block
% t_2       [vector of time]

clc
clear all
close all
```

Well and string dimensions

```
L_1 = 800;                                  % [ft] Length of drill collars
D_2 = 4.5;                                  % [in] DP OD
```

```
d_2 = 3.826;                                 % [in] DP ID
A_2 = (pi/4)*(D_2^2-d_2^2);                  % [in^2] Cross-sectional DP area
D_1 = 6.5;                                   % [in] DC OD
d_1 = 2.25;                                  % [in] DC ID
A_1 = (pi/4)*(D_1^2-d_1^2);                  % [in^2] Cross-sectional DC area
L_well = 8000;                               % [ft] Well MD
L_2 = L_well;                                % [ft] DP length
```

Operating parameters

```
WOB = 30000;                                 % [lbf] Weight on bit
RPM = [80, 90, 100];                                 % [RPM] Rotational rate
```

```
for x = 1:10
    disp(x)
end
```

```
f = 3*RPM/60                                 % [Hz] Excitations per sec
w = 2*pi*f;                                  % [rad/s] angular velocity
```

```
f =

    4.0000    4.5000    5.0000
```

Steel properties

```
E = 30*10^6;                                 % [psi] Modulus of elasticity for steel
c = 16800;                                   % [ft/s] Acoustic velocity in steel
gamma_1 = 5.0;                               % [(lb/ft)/(sec/ft)]Damping ratio of DC
gamma_2 = 0.7;                               % [(lb/ft)/(sec/ft)]Damping ratio of DP
```

Topside properties

```
k = 640000;                                  % [lbs/ft] Spring constant of drawworks
M = 20000/32.1741;                                 % [lbs*s^2/ft] Mass of swivel and
travelling block
t_2 = 0:0.01:6;                              % [s] vector of time

u_0 = 1;                                     % [in] Amplitude of bit displacement
for count = 1:length(RPM)
    w_1=w(count)
psi_1 = sqrt((w_1^2/c^2) - (i*gamma_1*w_1)/(A_1*E));

psi_2 = sqrt((w_1^2/c^2) - (i*gamma_2*w_1)/(A_2*E));

b_2 = atan((A_2*E*psi_2)/(M*w_1^2-k))-psi_2*L_2;

b_1 = atan(((A_1*E*psi_1)/(A_2*E*psi_2))*tan(psi_2*L_1+b_2))-psi_1*L_1;

B_2 = -(u_0*i)/(sin(b_1)) * (sin(psi_1*L_1+b_1))/(sin(psi_2*L_1+b_2));

B_1 = - (i*u_0)/sin(b_1);
```

```
w_1 =
```

```
   25.1327

w_1 =

   28.2743

w_1 =

   31.4159
```

Finds time of max bit displacement

```
bit_displacement = sin(w_1.*t_2);
finnmax = find(max(bit_displacement));
int = find(max(bit_displacement)==bit_displacement,1);
t = t_2(int);
```

Plot the displacement along the drillstring

```
[u,x] = axvib(u_0,B_1,psi_1,b_1,L_1,B_2,psi_2,b_2,L_2,w_1,t);
U = zeros(length(u),length(RPM));
U(:,count)= abs(u);


h(count) = char(RPM(count));
% txt = ['Frequency = ',num2str(f(count)),' Hz'];
txt = ['RPM = ',num2str(RPM(count))];
figure(1)
p = plot(U(:,count),x,'DisplayName',txt)

legend show
hold on
grid on

%title('Dynamic bit displacement')

ylabel('Distance from bit [ft]','fontweight','bold','fontsize',14)
xlabel('Normalized displacement','fontweight','bold','fontsize',14)
```

```
p =

  Line (RPM = 80) with properties:

              Color: [0 0.4470 0.7410]
          LineStyle: '-'
          LineWidth: 0.5000
             Marker: 'none'
         MarkerSize: 6
    MarkerFaceColor: 'none'
              XData: [1×1000 double]
              YData: [1×1000 double]
              ZData: [1×0 double]

  Use GET to show all properties
```

```
p =

  Line (RPM = 90) with properties:

              Color: [0.8500 0.3250 0.0980]
          LineStyle: '-'
          LineWidth: 0.5000
             Marker: 'none'
         MarkerSize: 6
    MarkerFaceColor: 'none'
              XData: [1×1000 double]
              YData: [1×1000 double]
              ZData: [1×0 double]

  Use GET to show all properties


p =
  Line (RPM = 100) with properties:
              Color: [0.9290 0.6940 0.1250]
          LineStyle: '-'
          LineWidth: 0.5000
             Marker: 'none'
         MarkerSize: 6
    MarkerFaceColor: 'none'
              XData: [1×1000 double]
              YData: [1×1000 double]
              ZData: [1×0 double]
  Use GET to show all properties
```

```
end

% p(1).Color = [0 0.4470 0.7410];
% p(2).Color = [0.8500 0.3250 0.0980];
% p(3).Color = [0.9290 0.6940 0.1250];

x0 = 60;
y0 = 60;
width= 350;
height= 700;

set(gcf,'position',[x0,y0,width,height])
```

Published with MATLAB® R2017b

APPENDIX B Supplementary Images and Documentation

Taper angle describes the abruptness of transition in OD between the stabilizer and BHA, as can be seen in the figure below.

APPENDIX B.1 Stabilizer Taper Angle

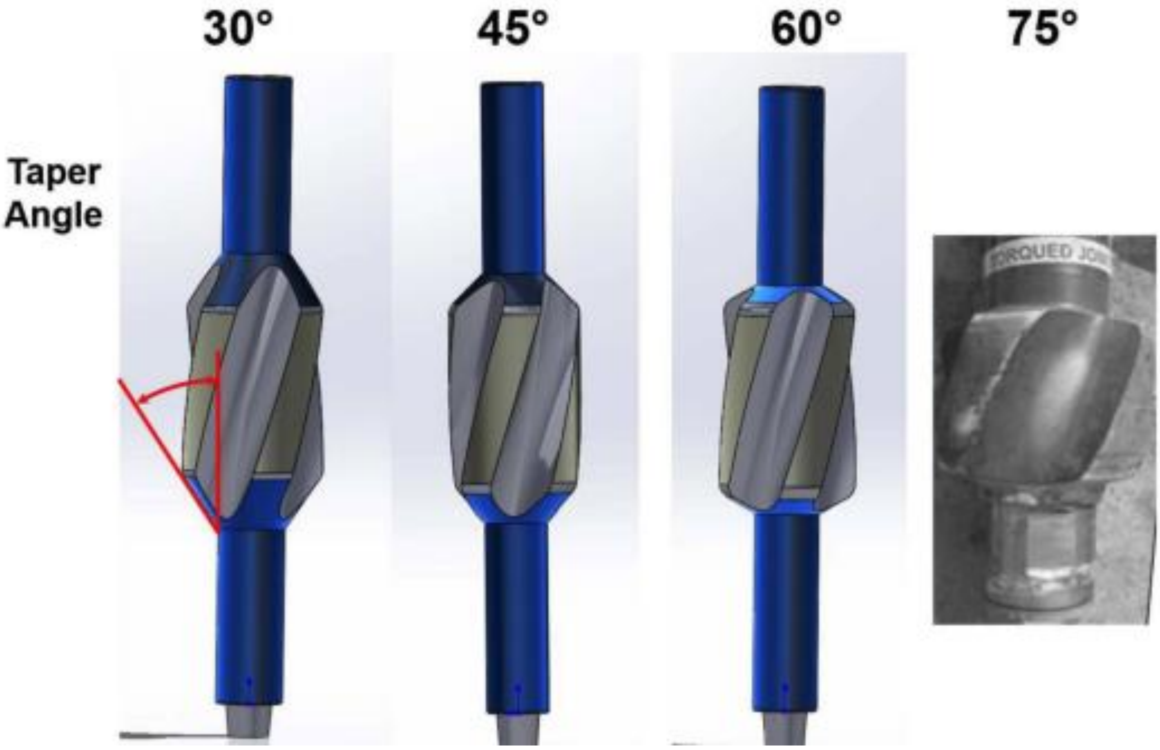

Stabilizers with varying degree of taper angle (Pastusek 2018).

The objective of the taper is to allow the stabilizer to bypass ledges in the borehole while tripping in and out. When tripping in and out, the overpull must overcome the static friction of the stabilizer contact. With ledges in the borehole, excess overpull can occur if the ledge angle and the taper angle is too large. The worst case scenario is the overpull generated by a 90° angled ledge when tripping with a 90° taper angle on the stabilizers. Pastusek (2018) demonstrated the forces acting on a free body diagram of a stabilizer as shown in **Error! Reference source not found.**.

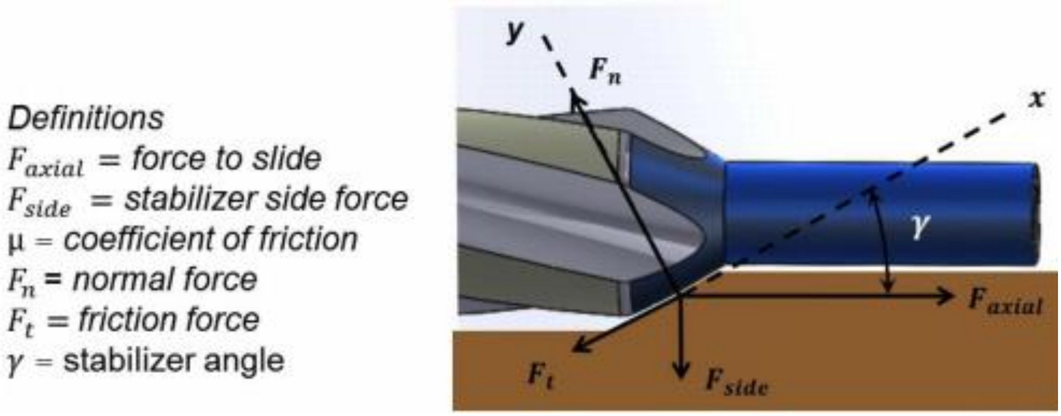

Forces acting on a stabilizer as the BHA is laying against the low side of the hole (Pastusek 2018).

By summation of forces in both horizontal and vertical directions, a term for the axial pulling force is derived:

$$\mathrm{F_{axial}} = F_{side}\left[\frac{\sin\gamma + \mu\cos\gamma}{\cos\gamma - \mu\sin\gamma}\right] \tag{3.14}$$

$$\text{for } \gamma < \tan^{-1}\left(\frac{1}{\mu}\right)$$

By using this equation, the pulling force necessary to pull the stabilizer out of the hole can be calculated using taper angle, side load and a coefficient of friction. With a taper angle of 0, the equation becomes directly proportional to the coefficient of friction. The pulling force needed for different coefficients of friction with varying taper angle given a side load of 4000 lbs is shown below.

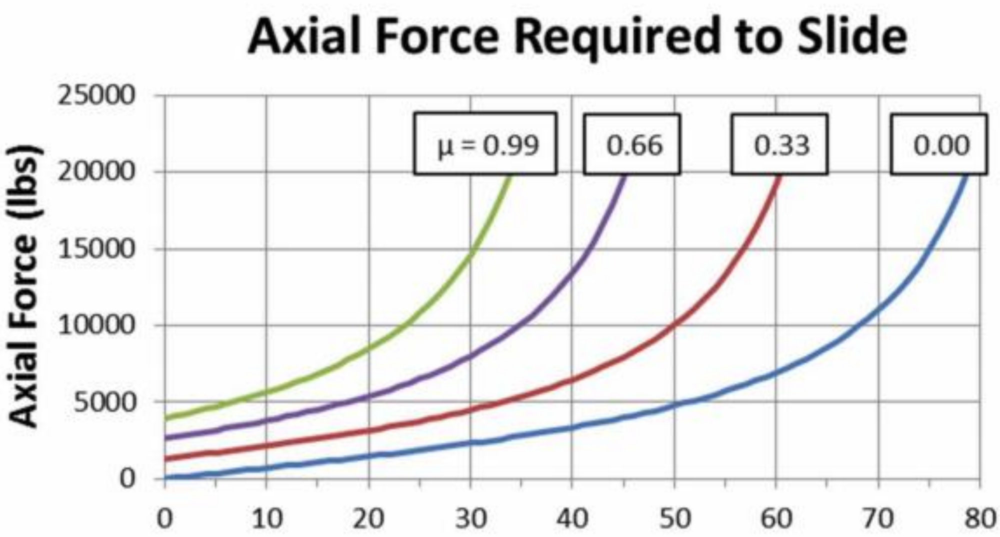

Axial pulling force with varying taper angle for a set of friction factors.

Pulling during rotation is most likely the scenario with the lowest coefficient of friction as the static friction is already overcome. The graph shows that it is possible to slide the stabilizer even at very high taper angles in this case, however there might be axial pulling constraints set by other components in the string which may put the BHA in jeopardy even at very low coefficients of friction. 45-degree tapers are commonly used in the industry, however as indicated by the graph, lower angled tapers may be preferential in order to reduce the overpull needed to slide the stabilizer.

APPE

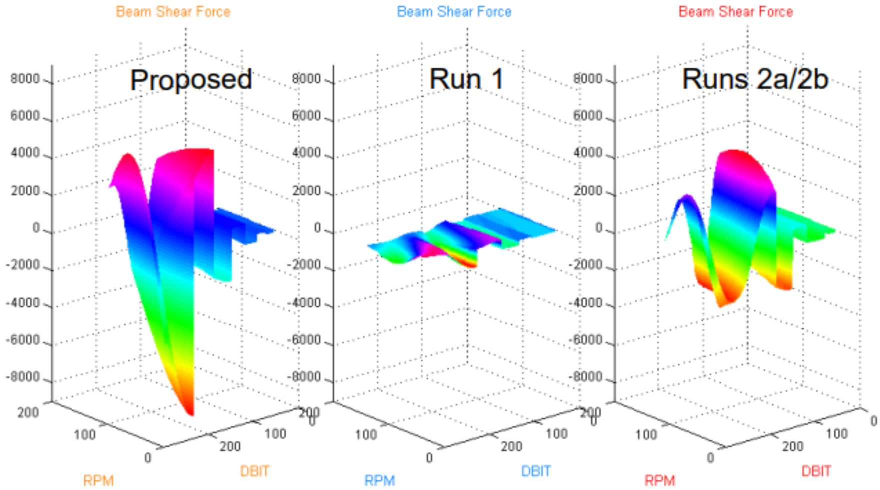

Beam sheer diagrams for the three BHAs (Bailey et al. 2008)

APPE

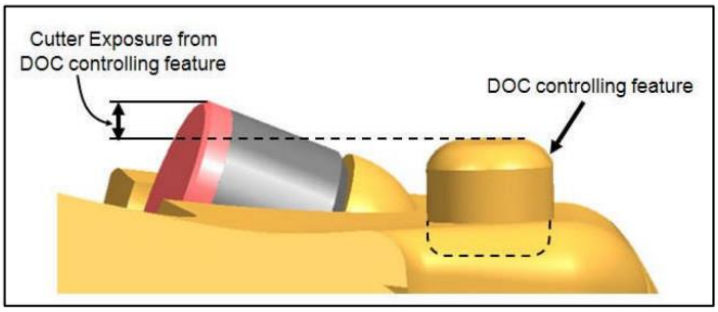

Feature based depth of cut control (DOCC)

To the left is the feature on a real bit used in the field and to the right is the DOC controlling feature illustrated (Schwefe et al. 2014)

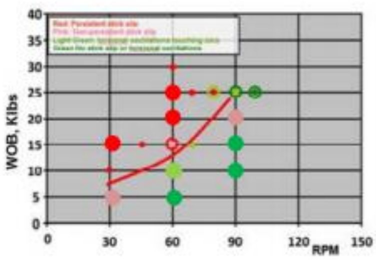

Fig. 8: Bit A without DOC control

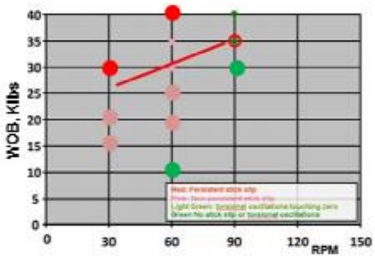

Fig. 9: Bit B with some DOC control

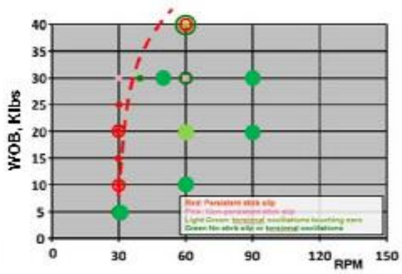

Fig. 10: Bit C with DOC control

Stability maps indicating the onset of stick-slip.

Red colors indicate persistent stick-slip, pink indicates non persistent stick-slip, while green indicates no stick-slip. The onset of stick-slip is delayed when applying WOB with increasing DOCC (Schwefe et al. 2014).

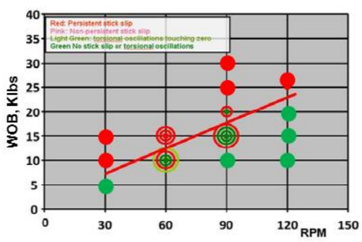

Bit B: Some DOC control

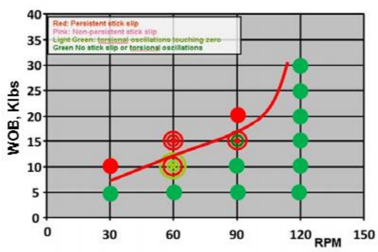

Bit C: DOC control

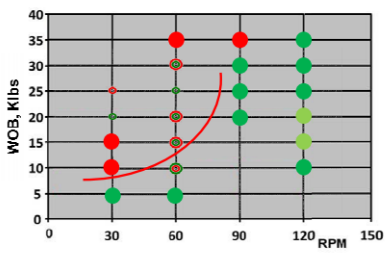

Bit D: Extreme DOC control

Stability maps from tests with varying DOC control

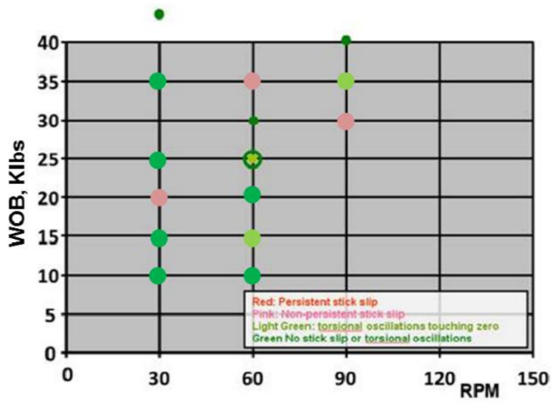

Fig. 19: Bit B with blade-based DOC control

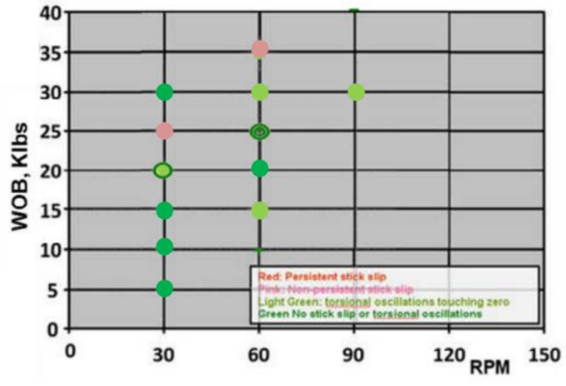

Fig. 20: Bit E with feature-based DOC control

Stability maps demonstrating blade based DOCC (left) vs feature-based DOCC (right) (Schwefe et al. 2014)

APPE

Results comparing wells drilled with and without STRS

	Well #	Footage (ft)	ROP (ft/hr)	Bit RPM	Surf RPM	WOB (k-lbs)	Torque (k ft-lbs) Min	Torque (k ft-lbs) Av	Torque (k ft-lbs) Max	Stick Slip (%)
STRS Installed	Well L	3316	68	279	81	25	16	24	27	9
	Well K	4035	69	263	79	29	20	23	26	8
	Well J	3436	78	279	80	27	25	27	28	8
	Well I	4136	76	280	84	29	16	24	27	9
	Well H	4093	79	297	101	27	19	24	27	10
	Well G	3614	93	264	74	26	19	22	25	11
No STRS	Well F	3204	84	281	81	29	22	26	29	12
	Well E	2535	59	303	101	32	17	27	30	15
	Well D	2827	69	265	70	23	21	23	26	16
	Well C	3079	36	305	103	21	23	27	29	10
	Well B	2866	66	280	99	20	17	25	28	28
	Well A	3088	43	288	97	22	16	20	22	8

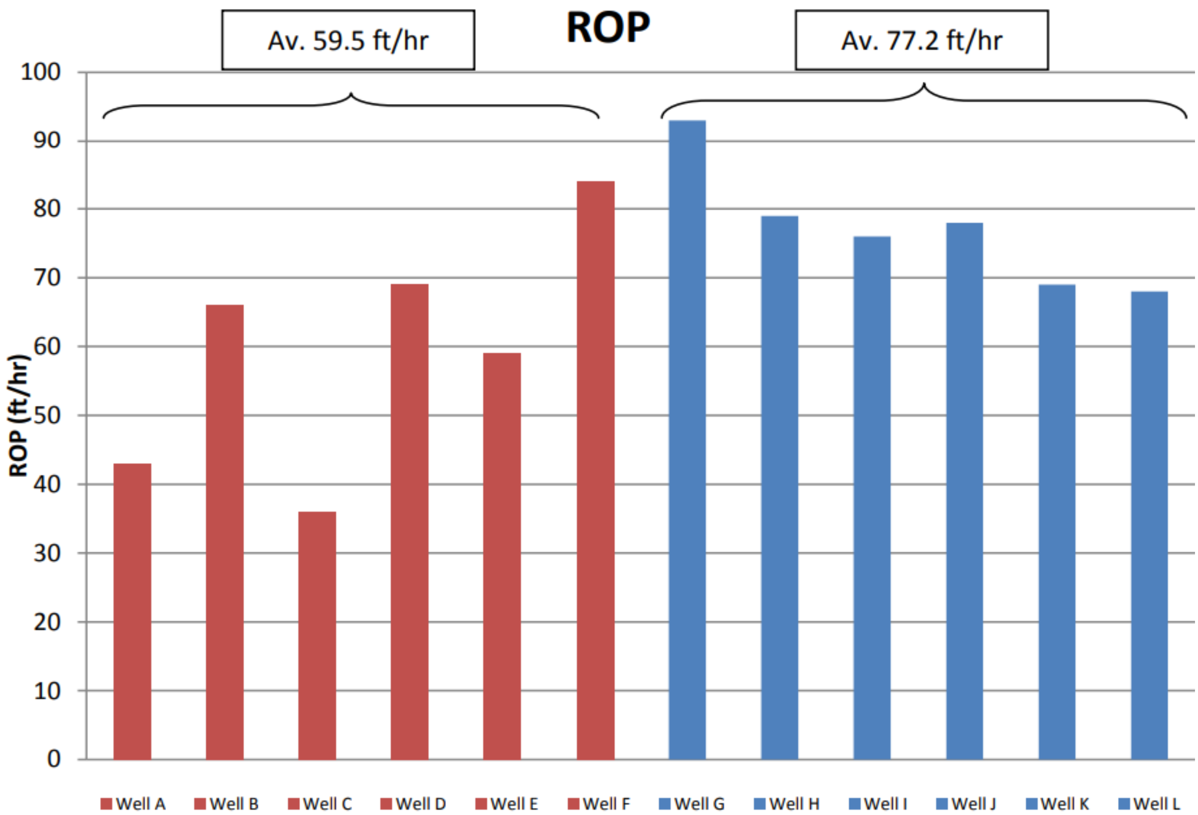

Graphical presentation of the ROP increases using STRS (Attar et al. 2014)

	feet/bit	Bit Wear	
		Inner Teeth	Outer Teeth
With-Out STRS	2371.9	1.5	3.2
With STRS	2567.6	1.0	2.0
% Improvement	8.2	34.2	37.1

Improvements in bit wear by implementing STRS (Attar et al. 2014)

Mads Berntsen

NTNU
Norwegian University of
Science and Technology

AkerBP